Sex- and species-specific CD99 expression of T cells and its implications in multiple sclerosis

Dissertation

zur Erlangung der Würde des Doktors der Naturwissenschaften
des Fachbereichs Biologie, der Fakultät für Mathematik, Informatik
und Naturwissenschaften der Universität Hamburg

vorgelegt von

Ingo Winschel

Hamburg 2024

Conducted at

Institute of Neuroimmunology and Multiple Sclerosis (INIMS)

Center for Molecular Neurobiology Hamburg (ZMNH)

University Medical Center Hamburg-Eppendorf (UKE)

Date of the oral defense: 10.04.2024

Chair: Prof. Dr. Thomas Oertner

Supervisor and referee: Prof. Dr. Manuel Alexander Friese

Referee: Prof. Dr. Tim-Wolf Gilberger

Dedication

This is dedicated to my wife and my children. Thank you.

Table of Contents

I. List of figures

II. List of tables

III. Abbreviations

AD	*Alzheimer's disease*
ADEM	*Acute disseminated encephalomyelitis*
AIRE	*Autoimmune regulator*
AML	*Acute myeloid leukemia*
ANO2	*Anoctamin 2*
AR	*Androgen receptor*
AREs	*Androgen response elements*
BBB	*Blood-brain barrier*
BCR	*B cell receptor*
BCSFB	*Blood-cerebrospinal fluid barrier*
cDCs	*Conventional dendritic*
CFA	*Complete Freund's adjuvant*
ChP	*Choroid plexus*
CIS	*Clinically isolated syndrome*
CMV	*Cytomegalovirus*
CNS	*Central nervous system*
CREB	*cAMP response element-binding protein*
DCs	*Dendritic cells*
DHT	*Dihydrotestosterone*
dpi	*Days post immunization*
E2	*17-beta estradiol*
EAE	*Experimental autoimmune encephalomyelitis*
EBNA1	*EBV nuclear antigen 1*
EBV	*Epstein-Barr virus*
ER	*Estrogen receptor*
EREs	*Estrogen response elements*
ERK1/2	*Extracellular signal regulated protein kinase1/2*
EWS	*Ewing sarcoma*
FCG	*Four Core Genotype*
FKBP	*FK506-binding protein*
GA	*Glatiramer acetate*
Gd	*Gadolinium*
GlialCAM	*Glial cell adhesion molecule*

GM-CSF	*Granulocyte macrophage-colony stimulating factor*
GPER	*G-protein-coupled estrogen receptor*
GTEx	*Genotype-Tissue Expression project*
GWAS	*Genome-wide association studies*
HHV-6	*Human herpesvirus 6*
HLA	*Human leukocyte antigen*
HSV	*Herpes simplex virus*
i.p.	*Intraperitoneally*
IFNγ	*Interferon-γ*
Ig	*Immunoglobulins*
IL-17	*Interleukin-17*
ILCs	*Innate lymphoid cells*
iNOS	*Inducible nitric-oxide synthase*
IP-10	*Interferon-gamma-inducible protein 10*
IRF	*IFN regulatory factor*
LN	*Lymph nodes*
LOY	*Loss of chromosome Y*
LPS	*Lipopolysaccharide*
mAb	*Monoclonal antibody*
MAIT cells	*Mucosal-associated invariant T cells*
MBP	*Myelin basic protein*
MHC	*Major histocompatibility complex*
MMP	*Matrix metalloproteinase*
MOG	*Myelin oligodendrocyte glycoprotein*
MRI	*Magnetic resonance imaging*
MS	*Multiple sclerosis*
mTECs	*Medullary thymic epithelial cells*
NDS	*Normal donkey serum*
NfL	*Neurofilament light chain*
NK	*Natural killer*
NMOSDs	*Neuromyelitis optica spectrum disorders*
PAR	*Pseudoautosomal region*
PBMCs	*Peripheral blood mononuclear cells*
PD	*Parkinson's disease*
pDCs	*Plasmacytoid dendritic cells*

PECAM1	*Platelet endothelial cell adhesion molecule 1*
PHA	*Phytohemagglutinin*
PILRs	*Paired immunoglobulinlike receptors*
PLP	*Proteolipid protein*
PMA	*Phorbol-12-myristat-13-acetat*
PPAR	*Peroxisome proliferator activated receptor*
PPIs	*Protein-protein interactions*
PPMS	*Primary progressive multiple sclerosis*
PTX	*Pertussis toxin*
RA	*Rheumatoid arthritis*
RRMS	*Relapsing-remitting* multiple sclerosis
RT	*Room temperature*
s.c.	*subcutaneous*
scRNAseq	*Single-cell RNA sequencing*
SEB	*Staphylococcal enterotoxin B*
SNP	*Single-nucleotide polymorphism*
snRNAseq	*Single-nucleus RNA sequencing*
SPMS	*Secondary progressive multiple sclerosis*
Sry	*Sex determining region of the Y*
T-ALL	*T-lineage acute lymphoblastic leukemia*
TCR	*T cell receptor*
TCRBV	*TCR variable beta chain*
TLR	*Toll-like receptor*
TMEV	*Theiler's murine encephalomyelitis virus*
TNF	*Tumor necrosis factor*
TRAIL	*tumor necrosis factor-related apoptosis-inducing ligand*
T_{reg} cells	*Regulatory T cells*
T_{RM}	*Tissue-resident memory T cells*
TYK2	*Tyrosine kinase 2*
VLA-4	*Very late antigen-4*
WT	*Wildtype*
Xa	*Activated X chromosome*
XCI	*X chromosome inactivation*
Xi	*Inactivated X chromosome*
Xist	*X-inactive specific transcript*

1 Introduction

1.1 Multiple sclerosis

Multiple sclerosis (MS) is a chronic autoimmune and inflammatory disease of the central nervous system (CNS) causing demyelination and neuroaxonal degeneration leading to progressive neurological disability[1,2]. It is the most frequently occurring neurological disease in young adults with approximately 2.8 million people being affected worldwide with a steadily increasing incidence[3]. Lesional sites of pathology within the CNS are a hallmark of MS and caused by immune cell infiltration across the blood-brain barrier (BBB). Depending on the location of these lesions, clinical manifestations include visual, sensory and motor disturbances as well as fatigue, pain and cognitive impairment among many other deficits[4,5]. Initially, such neurological dysfunction only appears for a limited time period of several days or weeks and marks the beginning of the early disease also known as clinically isolated syndrome (CIS). In most patients, this is followed by a relapsing course with intermittent periods of inflammation and subsequent relapses, called relapsing-remitting MS (RRMS)[6]. While initial symptoms may completely resolve, disability accumulates as the disease advances and recovery remains incomplete. Eventually, two third of the patients transition from the relapsing-remitting course to secondary progressive MS (SPMS) after 10-15 years, where superimposed relapses reflect ongoing inflammatory activity[7]. In primary progressive MS (PPMS), relapses are absent with 10-15% of patients suffering from a continuous worsening of neurological disability from the onset of disease. While this distinction in three disease subsets appears rather static, there is accumulating evidence that the clinical course is better considered as a continuum with partial shift from a predominantly localized acute injury to a widespread inflammation with failure of compensatory mechanisms[8]. Independent of clinical course, MS patients share qualitatively comparable pathology features, which include inflammation and neurodegeneration already from the onset of disease[9,10]. This is supported by the evidence that disability progression in RRMS patients is independent from relapses[11].

1.1.1 Epidemiology and aetiology

MS is considered to originate from a combination of genetic and environmental factors with multiple risk factors being discussed. Epidemiological data implies that inherited susceptibility accounts for >30% of the overall disease risk[12], with environmental factors, such as infections, nutrition, smoking and vitamin D levels contributing to MS pathogenesis in genetically vulnerable individuals[1,13]. However, individuals migrating from low-risk to high-risk countries are at lower risk to develop MS suggesting a subordinate role for environmental components[14]. Along that line, twin studies revealed that if one monozygotic twin is affected by MS, the other has only a 25% risk, whereas in dizygotic twins, this risk

decreases to 5%[15,16]. In addition, the risk for developing MS changes from 3% in first-degree relatives to 1% in second- and third-degree compared with a background risk in white northern Europeans of 0.3%[17]. Consequently, MS is discussed to arise from a combination of genetic predisposition with distinct environmental exposure, such as early-life obesity[18], smoking[19], low sun exposure and vitamin D deficiency[20,21] as well as the composition of gut microbiota[22] and infections like Epstein-Barr virus (EBV)[23] and human herpesvirus 6 (HHV-6)[1,24].

Genome-wide association studies (GWAS) identified 200 autosomal susceptibility variants outside the major histocompatibility complex (MHC), one chromosome X variant and 32 variants within the extended MHC[12]. Genes within the human leukocyte antigen (HLA) complex, which encode for the MHC involved in antigen presentation to T cells, are associated with strongest genetic risk factors for MS. Several HLA class II alleles drive disease risk (HLA-DRB1*15:01, HLA-DRB1*13:03, HLA-DRB1*03:01, HLA-DRB1*08:01 and HLA-DQB1*03:02) and some HLA class I alleles confer protection (HLA-B*38:01, HLA-A*02:01, HLA-B*44:02 and HLA-B*55:01)[1,25]. Due to HLA class II associations, research has focused on the relevance of antigen presentation to T cell receptors (TCR) of $CD4^+$ T cells, but targeted depletion of $CD4^+$ T cells was not clinically beneficial[26]. HLA class I peptide presentation to TCR of $CD8^+$ T cells has also been studied extensively, but HLA class I also shape immune responses of other immune cells like $CD56^{dim}CD16^+$ natural killer (NK) cells[27]. Thus, the broader antigen-independent effect of HLA class I and II on shaping the immune response beyond T cells in MS is likely not being driven by a single target molecule in all patients[1]. Non-HLA genetic associations with MS disease risk are located in *IL2RA* and *IL7RA* as well as *CD58, TYK2, STAT3* and *TNFRSF1A*[28,29] loci. A single-nucleotide polymorphism (SNP) within the tyrosine kinase 2 (*TYK2*) locus confers the largest reduction in MS risk outside the HLA complex[30]. While previous GWAS studies focused on susceptibility to MS and mainly discovered immune-related gene variants, the most recent GWAS study aimed to identify genetic variants that influence the outcome of the disease. By analyzing data from more than 22,000 MS patients, two genetic variants with respective significance have been identified[31]. A risk allele located in the *DYSF-ZNF638* locus is associated with a shortening in the median time to requiring walking aid by a median of 3.7 years in homozygous carriers and with increased brainstem and cortical pathology in brain tissue. A genetic variant in the *DNM3-PIGC* locus relates to significant heritability enrichment in CNS tissues suggesting a key role for CNS resilience in determining MS outcome in contrast to immune-driven susceptibility.

EBV infection has recently been postulated as a likely prerequisite for development of MS. A longitudinal study of 10 million US military personnel, who were followed for more than 20 years revealed a 32-fold increased risk of MS diagnosis in individuals who converted to EBV seropositivity as assessed by the presence of EBV-specific antibodies, but was not increased after infection with other

viruses like cytomegalovirus (CMV)[32]. EBV seropositivity was nearly ubiquitous at the time of MS onset, with only one of 801 cases being EBV seronegative and an average time of 7.5 years after seroconversion to MS onset. Of note, serum levels of neurofilament light chain (NfL), a biomarker of neuroaxonal degeneration, were elevated only after EBV seroconversion. It has previously been known that delayed exposure to EBV after childhood increases MS risk overall[33] and in individuals carrying the HLA-DRB1*1501 variant even fivefold[34].

The mechanisms how EBV infection contributes to MS development remain subject of investigation. Molecular mimicry is discussed as crucial mediator since three contiguous regions of mimicry of the EBV nuclear antigen 1 (EBNA-1) protein have been reported, potentially arose through epitope spreading[35]. Serum antibodies from MS patients are cross-reactive between EBNA-1 and the myelin basic protein[36] as well as the human chloride-channel protein anoctamin 2 (ANO2), which is associated with electrical conduction in axons[37]. More recently, a high-affinity cross-reactive CSF-derived antibody recognizing EBNA-1 and the CNS protein glial cell adhesion molecule (GlialCAM) has been identified[38]. However, while nearly everyone is infected with EBV, MS only evolves in a small proportion of population. A recent study discovered an ineffective control of EBV-induced autoimmunity, resulting from defined virus and host genetic predispositions, which increased risk for developing MS 260-fold[39]. Cytotoxic NK cells and EBV-specific T cells capable of eliminating autoreactive GlialCAM-specific cells, are impaired in MS patients due to an EBV-variant-specific upregulation of HLA-E inducing immune evasion of autoreactive cells[39].

1.1.2 Immunopathology of MS

Irrespective of the initial cause, a dysregulated immune response promoting CNS damage is shared across all MS patients. However, the series of events leading to disease state are still incompletely understood and may act more broadly than previously thought[1]. Immune cell subsets display dynamic plasticity and may exhibit pathogenic or protective roles at different stages of disease[1], which will be discussed in the following. Substantial evidence suggests a key role of $CD4^+$ T helper cells (Th cells) in MS pathogenesis especially of interferon-γ (IFNγ)-producing T_H1 cells and interleukin-17 (IL-17)-producing T_H17 cells, which can be found in active MS lesions[1,40,41]. They primarily contribute to activation and maturation of CNS-resident microglia in experimental autoimmune encephalomyelitis (EAE)[42] and T_H17 cells promote neuroinflammation by weakening the BBB integrity[43]. With regard to HLA class II association with MS, recognition of autoantigens by $CD4^+$ T cells have been subject of investigation. Indeed, $CD4^+$ T cells reactive against myelin oligodendrocyte glycoprotein 35-55 (MOG_{33-55}) have been identified in the CSF of MS patients[44]. In animal models, MS-like pathology with $CD4^+$ T cell infiltration can be induced by immunization with peptides of the myelin sheath (MOG, myelin basic

protein (MBP) or proteolipid protein (PLP))[45]. Similarly, β-synuclein-reactive $CD4^+$ T cells have recently been shown to directly damage neurons within the grey matter, thus promoting neurodegeneration, while MBP-specific T cells infiltrate the white matter and contribute to disease onset[46]. The ability of T cells to infiltrate specific brain regions is at least partially driven by the location of priming in the periphery as it has been shown that T cells from the mesenteric lymph nodes infiltrate the white matter, while T cells from the inguinal lymph nodes were recruited to the grey matter[47]. As counteracting mechanism, regulatory T cells (T_{reg} cells) are capable of maintaining self-tolerance as well as preventing hyperinflammation and autoimmunity[48,49]. While some studies describe increased frequency of T_{regs} in the CSF but not in the blood of MS patients with impaired suppressive functions, others describe reduced resting and increased activated T_{regs} in peripheral blood of MS patients[50-52]. These differences might be explained by T cell plasticity as well as the presence of different T_{reg} subsets depending on disease context[53,54], which need to be addressed in future studies.

The relevance of $CD8^+$ T cells in MS pathogenesis is underlined by the observation that $CD8^+$ T cells outnumber $CD4^+$ T cells in active lesions[55-57], exhibiting a tissue-resident memory phenotype and persisting behind the BBB[58]. $CD8^+$ tissue-resident memory T cells (T_{RM}) are thought to contribute to disease progression and tissue destruction by reactivating CNS-intrinsic inflammatory processes with subsequent immune cell infiltration[1,58,59]. This is supported by the presence of $CD8^+$ T_{RM}-like cells in the CNS of chronic demyelinating autoimmune disease like MS and neuromyelitis optica spectrum disorders (NMOSDs), but not in acute disseminated encephalomyelitis (ADEM), a monophasic acute inflammatory CNS disease[59]. In general, $CD8^+$ T cells interact with many different cell types in the CNS[1], but it has previously not necessarily been linked to a tissue-resident phenotype. Regarding their interplay with $CD4^+$ T cells, $CD8^+$ T cells are capable of recruiting $CD4^+$ T cells by secreting chemoattractants like IL-16 and interferon-gamma-inducible protein 10 (IP-10)[60], but also mediate the suppression of $CD4^+$ T cells by secreting perforin, which is cytotoxic[61]. In addition, cytotoxic $CD8^+$ T cells are able to induce oligodendrocyte cell death leading to exposed axons[62] and to directly damage neurons by the production of granzymes and perforins as well as through Fas/FasL-mediated cytotoxicity[63,64]. With regard to HLA class I association, antigen specificity of autoreactive $CD8^+$ T cells has been extensively studied, but no autoantigens have been identified to be recognized by CNS-resident $CD8^+$ T cells[65]. However, recent findings suggests that $CD8^+$ T cells also respond to GlialCAM and that EBV-infected B cells or monocytes might activate $CD8^+$ T cells within MS lesions through presentation of EBV-derived peptides[38,65-67]. Complementary to $CD4^+$ T cells, autoregulatory $CD8^+$ T cells ($CD8^+$ T_{reg} cells) have been described in EAE models and MS patients. Depleting $CD8^+$ T cells in EAE before disease onset exacerbates clinical symptoms in affected mice indicating their autoregulatory capacity, which includes suppression of $CD4^+$ T cells and especially myelin-reactive $CD4^+$ T cells[68-70].

Accumulating evidence point towards a substantial contribution of B cells to MS pathogenesis[1,71]. For example, B cell targeted therapy is effective in MS[72] and clonally expanded B cells or their immunoglobulin products are present in the CSF[73,74], meninges and brain of MS patients[71]. The importance of B cells in disease initiation and development is supported by the recent detection of EBV nuclear antigen 1 (EBNA1) reactive antibodies in the CSF of MS patients to cross-react with GlialCAM[38]. Mechanistically, B cells are capable of directly killing oligodendrocytes and neurons *in vitro* by secreting soluble factors, which was independent of immunoglobulins (Ig) or the complement system[75,76]. The migratory capacity of B cells into the CNS is at least partially regulated by T_{FH} cells[77] and bidirectional trafficking of B cells between lymph nodes and the CNS has been observed[78-80]. A recent study in mice found that B cells in the meninges are not blood derived but originate from the skull bone marrow representing a cell reservoir of continuously replenished B cells in the CNS with likely tolerogenic phenotype[81]. Furthermore, B cells in tertiary lymphoid follicles in the meninges have been demonstrated to produce IL-10 and IL-35[82] and elevated levels of IL-10 produced by plasmablasts have been detected in MS lesions[57] indicating an anti-inflammatory part as well.

Moving from adaptive to innate immunity, there is growing research about the role of unconventional T cells in MS pathogenesis with their IL-17 production as key factor[1,83-85]. Unconventional γδ T cells were found in chronic active lesions and CSF from MS patients[86] and possess the capability of lysing human brain-derived oligodendrocytes[87]. More recently, IL-17-producing $CD161^{hi}CCR6^{+}$ γδ T cells were described to be enriched in the CSF during MS relapse[88]. Mucosal-associated invariant T cells (MAIT cells) have been identified in MS brain lesions[89,90] and MAIT cells from the blood of MS patients produce higher levels of IL-17 and display increased IL-7 receptor surface expression[91]. Recent findings discovered an upregulation of gene signatures associated with tissue repair, when MAIT cells were activated via their TCR[92-94] and increased production of cytotoxic molecules, when activated via cytokines[95,96] indicating a dichotomous role depending on the inflammatory context. Their protective capacity is supported by an exacerbated EAE course in *Mr1*$^{-/-}$ mice, which lack MAIT cells[97].

Another innate cell type, which has just been discovered and investigated over the past decade, are innate lymphoid cells (ILCs). ILCs are considered as the innate counterparts to T cells, but do not express an antigen-specific TCR[98]. They are composed of five classes, including NK cells ($CD8^{+}$ T cell-like), ILC1s (T_H1-like), ILC2s (T_H2-like), ILC3s (T_H17-like) and lymphoid tissue-inducer cells (T_{FH}-like). They are largely tissue-resident, where they contribute to maintenance of tissue homeostasis and multiple immune pathways by cytokine secretion and direct interaction with other cell types in their local surrounding. ILC1s and a subset of NKp46-expressing ILC3s play a cardinal role in the initiation of $CD4^{+}$ T_H17-mediated neuroinflammation, while a loss of T-bet in these cells impaired the ability of myelin-reactive T_H17 cells to invade the CNS[99]. They are localized in the meninges and facilitate T cell entry

into the CNS by secreting proinflammatory cytokines, chemokines and matrix metalloproteinases. In addition, ILC3s have been described to infiltrate the CNS and present antigen to myelin-reactive $CD4^+$ T cells within the inflamed brain, whereas tissue-resident ILC3s in the periphery limit autoimmune T cell responses[100]. ILC2s are less well described in context of neuroinflammation, but have recently been described to induce CNS demyelination in a herpes simplex virus (HSV)-IL-2 mouse model of MS and to contribute to female susceptibility in an SJL mouse model of EAE[101]. NK cells are classically divided into two major groups known as immature NK cells ($CD56^{bright}CD16^{low}$), mainly located in tissue and lymph nodes, and mature NK cells ($CD56^{dim}CD16^{hi}$) composing 90% of circulating NK cells. In that regard, immature NK cells dominate in the CSF of individuals[102,103], while an increased $CD56^{bright}$ to $CD56^{dim}$ ratio has been observed in the CSF of MS patients[104]. As $CD56^{dim}$ NK cells are considered as pro-inflammatory effector and $CD56^{bright}$ as regulatory cells, this suggests a counteracting mechanism towards ongoing inflammation. Mechanistically, NK cells are capable of killing activated $CD4^+$ T cells by degranulation of cytotoxic molecules including perforin, granzymes and tumor necrosis factor (TNF)-related apoptosis-inducing ligand (TRAIL)[105]. Very little is known about the role of $CD56^{dim}CD16^{hi}$ mature NK cells in MS pathogenesis with only one study describing an increased percentage of circulating $CD56^{dim}perforin^+$ NK cells in PPMS and SPMS patients[106].

Monocytes consist of multiple subsets based on their expression of CD14 and CD16 with diverse functional specializations[107]. During acute inflammatory conditions, monocytes acquire pro-inflammatory effector functions, but can also contribute to tissue repair by developing regulatory functions. Once they migrated from the circulation into tissues by chemotaxis, they differentiate into macrophages or monocyte-derived dendritic cells to present antigen to T cells and to produce polarizing cytokines. In MS patients, counts ad phenotypic appearance of monocytes are tightly correlated with clinical severity[108,109] and have been observed to accumulate in the CNS at early onset of EAE[1,110]. Of note, a majority of these constantly replenished myeloid cells are not blood derived but originate from the cranial bone marrow[111]. Macrophages are the most abundant immune cells in acute inflammatory MS lesions, where they locally adapt their phenotype capable of switching from initial proinflammatory polarization to pronounced regulatory phenotype as it has been shown in EAE[112]. The recruitment and development of monocytes is controlled by IFNγ[113] and granulocyte macrophage-colony stimulating factor (GM-CSF)[114], with both not exclusively pathogenic but also exhibiting regulatory function[115-117].

Dendritic cells (DCs) can largely be grouped into conventional dendritic cells (cDCs) and plasmacytoid dendritic cells (pDCs), which can further be classified into multiple specialized subtypes[118,119]. Antigen presentation is mainly attributed to cDCs, whereas pDCs recognize intracellular viral or self RNA and DNA through Toll-like receptors (TLR) 7 and 9 and are a major source of type I interferons. cDCs isolated

from MS patients display reduced thymic stromal lymphopoietin receptor (TSLPR)-induced activation and effector function potentially resulting in impaired T_{reg} development in MS[120]. Moreover, *ex vivo* analysis of MS-derived DCs showed enhanced IL-12p70 production upon TLR ligation and increased expression of the migratory molecules CCR5 and CCR7[121]. Although IL-12 production by DCs and other APCs is crucial for the generation of T_H1 cells and cytotoxic $CD8^+$ T cell expansion, treatment with IL12/23 p40 neutralising antibody (ustekinumab) showed no benefit in RRMS patients[122]. As mentioned above, pDCs consist of at least two separate populations, which differ in their capability to induce IL-17- or IL-10-producing T cells[1,119]. While type 1 pDCs ($CD123^{hi}CD86^{low}TLR2^{low}$) produce IFNα and induce T_{reg} cell expansion, type 2 pDCs ($CD123^{low}CD86^{hi}TLR2^{hi}$) produce IL-6 and TNF and induce T_H17 cell expansion. In MS patients, the pDC1/pDC2 ratio is shifted towards pDC2s with propensity to prime IL-17 secreting cells over IL-10-secreting $CD4^+$ T cells.

The parenchyma of the CNS is an immune-privileged compartment with only tissue-resident macrophages, known as microglia, permanently residing under homeostatic conditions capable of self-repleneshing[1,123]. Although microglia in the CNS of MS patients are able to present MBP via MHC II in active MS lesions[124], microglial MHC class II is described to be dispensable for EAE and cuprizone-induced demyelination[125]. Besides antigen presentation, microglia participate in tissue homeostasis and inflammation[126], which is considered to be dysbalanced in MS patients shifted towards an activated, tissue-destructive role[1]. This is in concordance with a recent GWAS study reporting association of MS risk genes with microglial activation[12]. Single-cell analysis of human and murine brain samples revealed three MS-associated microglia cluster exhibiting an activated status shown by increased expression of apolipoprotein E and MAF BZIP transcription factor B[127,128]. Furthermore, activated microglia induce reactive astrocytes by secreting Il-1α, TNF and C1q, which in turn induces the death of neurons and oligodendrocytes because these astrocytes lose their ability to promote neuronal survival, outgrowth and synaptogenesis[129].

1.1.3 Animal models in MS

Animal models are crucial in elucidating cellular and molecular mechanisms in MS pathogenesis through experimental manipulation and hence to develop effective pharmacological treatment options. They allow collection of CNS tissue samples already at early time points of CNS inflammation, while research in humans mostly relies on post-mortem tissue with long-lasting impact of inflammatory and neurodegenerative processes.

To account for complexity of MS pathology and to probe different aspects of the disease, different models can be used. The best characterized models include EAE, Theiler's murine encephalomyelitis virus (TMEV) infection and the toxin-induced demyelination model with cuprizone[130]. The virally

induced TMEV model is more suitable than classical EAE to study the role of $CD8^+$ T cells and the disease association with viral infections[131]. In contrast, the neurotoxic copper chelator cuprizone results in only little inflammation, but oligodendrocyte damage as well as demyelination allowing to investigate neurodegenerative mechanisms[132,133]. As both models induce demyelination, they can be used to study axonal damage as well as remyelination processes[130].

The most commonly used MS animal model to study inflammation-induced neurodegeneration is EAE, which is initiated by autoreactive T cells and most suited to reflect the autoimmune pathogenesis of MS[130,134]. In mice and rats, autoimmunity to CNS components is induced by a single subcutaneous (s.c.) injection of specific peptides of myelin sheath proteins emulsified in complete Freund's adjuvant (CFA), which consists of non-metabolizable oils and heat-killed *Mycobacterium tuberculosis* to enhance and maintain a strong immune response against injected CNS antigens[135,136]. The immunization is often amplified by an injection of pertussis toxin (PTX), which facilitates immune cell entry through a disrupted BBB[137]. CNS antigens include MOG, PLP and MBP peptides, which dictate together with the respective mouse strain the EAE disease course. The most commonly used combination is induced in C57BL/6 mice immunized with the MOG_{35-55} peptide, whereas an immunization with $PLP_{139-151}$ in SJL mice results in a relapsing-remitting phenotype[138]. During active immunization myelin-reactive T cells are activated in the lymph nodes (LN) and migrate to the CNS[139], where they are reactivated by CNS-resident APCs presenting myelin antigens on their surface[140]. Infiltrating T cells secrete pro-inflammatory cytokines, which in turn recruit further immune cells to the CNS[141,142]. These processes lead to demyelination in the CNS, which is reflected in clinical EAE symptoms with ascending paralysis from the tail to the hindlimbs correlating with spinal cord injury[138]. These symptoms usually occur 7-11 days post immunization (dpi) with disease peak after 13-15 dpi, followed by a recovery phase before animals enter a chronic or relapse phase 25-30 dpi. In addition to active immunization, passive immunization protocols exist and spontaneous EAE models in transgenic mice can be observed. 2D2 TCR transgenic mice harbor a MOG_{35-55}-specific T cell receptor and can develop spontaneous EAE. During passive immunization, activated myelin-specific T cells from TCR transgenic mice or from actively immunized mice are transferred after *in vitro* activation into recipient mice[143]. Further expansion of transgenic mice led to the development of double-transgenic mice expressing T and B cell receptors that recognize MOG ($TCR^{MOG}xIgH^{MOG}$ mice)[144,145]. B cell receptor (BCR) transgenic mice (IgH^{MOG} mice) were generated by knock-in of recombined heavy chain of an anti-MOG antibody in the Ig J region resulting in B cells with MOG-specific BCR and production of anti-MOG antibodies[146,147].

As in all animal models, there are limitations with respect to how well EAE actually reflects complex MS pathogenesis. Firstly, T cells in EAE react to a specific myelin antigen, which is not known for MS yet and the EAE model provides few information about MS progression as well as about

neuroprotective mechanisms such as remyelination and neuronal survival[130]. Moreover, very few studies have addressed the role of $CD8^+$ T cells as in most EAE models $CD4^+$ T cells are predominantly activated[148] and EAE is mainly affecting the spinal cord, whereas MS is considered a brain disease with demyelination in the cortex[149].

1.2 Sex differences in immunity

Historically, medical research has been centered on male physiology since evidence-based medicine was defined by clinical trials done predominantly in men[150,151]. Women of childbearing age were excluded from clinical trials for several reasons, including safety concerns for their offspring. While this was intended to protect women and children, it created a gap surrounding women's health and an assumption that female and male cells and animals were biologically identical[150,152]. A study found that eight out of the ten prescription drugs withdrawn from the market between 1997 and 2000 had greater health risks for women than for men[153]. In 2014, the NIH developed policies that require a balance of female and male cells and animals in preclinical studies and to include sex as a biological variable[154]. Women display higher rates of adverse drug reactions than men do[155] and pharmacokinetic as well as pharmacodynamic differences including zolpidem[156] and TNF inhibitor[157] were reported. In addition, women develop higher antibody responses and experience more adverse reactions in response to vaccines than males[158]. The exclusion of female mice from animal experiments is often justified by confounding contributions from estrus cycle, but female mice tested throughout their hormone cycles display no more variability than males[154,159].

While sex differences in disease prevalence, manifestation and treatment are mainly rooted in the genetic differences between women and men, gender interacts with sex and poses a major contributor to disease incidence and outcome[150,152]. To understand and dissect these differences properly, it is crucial to define and understand these terms. Sex is based on the composition of sex chromosomes (e.g. 46XX or 46XY), gonads (e.g. ovaries or testes), and gonadal hormones (e.g. estrogens or androgens) and is mainly categorized as female, male and intersex[150,152]. Gender refers to the socially constructed norms that impose certain roles, behaviours, activities and attributes for women and men and people with non-binary gender identities[160]. These attributes are context and time-specific and include the understanding that in many people, traits of masculinity or femininity coexist and are expressed to different degrees[150]. These attributes are fluid and in transgender people, gender identity often differs with the sex attributed at birth. Gender is an equally important variable as biological sex in human health as gender-related characteristics determine access to health care, help-seeking behaviours, the individual use of the health-care system and the perception of clinicians as well as gender-related behaviour like smoking, physical activity and nutritional habits[150]. For instance, in the

cardiovascular field, women often underestimate their risk and seek consultation later than men for treatment of myocardial infarction[161]. Intriguingly, for premature acute coronary syndrome, the presence of risk factors was more robustly associated with gender than with sex[162].

1.2.1 Sex differences in steady-state immunity

Immune responses require metabolic resources that might otherwise be used for biological processes, such as growth and reproduction[163]. There are theories stating that reduced immune function in males can be seen as a trade-off of positive selection for other traits enhancing survival and reproductive success[164]. This is supported by observations of decreased immune responses in females across many species including lizards and birds[165,166]. Even in *Drosophila melanogaster* immune-related genes are located on the X chromosome and their expression varies between the sexes upon infection[167,168].

In humans, the number and properties of innate and adaptive immune cells differ profoundly between the sexes. At baseline, women display a lower percentage of NK cells and a higher percentage of plasma cells[169,170], but no significant differences were observed in other subsets including T cells, B cells, DCs and monocytes by single-cell RNA sequencing (scRNAseq) in this study[170]. However, other studies found higher B cell and $CD4^+$ T cell counts as well as higher CD4/CD8 ratios in women, while males display higher $CD8^+$ T cell and T_{reg} frequencies[169,171-173].

Similarly, effector functions like cytokine production, signaling pathways and antibody responses show sex disparity as well. The TLR 7 pathway is one of the best described pathways in that regard. The *TLR7* gene is encoded on the X chromosome and has been demonstrated to escape X chromosome inactivation (XCI) resulting in transcription from both X chromosomes in a large proportion of B lymphocytes, monocytes and DCs in women and Klinefelter syndrome individuals harboring a XXY genotype[174]. Biallelic *TLR7* expression in B cells led to higher transcriptional levels compared to monoallelic cells and correlated with higher TLR7 protein levels in women compared to men. Functionally, TLR7 ligands induce higher IFNα production in female peripheral blood lymphocytes[175], which is driven by higher basal levels of IFN regulatory factor (IRF) 5 in pDCs[176]. More recently, IRF5 positive B cells were associated with higher production of TNFα in women upon TLR9 stimulation[177], whereas stimulation of DCs with a TLR9 did not alter sex-specific IFNα expression[175]. Peripheral blood mononuclear cells (PBMCs) isolated from men produced higher amounts of IL-10 after stimulation with TLR8 and TLR9 ligands or viruses[178] as well as TNF upon lipopolysaccharide (LPS) stimulation[179]. Male neutrophils showed higher expression of TLR4 and higher responsiveness to LPS and IFNγ with subsequent TNFα production[180]. In women, $CD4^+$ and $CD8^+$ T cells had a significantly higher level of activated phenotype in peripheral blood in the absence of pathology[181] and their upregulation of pro-

inflammatory genes upon Phorbol-12-myristat-13-acetat (PMA)-ionomycin stimulation indicate stronger cytotoxic capacities[182]. Phytohemagglutinin (PHA)-stimulated male PBMCs exhibit higher levels of IFNγ and IL-2, but lower levels of IL-4 and IL-10[183] and female naïve $CD4^+$ T cells produce higher levels of IFNγ upon anti-CD3/-CD28 stimulation, whereas male $CD4^+$ T cells produced higher levels of IL-17A[184]. Moreover, women harbor greater basal immunoglobulin levels and are capable of inducing stronger antibody responses than males[185].

1.2.2 Sex differences in autoimmunity

From epidemiological studies and clinical observations, it is known that females and males differ in their immunological responses. Women are generally able to mount stronger innate and adaptive immune responses resulting in better control of infections compared to males (**Figure 1.1**)[152,163]. However, this is accompanied by an increased female preponderance and susceptibility to autoimmune diseases such as systemic lupus erythematosus (SLE), rheumatoid arthritis (RA), autoimmune liver diseases and MS[186,187]. Sexual disparity in autoimmunity is driven by a complex interplay of (epi)genetic and environmental factors as well as sex hormones, which will be discussed in the following.

The most striking contributor comprises the different sex chromosome composition (XX versus XY). While the Y chromosome harbors 106 protein-encoding genes[188], the X chromosome encodes more than 800 protein-coding genes, from which several contribute to sex-based differences in immune responses. Among those immune genes are receptors like IL-2 receptor γ-chain (*IL-2RG*), *TLR7* and proteins involved in transcriptional and translational control like forkhead box P3 (*FOXP3*) as well as proteins related to immune response like CD40 ligand (*CD40L*) and *CD99* (**Figure 1.1**)[189]. Recently, two studies investigated the role of the Y chromosome in colorectal and bladder cancer. While the loss of the entire Y chromosome (LOY) raises the risk for bladder cancer by evading detection from immune cells[190], another study discovered a detrimental role for the Y chromosome gene *KDM5D* in colorectal cancer[191].

Regarding epigenetic factors, the mechanism of XCI is of particular importance. To maintain equal X-chromosomal gene expression in women, the paternal or maternal X chromosome in each cell is randomly inactivated during early embryonic development and propagated through subsequent cell divisions (**Figure 1.1**)[152]. The long noncoding RNA X-inactive specific transcript (Xist) is considered the master-regulator of XCI and responsible for the cis-coating of the chromosome from which it is expressed, initiation of gene silencing and changing the chromatin state to maintain silencing[192]. Xist includes highly conserved repeat domains (A-F), that orchestrate XCI by interaction with specific epigenetic regulators like SPEN or polycomb proteins that induce chromatin modifications leading to

the formation of an inactivated X chromosome (Xi, Barr body). However, XCI is often incomplete with at least 23% of X-chromosomal genes escaping XCI that varies between genes, individuals, tissues and cells[193]. XCI often results in relative overexpression of certain genes in females compared to males[194] possibly contributing to female preponderance in autoimmune susceptibility[195] as exemplified for *TLR7* and SLE[174]. Expression from a Y chromosome homolog could potentially compensate for expression from the Xi, but often results in different degrees of gene expression[194]. Another example, the X-linked histone demethylase *Kdm6a* encoding the epigenetic regulator UTX, escapes XCI resulting in sexually dimorphic expression, has been reported as a critical molecular determinant of sex differences in NK cells and antiviral immune responses[196]. Although lower in numbers, female murine NK cells display increased effector function compared to males likely contributing to less viral susceptibility in females. This effect is at least partially explained by a greater expression of UTX in female NK cells since loss of one *Kdm6a* allele in female mice led to increased NK cell counts and decreased effector function as it was observed in wildtype (WT) male mice. Notably, UTX-mediated effects were independent from gonadal hormones and UTY, the Y-linked homolog, could not compensate for reduced dosage in males.

However, generally speaking, sex hormones including estrogens, progesterone and androgens are crucial mediators of sex differences in autoimmunity (**Figure 1.1**). Low serum testosterone levels in men are associated with increased incidence of RA and in MS patients androgen levels are lower compared to age-matched healthy controls[197]. Estrogen on the other hand worsens disease course in an SLE model, but shows immune-protective effect in other autoimmune diseases such as MS and RA, although results are heavily context-dependent and thus remain elusive[198]. The molecular mechanism of estrogen is mediated by the two estrogen receptors alpha and beta (ERα and ERβ). T cells mainly express ERα, which promotes the pathogenic potential of Th1 and Th17 cells and limits the suppressive capacity of T_{regs} in a mouse model of colitis[199]. On the contrary, androgens promote local expansion of T_{regs} in visceral adipose tissue indirectly via differentiation of unique IL-33-producing stromal cells[200]. In addition, androgens upregulate the expression of Foxp3, the transcription factor for T_{reg} differentiation, by direct binding of the androgen receptor (AR) complex to the *Foxp3* locus. More recent studies investigated the contribution of sex hormones in autoimmune predisposition by influencing the autoimmune regulator (AIRE) in the thymus (**Figure 1.1**)[152]. After developing in the bone marrow, T cells undergo negative selection in the thymus by eliminating T cells, which could potentially recognize self-antigens. While expression of these self-antigens is usually restricted to one specific tissue, they are also ectopically expressed by medullary thymic epithelial cells (mTECs), where expression of a majority happens under control of the *Aire* gene[201]. In humans and mice, females expressed less AIRE on mRNA and protein level in the thymus and estrogen downregulated AIRE expression in human cultured TECs[202]. In addition, androgen recruits the AR to *Aire* promoter regions leading to an enhancement of *Aire* transcription with higher Aire-mediated antigen expression and

consequent more efficient negative selection of self-reactive T cells in males[203]. The same study showed a protective effect of androgen administration and male gender in an Aire-dependent manner in EAE.

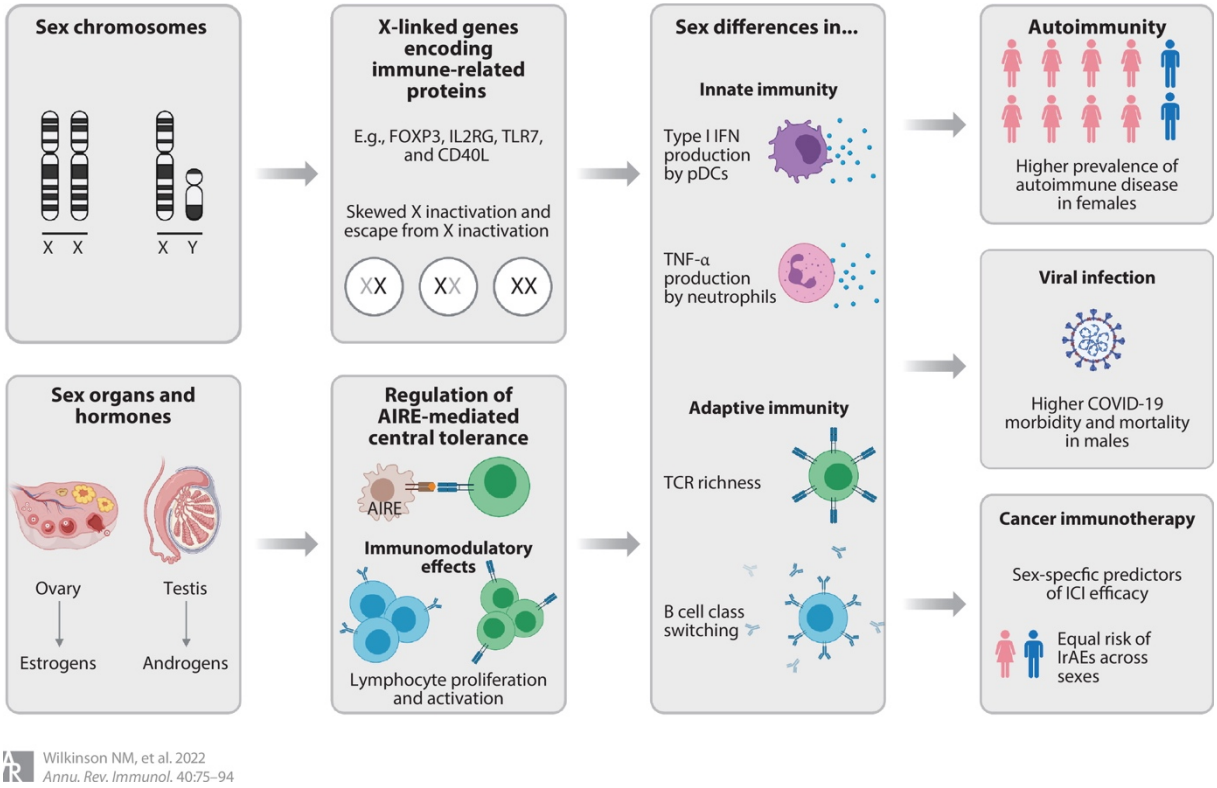

Figure 1.1: Overview of sex-related differences in immunity. Sex chromosomes and sex hormones as central mediator leading to sex differences in innate and adaptive immunity and subsequently altered incidence of autoimmune disease, outcome of viral infections as well as cancer immunotherapy. *Figure from Wilkinson NM et al. Sex Differences in Immunity. Annu Rev Immunol. 2022 Apr 26;40:75-94*[152].

1.2.3 Sex differences in MS and EAE

Sex differences in MS and EAE have been extensively studied over the past years with often contradictory or inconsistent results indicating the necessity for further mechanistic studies[187,204-206]. Depending on geographic regions, overall MS sex ratio varies between 2:1 and 3:1[207] with a steadily increasing incidence in female MS patients in past decades making sex one of the most important risk factors for developing MS[208]. Nowadays, the sex ratio in RRMS seems to be stable at approximately 2.5:1, which is indicated by a large cohort study from Canada from 1996 to 2009[209]. While MS sex ratio is almost equal in children and late-onset MS (> 50 years), it increases in adolescent-onset MS after puberty suggesting gonadal hormones as key regulator[206,210]. Intriguingly, PPMS affects women and men equally[187].

1.2.3.1 Development and clinical manifestation

With regard to a stronger female immune system, women experience a 17.7% higher relapse rate compared to male RRMS patients[211] and display IFNγ-skewed cytokine responses to multiple MS-related myelin antigens including PLP, MOG and MBP[212]. Inflammatory-demyelinating lesions can be visualized with magnetic resonance imaging (MRI) after injection of the contrast agent gadolinium (Gd) and are considered as source of relapses[213]. Gd-enhancing inflammatory lesions are more prevalent in female MS patients[214], whereas chronic-active lesions are relatively more present in male patients suggesting ongoing T cell inflammation[215]. Chronic-active lesions are characterized by an inactive demyelinated center with residual $CD8^+$ T cell and microglia inflammation along the lesion edge, while active lesions contain abundant leukocytes and inactive lesions display no immune cell infiltrates[206]. In contrast to female biased inflammatory disease onset, male sex has been shown to be among the strongest early predictors of future permanent disability in RRMS[216]. Faster accumulation of disability[217] and more rapid progression[218] indicate stronger neurodegeneration in male RRMS patients (**Figure 1.2**). However, male preponderance in neurodegenerative processes is limited to the relapsing subgroup as male PPMS patients do not show more rapid disease accumulation[187,219]. Lower performance of male MS patients in cognitive tests[220] as well as pronounced localized brain atrophy in several deep gray matter structures[221], as surrogate marker for neurodegeneration, point towards a male bias. Additionally, conversion to SPMS progresses faster in male RRMS patients[222]. Collectively, the initiation of disease with immune cell infiltration and formation of inflammatory lesions is stronger in female patients, whereas neurodegenerative processes and smouldering inflammation display a male bias (**Figure 1.2**).

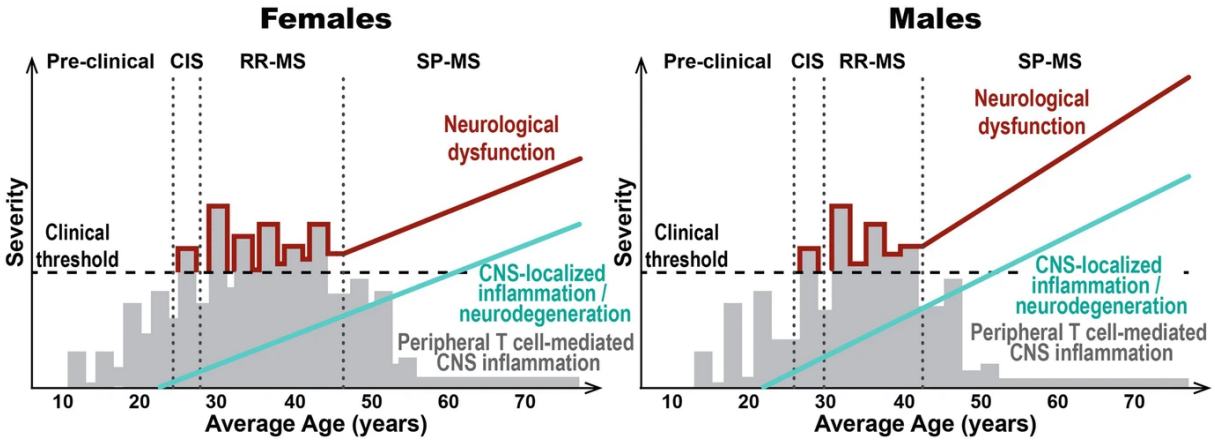

Figure 1.2: Sex differences in disease course and clinical manifestations of MS patients. The onset of MS is thought to start as subclinical autoimmune activity during childhood, but does not reach the clinical threshold until first CIS in adulthood. This is often followed by episodes of inflammation and subsequent remission until patients eventually transition to SPMS. In women, the disease course is characterized by an earlier onset with more associated T cell inflammation, whereas men show increased progression of neurological dysfunction and transition to SPMS. *Figure from Alvarez-Sanchez N et al. Immune Cell Contributors to the Female Sex Bias in Multiple Sclerosis and Experimental Autoimmune Encephalomyelitis. Curr Top Behav Neurosci. 2023;62:333-373*[206].

As already indicated above, certain EAE models reflect the female sex bias observed in MS patients. While female SJL and ASW mice develop a greater severity and female ASW mice a higher incidence, male B10.PL and PL/J mice showed more severe disease[223]. However, no sex differences were reported for the NOD strain and inconclusive results for C57BL/6 mice, which might be due to different concentrations of PTX administered[206,223]. SJL mice became the strain of choice to study sex differences in CNS autoimmunity for multiple reasons. Regardless of injected myelin peptide ($PLP_{139–155}$, MBP or $MOG_{92–106}$) female SJL mice demonstrate higher incidence and are more prone to relapses[223,224]. Transgenic mice with SJL background carrying a TCR specific for MOG_{92-106} (TCR^{1640} mice) develop spontaneous EAE more often in female mice[225,226]. However, the latter also applies to 2D2 mice on a C57BL/6 background carrying a MOG_{35-55}-specific T cell receptor[227]. Furthermore, in $MOG_{35–55}$-induced EAE, female C57BL/6 mice exhibit more severe spinal cord and optic nerve inflammation[228] and female $MOG_{35–55}$-specific Th cells are more efficient in transferring EAE to recipient mice compared to male cells[206]. Further transfer studies contributed to decipher between the effect of sex on T cell priming versus secondary mechanisms in the effector phase including BBB permeability and immune cell processes in the CNS. Myelin-specific T cells isolated from female immunized SJL mice also transfer disease more effectively, while the sex of the host mice does not influence disease activity arguing for a female bias in the induction phase[206,229,230].

1.2.3.2 Role of sex hormones

The influence of sex hormones in MS manifestation is supported by the peak of sex bias arising with puberty and a decrease with menopause[206]. In a phase 2 multicenter trial, estriol treatment together with glatiramer acetate (GA), an immunomodulatory therapy, showed additional reduction in MS relapses compared to placebo plus GA[231]. Treatment with daily testosterone (androgel) in ten male MS patients suggested a neuroprotective effect[232]. Moreover, a possible worsening of MS disabilities can be observed with menopause[233] while evidence of effects of contraceptives have yielded conflicting results[234], suggesting the necessity of further studies on the role of female sex hormones in MS.

Studies in EAE suggest a protective role of androgens on disease activity since castration of male SJL mice increased disease severity, whereas androgen supplementation protected against EAE[235,236]. The same studies attribute a possible disease protection to ovariectomy, if removal of ovaries is performed prior to pubertal onset. Functionally, protective mechanisms involving ERα in peripheral immune cells[237] as well as ERβ in oligodendrocytes and myeloid DCs within the CNS[238] have been described. More recently, the protective effect of androgens has been investigated. In SJL mice, mast cells produce IL-33 in response to testosterone leading to a protective phenotype in EAE by shifting the T cell response to a less pathogenic Th2 myelin-specific response[101].

1.2.3.3 Role of sex chromosomes

While it is generally not possible to study the genetic status independently of sex hormones in humans, studies in people with sex chromosome disorders show an increased risk of autoimmune diseases like SLE and MS in men with Klinefelter's syndrome (XXY) and an underrepresentation of women with Turner's syndrome (45,X) among SLE patients[239,240]. To examine the effect of sex chromosomes independently of hormones, the Four Core Genotype (FCG) mice were established[241,242]. Here, the sex determining region of the Y *(Sry)*, responsible for testis formation, was deleted from the Y chromosome and transferred as a transgene to an autosome. Consequently, the Y chromosome is no longer responsible for testis formation and mice lacking the *Sry* develop ovaries. This results in two types of male (with sex determined by gonadal type), XY$^-$*Sry* and XX*Sry*, and two types of female, XY$^-$ and XX allowing to assess the effects of sex chromosomes in mice with either ovarian or testicular hormones[243]. Mice with XX sex chromosome background demonstrated a more proinflammatory phenotype and greater susceptibility to EAE and lupus compared with XY mice[244], indicating that X-chromosomal encoded genes show an independent risk of hormonal regulation. Moreover, CD4$^+$ T cells isolated from XX FCG mice had higher levels of the X-linked gene *Utx* compared to XY FCG mice independent of their gonadal status showing that elevated expression in female mice at baseline is not regulated by sex hormone, but chromosomal composition.[152,245]. Deletion of *Kdm6a* in T cells ameliorated disease course and reduced neuropathology in EAE, while being associated with upregulation of Th2 and Th1 activation pathways.

1.2.3.4 Mechanistic contribution of immune cells

Mechanistic studies providing insight into immune processes contributing to sex differences in CNS autoimmunity mostly focused on CD4$^+$ T cells, since such studies in humans remain challenging and thus EAE as a CD4$^+$ T cell driven disease serves as a substitute. Sexual disparity in EAE and MS may result from differences in priming of T cells, their interaction with APCs and functional capacities, their trafficking to the CNS as well as the contribution of other immune cell subsets[206].

As already mentioned above, AIRE in mTECs is increased in males and induced by androgens and suppressed by estradiol suggesting a more efficient negative T cell selection in males[202,203]. Specifically, in EAE, the female preponderance and the suppressive effect of androgens were not observed in Aire-deficient mice[203,206]. After EAE induction, myelin-loaded APCs traffic to peripheral lymphoid organs and foster CD4$^+$ Th cell differentiation with female Th cells more prone towards Th1 cells, while male cells are more skewed towards Th2 or Th17 cells[101,206]. This female bias in Th1 responses implicates differences in IFNγ production, which is additionally regulated by sex hormones itself. Androgens increased the expression of the peroxisome proliferator activated receptor (PPAR)α, which is

correlated with decreased IFNγ production in SJL mice[184] and testosterone levels are inversly associated with production of Th1 cytokines in SJL EAE[246]. In contrast, low dosis of estradiol supplementation to ovariectomized mice increased Th1 cell responsiveness and development of IFNγ producing cells, which was attributed to ERα but not ERβ[247]. While this could be mediated by indirect pathways, a direct effect of estradiol on the *Ifng* promoter could be shown as estradiol enhances its activity[248].

After peripheral activation, myelin-specific cells traffick to the CNS through a partially disrupted BBB, which is formed by endothelial cells of microvessels connected by tight junction proteins[206]. More Gd-enhancing lesions in female MS patients indicate a less intact BBB compared to males[214], which might relate to increased myelin-specific Th1 cell expansion in females seen in recall assays, where Th1 cells from immunized mice are challenged with the same antigen *in vitro*[249]. Moreover, several proteins known to be involved in BBB transmigration show higher expression in females. For instance, matrix metalloproteinase (MMP)-9, which participates in BBB degradation was shown to be elevated in the CSF of female RRMS patients[250]. In mice, female and castrated male MBP-primed T cells exhibited both subunits (α_4 and β_1) of very late antigen-4 (VLA-4), a key player of BBB trafficking and target of natalizumab, whereas β_1 was absent in males, which could be directly mediated through androgens[251].

Once in the CNS, interaction of invading T cells with microglia play an important role. However, there is currently not much known about sex-specific involvement of microglia in MS or EAE. No sex differences in terms of macrophages/microglia density were found in post-mortem tissue[252] and further human studies on that topic remain sparse. In EAE, MBP-primed T cells from female and castrated male mice but not from male mice enhanced expression of neurotoxic inducible nitric-oxide synthase (iNOS) and proinflammatory molecules, such as IL-1α, IL-1β, IL-6 and TNFα in microglia by cell-cell contact[253]. Further implementations can be derived from general profiling studies or studies in other neurodegenerative diseases. Gene expression analysis demonstrated a higher type I IFN signature of female microglia[254] and a higher metabolic activity in aged WT and APP/PS1 transgenic mice (Alzheimer's mouse model)[255], whereas male microglia tend to be more reactive to LPS treatment *in vitro*[256].

With $CD4^+$ T cells being the best characterized cells in EAE and MS, data on sex-specific mechanisms of other immune cells contributing to CNS neuroinflammation remains limited and partially inconclusive. Male $CD8^+$ T cells from MS patients display higher degrees of TCR variable beta chain (TCRBV) pertubation shaped by a distinct MHC-I repertoire and concerted selection and expansion seem to be less dependent on high HLA-binding similarity[257]. This suggests a more pronounced expansion of low-avidity T cell clones and epitope spreading in males and might be interpreted to contribute to a higher disease burden in males[257]. Along this line, post-mortem studies in MS observed more chronic-active

lesions[215], which are characterized by $CD8^+$ T cell persistence possibly indicating a contribution of these smouldering lesions to a more rapid progression in male MS patients[206]. Moreover, male mice are more susceptible to TMEV-induced demyelination correlating with weaker immune response and chronic viral persistence[258,259].

The expansion and activity of T_{regs} in EAE and MS might be more pronounced in females as indicated by a higher frequency of $CD4^+$ T_{regs} in the CSF of female MS patients compared to males[260] and a higher association of T_{reg} function or differentiation gene signature in female TCR^{1640} cells, which induce a remitting disease course only in female mice[226]. While these findings seem counterintuitive first, since T_{regs} are generally considered to confer protecitve effects in MS and EAE, increased T_{reg} function can also be interpreted as a measure of increased inflammatory processes in females as they are needed in higher numbers to restrict ongoing inflammation. In contrast, IL-10 production has been demonstrated to be protective in EAE[261] and male myelin-specific T cells secrete higher levels of IL-10[262] and treatment of SJL mice with 5-α dihydrotestosterone (DHT) increases IL-10 production of $CD4^+$ T cells upon TCR stimulation[206,263].

With $CD11b^-CD11c^+$ cDCs (DC1) being most efficient at priming $CD8^+$ T cells in the draining lymph nodes and myelin-reactive Th cells in the CNS and $CD11b^+CD11c^+$ cDCs (DC2) being effective in priming Th cells in peripheral lymphoid organs[206], sex-intrinsic differences of DCs would pose a major contributor to sex disparity in MS. However, no sex differences in the composition of DCs were found in the peripheral blood of MS patients[264] once again showing limitations of tissue access in human MS studies. Splenic DCs or macrophages from female SJL mice are more capable in priming myelin-specific $CD4^+$ T cells *in vitro*[265] and when in a co-culture of both cell types, female DCs induce IFNγ production more efficiently, which also correlated with IL-12p40 levels[184,206]. Additionally, IL-12 was decreased in the draining lymph nodes from male mice during EAE compared to females[249] and it was found at higher levels in the serum of female MS patients[266]. 17-beta estradiol (E2) has been demonstrated to facilitate differentiation of bone marrow progenitors into $CD11b^+CD11c^+MHCII^+$ DCs, enhance expression of co-stimulatory molecules (CD40 and CD86) and IL-12p40 secretion in response to TLR ligands CpG and LPS[267].

Very little is known about sex-specific regulation of NK cells in MS pathogensis with only one study assessing NK and NKT cell frequencies in peripheral blood of female and male MS patients[268]. No differences were found between MS women and men in total NK and NKT cells, but female MS patients display an increased frequency of $CD56^{bright}$ NK cells compared to healthy females, while a more activated state of $CD56^{low}$ NK cells and NKT cells was observed in male MS patients compared to healthy counterparts[206,268].

Similar to NK cells, the data on sex differences of B cell in the context of MS is even more scarce. In MS, oligoclonal bands are less likely to be detected in male patients[269] with humoral responses and development of autoantibodies generally more pronounced in females[206].

Taken together, a large body of evidence indicates an increased expansion of Th1 cells in female MS patients and mice, while males are more skewed towards a Th2 immune response and increased IL-10 production. Female DCs seem to be more efficient in $CD4^+$ T cell priming, which leads to an increased probability of female T cells trafficking to the CNS by enhanced expression of VLA-4 accompanied by increased MMP-9 levels in the CSF implying a more desintegrated BBB. In the CNS, female microglia display an elevated metabolic activity as well as increased capability of secreting proinflammatory cytokines, whereas male MS patients exhibit more chronic-active lesions with $CD8^+$ T cell persistence (**Figure 1.3**). However, the contribution of other immune cells and their detailed mechanisms require further investigations as many observations remain elusive showing the necessity for further in-depth characterization.

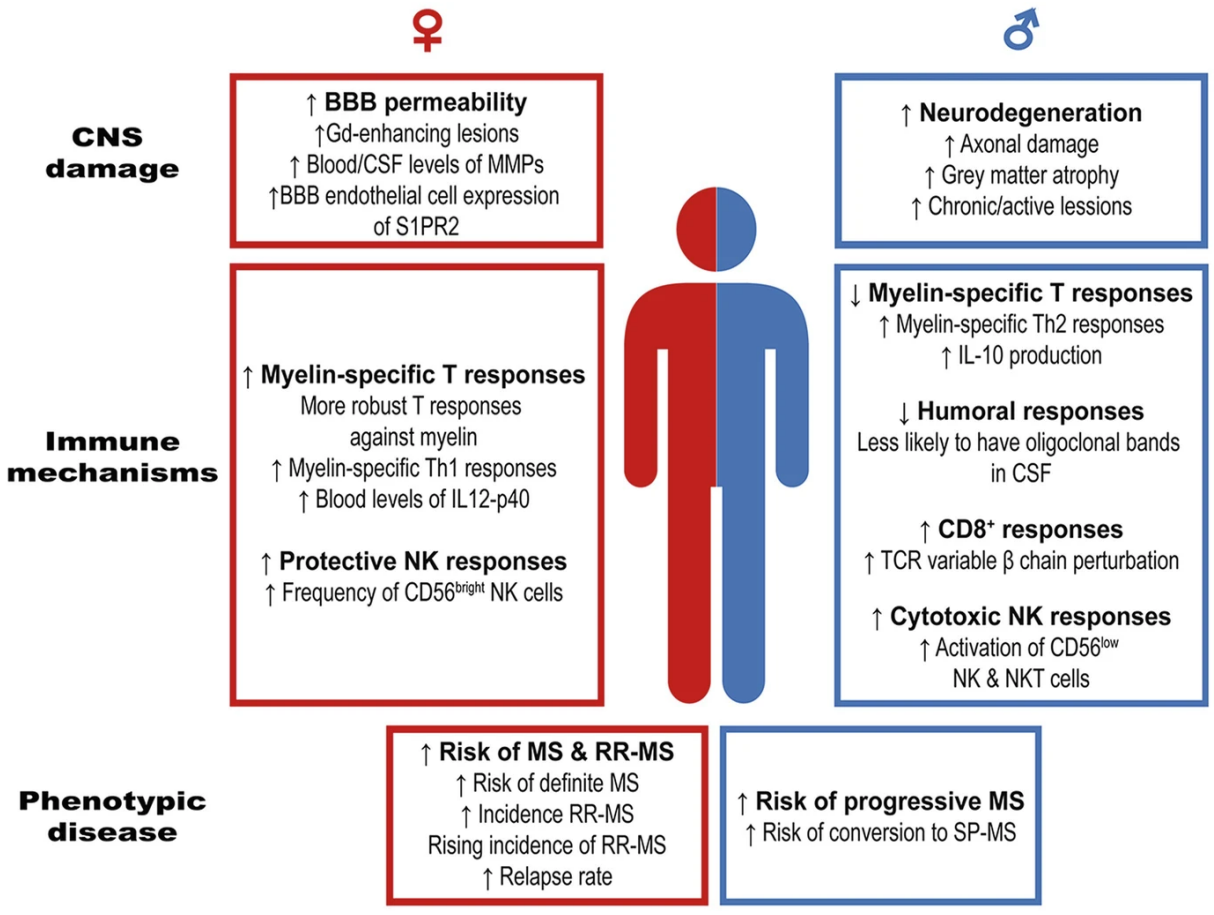

Figure 1.3: Overview of mechanisms driving sexual disparity in MS. Mechanisms peripheral immune responses and CNS autoimmunity including neurodegenerative processes are considered as distinct processes resulting in disparate clinical outcomes in women and men. *Figure from Alvarez-Sanchez N et al. Immune Cell Contributors to the Female Sex Bias in Multiple Sclerosis and Experimental Autoimmune Encephalomyelitis. Curr Top Behav Neurosci. 2023;62:333-373[206].*

1.2.3.5 Disability progression

While the majority of these findings points towards more pronounced immune responses and hence female preponderance in MS incidence and disease activity, some of these results indicate stronger inflammatory processes in males and appear counterintuitive at first sight. However, they might explain faster disability progression in male MS patients as it is hypothesized that sex-related factors play different roles in the immune system versus the CNS[205]. Regional differences in substructure volumes between healthy women and men can be detected already at steady state[270], but also in other neurodegenerative diseases like Parkinson's disease (PD)[271], which occurrs more often in men as well as in Alzheimer's disease (AD), which presents female dominant[272]. Similar to its importance in immunity, the X chromosome possesses a key role in brain development as X chromosomal genes are expressed more than from any autosome as also indicated by a wide array of X-linked deficits in brain development[205]. Also here, the FCG model was used to study CNS-intrinsic response to injury and it was found that EAE mice with an XY background demonstrated greater clinical severity and increased neuropathology in the CNS than mice with XX background[244,273]. In terms of sex hormones, recent findings indicate a neuroprotective effect of estriol, a hormone produced by the fetoplacental unit, when applied after disease onset in EAE[274]. This decreased cerebral cortex atrophy was associated with an increased cholesterol synthesis proteins in oligodendrocytes and more newly formed remyleinating oligodendrocytes as well as with a reduced loss of cortical layer V neurons[274]. While the rationale for estriol rather arises from a protective effect of pregnancy in MS, a selective deletion of ERβ in astrocytes in gonadally intact female mid-aged mice induced cognitive impairment as well as astrocyte and microglia activation with synaptic loss, which was also accompanied by metabolic changes in gluconeogensis and glycolysis[275]. Further mechanistic pathways involve a more pronounced microglia activation at the rim of white matter lesions possibly arising from local T cell presence, increased astrocytic activation and iron release from oligodendrocytes in males as well as a greater susceptibility of male neurons towards oxidative and nitrosative stress[276].

1.3 The surface protein CD99

T cell infiltration from the periphery across the BBB promotes inflammation, demyelination and neurodegeneration leading to lesions in the CNS, which are hallmarks of MS[4]. The cell surface receptor CD99 has been suggested to be important in transmigration of immune cells through endothelial layers including the BBB[277-279]. The 32-kDa transmembrane protein CD99 is broadly expressed in many human cell types including leukocytes and endothelial cells[277,280]. It is mostly described in the context of cancer research being overexpressed and regulated in several tumors[281]. In Ewing sarcoma (EWS) CD99 serves as a diagnostic marker[282,283] and functionally regulates tumor cell growth and survival, which can be

targeted by an anti-CD99 monoclonal antibody (mAb) *in vitro*[284]. More recently, CD99 has been analyzed and discussed as a potential therapeutic target in hematological malignancies such as acute myeloid leukemia (AML) and T-lineage acute lymphoblastic leukemia (T-ALL), but it is also described in the context of osteosarcoma, breast cancer and malignant gliomas along other tumors[285]. Aside from its role in malignancies, CD99 has mostly been characterized in regard to leukocyte diapedesis and T cell regulation.

1.3.1 CD99 in immune cell transmigration

CD99 involvement in T cell transmigration has been extensively studied[286-288]. Human CD99-specific antibodies blocked monocyte migration through endothelial monolayers[277] and mouse CD99-specific antibodies inhibited lymphocyte entry into the inflamed skin[289] as well as neutrophil recruitment into the inflamed peritoneum[290]. Additionally, blocking CD99 lead to neutrophil accumulation between endothelial cells with most cells trapped between the basement membrane[291]. Furthermore, by using human stem cell-derived *in vitro* models, it has been shown that CD99 mediates the migration of human $CD4^+$ T cells across the BBB endothelium[292] and is possibly also used by different human $CD4^+$ T cells when crossing the epithelial blood-cerebrospinal fluid barrier (BCSFB) of the choroid plexus (ChP)[293]. Diapedesis can be seen as a multistep process, in which platelet endothelial cell adhesion molecule 1 (PECAM1) and CD99 act sequentially. Blockade of CD99 by a specific antibody resulted in accumulation of leukocytes partly entering the endothelial layer, while blockade of PECAM1 stopped leukocytes apically of endothelial cells[286].

During transendothelial migration homophilic engagement of endothelial and leukocyte CD99 activates protein kinase A (PKA) via its juxtamembrane cytoplasmic tail and the A-kinase anchoring protein ezrin and soluble adenylyl cyclase (sAC), thereby elevating cAMP levels[291]. PKA in turn stimulates membrane trafficking from the lateral border recycling compartment (LBRC) to the sites of transendothelial migration promoting leukocyte diapedesis. In a different study, it has been shown that binding of growth and differentiation factor 6 (GDF6) to the CD99 extracellular domain results in recruitment of C-terminal Src kinase (CSK) inhibiting Src activity[294]. However, parts of the signaling cascade and its implication in leukocytes is still unknown.

1.3.2 CD99 in T cell regulation

CD99 association with T cell regulation and a potential role as co-stimulatory factor in T cell activation has been substantial subject of investigation[287]. Engagement of CD99 with an agonistic antibody enhanced the expression of several T cell activation markers on anti-CD3-stimulated T cells and

induced the elevation of intracellular calcium and tyrosine phosphorylation of cellular proteins[295] as well as translocation of TCR complexes to lipid rafts[296] and the necessity of CD99 for the effect of IFNγ on HLA class I expression[297]. More recent data showed that anti-CD99 mAb MT99/3 downregulated the expression of CD86, but upregulated IL-6, IL-10 and TNFα production by monocytes and that cell to cell contact between monocytes and lymphocytes is required for that mechanism[298]. The same group showed that recombinant CD99 proteins induced the upregulation of IL-6 and TNFα, but not IFNγ in anti-CD3 activated T cells and that cytokine upregulation was not observed in unstimulated T cells[299]. However, recombinant CD99 did not affect upregulation of T cell activation marker like CD25, CD69 or MHC II or T cell proliferation upon T cell activation. Whether its own upregulation or the upregulation of T cell activation markers or cytokine expression is differentially regulated between the sexes requires more investigation and is subject of this thesis.

1.3.3 CD99 ligands

The homophilic interaction of CD99 has been demonstrated by using CD99 transfected cells, which only bound to other CD99 transfectants but not to control transfectants[277]. However, the existence of other CD99 ligands has always been proposed. In a recent study, it has been shown, that the inhibitory effect of the mAb clone MT99/3 on T cell activation requires cell-to-cell contact between monocytes and T cells as soluble mediators are insufficient to induce hypo-responsiveness[298]. In a follow-up study, the same group used recombinant CD99 protein to determine the role of CD99 and its ligand interaction and showed that the so far undescribed ligands are expressed on monocytes, NK cells and DCs, but not on T and B cells and that interaction between CD99 and its ligand modifies the production of IL-6 and TNFα[299]. Furthermore, recombinant CD99 was used in a pulldown-assay to identify CD99 ligand candidates via LC-MS/MS in several hematopoietic cell lines including monocytic THP-1 cells[300]. Another group demonstrated that the GDF6 prodomain is a ligand for CD99 and maintains ES growth[294]. Moreover, another study investigating mouse CD99 showed that only CD99 on endothelial cells, but not on neutrophils participates in neutrophil extravasation[301]. Therefore, the authors searched for heterophilic ligands of endothelial CD99 on neutrophils and found that endothelial cells bind to the paired immunoglobulinlike receptors (PILRs) in a strictly CD99-dependent way. This finding was specified by the same group showing that binding of CD99 to PILR-β1 lead to neutrophil attachment to the endothelium[302].

1.3.4 Sex-specific CD99 regulation

CD99 is encoded by the gene *MIC2*, which is located at the very edge of the pseudoautosomal region (PAR) 1 of the X and Y chromosome. This region is known to escape XCI, which also applies for *CD99*[193,303]. However, this escape might not always happen to a full extent across all tissues leading to a differential expression in females and males[193,304]. Allelic expression form the Xi is reduced compared to expression from the activated X chromosome (Xa)[193,303] likely due to its embedding within the silenced chromatin structure surrounding the Xi resulting from its proximity to *XIST*[305]. Consequently, males display an increased *CD99* expression as it is transcribed from the X and Y chromosome[193,303]. Moreover, mosaic LOY in leukocytes, which happens in at least 10% of the peripheral blood cells in 10-40% of 60-80 year old men, is associated with reduced CD99 surface expression in immune cells[306]. Accordingly, individuals with Turner syndrome (45,X), a unique sex chromosome aneuploidy, show a decreased *CD99* expression compared to euploidic females (46,XX) and males (46,XY)[307,308].

1.4 Aim of the study

GWAS in MS have only focused on autosomal chromosomes and their contribution to MS susceptibility. Although recent GWAS partially included analysis of sex chromosomes, no protein-coding X- or Y-linked risk variants were detected[12,309]. This was possibly due to exclusion of SNPs from the X and Y chromosome as they did not pass quality control criteria with limited statistical power for both sex chromosomes. Having these limitations in mind, together with the observation that genetic variation accounts for approximately 30% of the overall disease risk[310], we hypothesized that there are undetected gene expression differences between women and men that could explain part of the sexual disparity in incidence of MS and other autoimmune diseases. Our findings identified CD99 as a protein with sexually dimorphic expression in humans. The overarching aim of this study was to understand whether and how CD99 contributes to sex-specific differences in autoimmunity with MS as a prototypic disease.

To achieve this, the following aims were addressed:

1. Identifying human candidate genes with sexually dimorphic expression pattern in immune cells.
2. Deciphering drivers of sex-specific CD99 expression on epigenetic, genetic and hormonal level.
3. Profiling of functional relevance of differential CD99 surface expression on T cells of women and men.
4. Translating findings into a mouse model of neuroinflammation.
5. Identifying CD99 ligands, downstream signaling pathways and their sex-specific modulation.

2 Material & methods

2.1 Material

2.1.1 Study cohorts

MS patients, NND patients and healthy individuals were recruited through the MS day clinic and the Department of Neurology, University Medical Center Hamburg-Eppendorf (UKE). The study was approved by the local ethics committee (Hamburger Patienteninformationssystem Multiple Sklerose – HAPIMS, Ethikkommission der Ärztekammer Hamburg, registration number PV4405) and informed consent was obtained from all patients and healthy individuals. These patients were not on any immunomodulatory medication at the time of sampling. Cryopreserved samples were collected in the biobank of the UKE Institute of Neuroimmunology and Multiple Sclerosis (INIMS). Trans men were recruited through the medical practice amedes Medizinisches Versorgungszentrum Hamburg GmbH. The study was approved by the local ethics committee (Ethikkommission der Ärztekammer Hamburg, registration number PV5245) and informed consent was obtained from all individuals. Cryopreserved samples were collected at the Research Department Virus Immunology, Leibniz Institute of Virology, Hamburg. Study participants were screened for chronic infections, autoimmune and metabolic diseases and cancers by medical history and blood tests. Participants received 1000 mg testosterone undecanoate i.m. (Nebido, Jenapharm) injections. After the first testosterone injection, the second injection was scheduled 6 weeks later, followed by a steady rhythm of 3 months. Further characteristics of the cohorts are detailed in **Table 2.1, Table 2.2 and Table 2.3**.

Table 2.1: Characteristics of MS patients and healthy individuals included in CD99 surface expression analysis of PBMCs.

	n	**% female**	**Age (years)**	**Disease duration (years)**	**Median EDSS[1] ± IQR**
RRMS[2]	60	50	33.3 ± 9.8	5.1 ± 5.7	1.5 ± 2.0
HI[3]	60	50	33.0 ± 9.7	NA[4]	NA

[1]Expanded disability status scale; [2]Relapsing remitting MS; [3]Healthy individuals; [4]Not applicable. Data are presented as mean ± SD unless otherwise indicated.

Table 2.2: Characteristics of MS patients and non-neuroinflammatory disease patients included in CD99 surface expression analysis of blood and CSF samples.

	n	**% female**	**Age (years)**	**Disease duration (years)**	**Median EDSS[1] ± IQR**
RRMS[2]	33	73%	33.8 ± 9.8	1.6 ± 2.4	1.5 ± 1.0
NND[3]	16	69%	41.3 ± 13.2	NA[4]	NA

[1]Expanded disability status scale; [2]Relapsing remitting MS; [3]Non-neuroinflammatory disease patients; [4]Not applicable. Data are presented as mean ± SD unless otherwise indicated.

Table 2.3: Characteristics of healthy individuals included in CD99 surface expression analysis of PBMCs in trans men cohort.

n	Mean age of treatment start (years)	Median injection date TP1[1] (months)	Median injection date TP2 (months)	Treatment
5	23.3 ± 2.9	6.7 ± 0.4	11.9 ± 0.7	1000 mg testosterone undecanoate i.m.

[1]Time point. Data are presented as mean ± SD unless otherwise indicated.

2.1.2 Mice

C57BL/6 WT and C57BL/6-CD99$^{em2\text{-}8/Hhtg}$ (*Cd99*$^{-/-}$) were kept under specific pathogen-free conditions in the animal facility of the ZMNH, University Medical Centre Hamburg-Eppendorf. 8–12-week-old mice were used for experiments. All animal experimental procedures were in accordance to international and national animal welfare guidelines. Ethical approvals were obtained from the State Authority of Hamburg, Germany (approval no. 083/19 and 107/21).

2.1.3 Antibodies

Table 2.4: Primary antibodies used for flow cytometry.

Antigen	Clone	Supplier
PBMC cohort		
CD4	RPA-T4	BioLegend
CD161	HP-3G10	BioLegend
CD45RA	HI 100	BioLegend
CD8a	HIT8a	BioLegend
CD197 (CCR7)	G043H7	BioLegend
CD3	OKT3	BioLegend
Anti-Human Lineage (CD3,CD14,CD19,CD20,CD56)	UCHT1, HCD14, HIB19, 2H7, HCD56	BioLegend
CD11c	3.9	BioLegend
CD16	3G8	BioLegend
CD304	12C2	BioLegend
CD123	6H6	BioLegend
HLA-DR	G46-6	BD Bioscience
CD45	HI30	BioLegend
CD56	B159	BD Bioscience
CD19	SJ25C1	BioLegend

CD14	HCD14	BioLegend
CD20	2H7	BD Bioscience
CD99	HCD99	BioLegend

CSF cohort		
CD4	RPA-T4	BioLegend
CD161	HP-3G10	BioLegend
CD45RA	HI 100	BioLegend
CD8a	HIT8a	BioLegend
CD197 (CCR7)	G043H7	BioLegend
CD3	OKT3	BioLegend
CD99	HCD99	BioLegend

CD99 dynamics		
CD3	SK7	BD Bioscience
CD8	RPA-T8	BD Bioscience
CD4	SK3	BD Bioscience
CD69	FN50	BioLegend
CD99	3B2/TA8	BioLegend
CD45RA	HI100	BioLegend

***in vitro* testosterone**		
CD3	SK7	BD Bioscience
CD8	RPA-T8	BD Bioscience
CD4	SK3	BD Bioscience
CD69	FN50	BioLegend
CD99	3B2/TA8	BioLegend
CD45RA	HI100	BioLegend

Trans men cohort		
CD3	SK7	BD Bioscience
CD8	RPA-T8	BD Bioscience
CD4	SK3	BD Bioscience
CD161	DX12	BD Bioscience
MR1 tetramer		NIH

CCR7	G043H7	BioLegend
CD99	3B2/TA8	BioLegend
CD45RA	HI100	BioLegend
CD16	3G8	BD Bioscience
HLA-DR	G46-6	BD Bioscience
CD11c	B-ly6	BD Bioscience
CD14	HCD14	BioLegend
CD20	2H7	BioLegend
CD19	SJ25C1	BioLegend
CD56	HCD56	BioLegend
CD123	6H6	BioLegend
CD45	HI30	BioLegend

CD99 expression in C57BL/6		
CD11b	M1/70	BD Bioscience
TCRb	H57-597	BD Bioscience
MHC II	M5/114.15.2	BioLegend
CD19	6D5	BioLegend
CD4	GK1.5	BioLegend
CD8a	53-6.7	BioLegend
CD45	30-F11	BioLegend
NK1.1	PK136	BioLegend
CD11c	N418	BioLegend
CD317	927	BioLegend
Ly-6G	1A8	BioLegend
CD99	polyclonal	R&D systems

***CD99*-deficient mouse validation**		
CD11b	M1/70	BD Bioscience
B220	RA3-6B2	BD Bioscience
TCRb	H57-597	BD Bioscience
TCRgd	GL3	BD Bioscience
CD4	GK1.5	BioLegend
CD8	53-6.7	BioLegend
CD44	IM7	BioLegend

CD45	30-F11	BioLegend
CD99	polyclonal	R&D systems

Mouse CFSE proliferation		
CD4	GK1.5	BD Bioscience
TCRb	H57-597	BD Bioscience
CD8a	53-6.7	BioLegend
CD44	IM7	BioLegend

EAE infiltration day 30		
CD11b	M1/70	BD Bioscience
CD19	1D3	BD Bioscience
TCRb	H57-597	BD Bioscience
MHC II	M5/114.15.2	BD Bioscience
F4/80	BM8	BioLegend
NK1.1	PK136	BD Bioscience
CD8a	53-6.7	BioLegend
CD45	30-F11	BioLegend
Ly6G	1A8	BioLegend
CD11c	N418	BioLegend
CD317	927	BioLegend
CD99	polyclonal	R&D systems

EAE infiltration day 15		
CD11b	M1/70	BD Bioscience
CD19	1D3	BD Bioscience
TCRb	H57-597	BD Bioscience
MHC II	M5/114.15.2	BD Bioscience
F4/80	BM8	BioLegend
NK1.1	PK136	BD Bioscience
CD8a	53-6.7	BioLegend
CD45	30-F11	BioLegend
Ly6G	1A8	BioLegend
CD11c	N418	BioLegend
CD317	927	BioLegend

TCRgd	GL3	BD Bioscience
PD-1/CD279	29F.1A12	BioLegend
CD103	2E7	BioLegend
CD44	IM7	BioLegend
CD69	H1.2F3	BioLegend
CD4	GK1.5	BioLegend
CD99	polyclonal	R&D systems

***Cd99*$^{-/-}$ mice adhesion molecules**		
CD11b	M1/70	BD Bioscience
CD19	1D3	BD Bioscience
TCRb	H57-597	BD Bioscience
CD99l2	polyclonal	R&D systems
CD8a	53-6.7	BioLegend
CD11a	M17/4	BioLegend
CD44	IM7	BioLegend
CD99	polyclonal	R&D systems
CD29	HMb1-1	BioLegend
CD49d	R1-2	BioLegend
CD45	30-F11	BioLegend

2.1.4 Primer, oligonucleotides and plasmids

Table 2.5: Primer for mouse genotyping.

Abbreviation	Name	Full sequence
Cd99_mut_for	CD99-F1-4A2C	CCTCAGCGAGTGACGACTTCAAAACC
Cd99_wt_for	CD99-F1-2A2C	CCTCAGCGAGTGACGACTTCAACC
Cd99_rev	CD99-591-rev	CCCAGAGCCCCGGGTATGTAAATGACTC
Cd99_ctrl_for	MK-F4	GTCCATTGCAAGGTGCCCTGCAACTG
Cd99_ctrl_rev	MK-rev5	CCTTCCTCAGTTGACAAAGACAAGCCTTTC

Table 2.6: Primer, oligonucleotides and restriction sites used for the generation of CD99 vectors.

Abbreviation	Name	Full sequence
Primer_f_1	for_hsCD99_BamHI	TAGGGATCCGATGGTGGTTTCGATTTATCCGATG
Primer_r_1	rev_hsCD99_XbaI	TAGTCTAGATTTCTCTAAAAGAGTACGCTGAACAGC
Oligo_f_1	LCv2-hsCD99-sgRNA01_FWD	CACCGCGGCGACCAGAACACCCAGC
Oligo_r_1	LCv2-hsCD99-sgRNA01_REV	aaacGCTGGGTGTTCTGGTCGCCGC
Oligo_f_2	LCv2-hsCD99-sgRNA02_FWD	CACCGATCCCCAAGAAACCCAGTGC
Oligo_r_2	LCv2-hsCD99-sgRNA02_REV	aaacGCACTGGGTTTCTTGGGGATC
Oligo_f_3	LCv2-hsCD99-sgRNA03_FWD	CACCGAAAGTCATCCCCTAAAAGAG
Oligo_r_3	LCv2-hsCD99-sgRNA03_REV	aaacCTCTTTTAGGGGATGACTTTC
Oligo_f_4	LCv2-hsCD99-sgRNA04_FWD	CACCGCACCTGAAACGCCATCCGCA
Oligo_r_4	LCv2-hsCD99-sgRNA04_REV	aaacTGCGGATGGCGTTTCAGGTGC
Primer_f_2	97_for_hsCD99_AgeI	TAGACCGGTATGGCCCGCGGGGCTGC
Primer_r_2	98_rev_hsCD99_BsiWI	TAGCGTACGTTTCTCTAAAAGAGTACGCTGAACAGC
Primer_f_3	96_for_hsCD99_BamHI	TAGGGATCCGATGGTGGTTTCGATTTATCTGATGC
Primer_r_3	90_rev_hsCD99_XbaI	TAGTCTAGATTTCTCTAAAAGAGTACGCTGAACAGC
Primer_f_4	S011_Seq_CMV_promoter_FWD	CGCAAATGGGCGGTAGGCGTG
Primer_r_4	P001_Frag1_Rec-PCR_FKBP[-BshTI]-rev	TTCGAGCATACCcGTGTAGTGCA
Primer_f_5	P002_Frag2_Rec-PCR_FKBP[-BshTI]-for	TGCACTACACgGGTATGCTCGAA
Primer_r_5	S01_CD99-rev	GGTTTGGGTGGGTTCGGTGGTC
CD99-SP-for	O01_CD99-SP-FLAG-for	CCGGTATGGCCCGCGGGGCTGCGCTGGCGCTGCTGCTCTTCGGCCTGCTGGGTGTTCTGGTCGCCGCCCCGGACTACAAAGACGATGACGACAAGC
CD99-SP-rev	O02_CD99-SP-FLAG-rev	GTACGCTTGTCGTCATCGTCTTTGTAGTCCGGGGCGGCGACCAGAACACCCAGCAGGCCGAAGAGCAGCAGCGCCAGCGCAGCCCCGCGGGCCATA

Table 2.7: Plasmids.

Name	RRID	Origin
Lenti-Cas9-gRNA-GFP	Addgene_124770	Jason Sheltzer
pEF6a-CD28-PafA	Addgene_113400	Min Zhuang
pEF6a-FKBP-CD28	Addgene_113401	Min Zhuang
pLVX-TRE3G-BCCP-PupE-IRES-BFP	Addgene_113405	Min Zhuang
pGEX6p-1-BCCP-PupE	Addgene_113403	Min Zhuang
pGEX6p-1-FRB-PafA	Addgene_113404	Min Zhuang
pMDLg/pRRE	Addgene_12251	Didier Trono
pRSV-Rev	Addgene_12253	Didier Trono
pMD2.G	Addgene_12259	Didier Trono

2.1.5 Chemicals and reagents

Table 2.8: Reagents for mouse genotyping.

Reagent	Supplier
Agarose Ultra Pure	Merck
ddH_2O	Generated in house
dNTP Mix (10 mM)	Thermo Fisher Scientific
DreamTaq Green Hot Start Buffer 10x	Thermo Fisher Scientific
DreamTaq Hot Start Green DNA Polymerase	Thermo Fisher Scientific
GeneRuler 1 kb DNA Ladder	Thermo Fisher Scientific
Genotyping master mix (2x)	Thermo Fisher Scientific
QuickExtract DNA Extraction Solution	Lucigen
RotiSafe	Carl Roth

Table 2.9: Reagents for animal experiments.

Reagent	Supplier
CO_2/O_2 gas	SOL Deutschland
DietGel Recovery	Clear H_2O
Incomplete Freund‘s adjuvant	BD Bioscience
MOG_{35-55} peptide	Peptides & elephants
Mycobacterium tuberculosis	BD Bioscience
Pertussis toxin (*Bordetella pertussis*)	Merck

Table 2.10: Reagents for cell culture.

Reagent	Supplier
5α-dihydrotestosterone (DHT)	Sigma-Aldrich
Biocoll Separating Solution	Biochrom
CellTrace™ CFSE Cell Proliferation Kit	ThermoFisher
CellTrace™ Violet Cell Proliferation Kit	ThermoFisher
Collagenase I	Sigma-Aldrich
Dextran-coated charcoal (DCC)	Merck
Dimethyl sulfoxide (DMSO)	AppliChem
DMEM with glutamine and high glucose	Thermo Fisher Scientific
DNase I	Merck
EDTA	ThermoFisher Scientific
Heat-inactivated fetal calf serum (FCS)	Biochrom
Human Pan T Cell Isolation Kit	Miltenyi Biotec
Human Ultra-LEAF Purified anti-CD3 (clone OKT3)	BioLegend
Human Ultra-LEAF Purified anti-CD28 (clone CD28.2)	BioLegend
Human Purified anti-CD99 (clone hec2)	BioLegend
Human Purified anti-CD99 (clone HCD99)	BioLegend
Lipofectamine 2000	Thermo Fisher Scientific
MojoSort™ Mouse CD3 T Cell Isolation Kit	BioLegend
Mouse Ultra-LEAF Purified anti-CD3 (Clone 145-2C11)	BioLegend
Mouse Ultra-LEAF Purified anti-CD28 (Clone 37.51)	BioLegend
PBS (1x and 10x)	Pan-Biotech
Percoll (1.13 g/ml)	GE Healthcare
Polybrene	Sigma-Aldrich
Purified Mouse IgG1, κ Isotype Ctrl Antibody (clone MOPC-21)	BioLegend
Purified Mouse IgG2a, κ Isotype Ctrl Antibody (clone MOPC-173)	BioLegend
Recombinant mouse IL-2	Peprotech
Testosterone	Sigma-Aldrich
Trypanblue solution	Sigma-Aldrich

Table 2.11: Reagents for flow cytometry and cell sorting.

Reagent	Supplier
BD CompBeads (Anti-rant and anti-hamster Ig κ/ negative control compensation particles set)	BD Bioscience

BD Cytofix (fixation buffer)	BD Bioscience
BD FACS Clean Solution	BD Bioscience
BD FACSDIVA CS&T Research beads	BD Bioscience
BD FACS Flow	BD Bioscience
BD FACS Lysing Solution	BD Bioscience
BD FACS Rinse Solution	BD Bioscience
BD Fixable Viability Stain 700	BD Bioscience
Brilliant Stain Buffer	BD Bioscience
Ethanol absolute	Th. Geyer
Fetal calf serum (FCS)	Merck
Fixable Aqua Dead Cell Stain Kit	Invitrogen (Thermo Fisher Scientific)
Fixation Buffer	BioLegend
Precision Count Beads™	BioLegend
Propidium Iodide	BioLegend
Streptavidin, R-phycoerythrin-conjugate (SAPE)	Invitrogen (Thermo Fisher Scientific)
TruStain FcX (anti-mouse CD16/32) antibody	BioLegend
UltraComp eBeads (compensation beads)	Invitrogen (Thermo Fisher Scientific)
V500 live/dead stain	Thermo Fisher Scientific

Table 2.12: Reagents for vector cloning.

Reagent	**Supplier**
5X Q5 Reaction buffer	New England BioLabs
10X FastDigest Buffer	Thermo Fisher Scientific
Ampicillin	Carl Roth
ddH_20	Generated in house
dNTP Mix (10 mM)	Thermo Fisher Scientific
FastDigest Restriction Enzymes	Thermo Fisher Scientific
Q5 High-Fidelity DNA Polymerase	New England BioLabs
SOC outgrowth medium	New England Biolabs
T4 DNA Ligase Buffer (10X)	New England BioLabs
T4 DNA Ligase	New England BioLabs
Top10 *E.Coli*	Invitrogen (Thermo Fisher Scientific)

Table 2.13: Reagents for recombinant protein expression and purification.

Reagent	Supplier
Acetic acid	Carl Roth
ddH20	Generated in house
Glutathione-Sepharose™ 4B beads	GE Healthcare
Methanol	Carl Roth
MOPS SDS Running buffer (20X)	Invitrogen (Thermo Fisher Scientific)
PageRuler PreStained Protein Ladder	Thermo Fisher Scientific
PBS (1×)	Pan-Biotech
PreScission protease	Cytiva
Roti-Blue	Carl Roth
Triton-X®100	Carl Roth

Table 2.14: Reagents for immunofluorescent staining.

Reagent	Supplier
High Precision Microscope Cover Glasses	Marienfeld
Hoechst 33342	Thermo Fisher Scientific
Microscope Slides	Carl Roth
Normal Donkey Serum (NDS)	Merck
Paraformaldehyde (PFA)	Sigma-Aldrich
PBS (1×)	Pan-Biotech
ROTI®Mount FluorCare	Carl Roth
Streptavidin, Allophycocyanin	Thermo Fisher Scientific
Triton-X®100	Carl Roth

2.1.6 Solutions, buffers and media

Table 2.15: Solutions, buffers and media.

Name	Reagent	Concentration	Supplier
Calcium chloride solution (2.5 M)	$CaCl_2 \cdot 2\ H_2O$	18.4 g	Carl Roth
	ddH_2O	50 ml	Generated in house
Charcoal stripped human T cell medium	Charcoal stripped FBS Standard	5%	Pan-Biotech
	GlutaMAX™ Supplement	1%	Gibco
	Penicillin and streptomycin	1%	Thermo Fisher Scientific

	RPMI 1640 without L-glutamine and phenolred	500 ml	Capricorn Scientific
Cleavage buffer	Tris	50 mM, pH 7.0	AppliChem
	Sodium chloride	150 mM	Sigma-Aldrich
	EDTA	1 mM	Thermo Fisher Scientific
	DTT	1 mM	Thermo Fisher Scientific
CNS digestion solution	Collagenase A	1 mg/ml	Roche
	DNaseI	0.1 mg/ml	Merck
	RPMI 1640 medium	50 ml	Pan-Biotech
Erylysis buffer (pH 7.3 – 7.4)	Potassium bicarbonate ($KHCO_3$)	10 mM	Sigma-Aldrich
	Amoniumchloride (NH_4Cl)	0.15 M	Sigma-Aldrich
	Na_2EDTA	0.1 mM	Thermo Fisher Scientific
	ddH_2O	500ml	Generated in house
FACS buffer	BSA	2.5 g	Merck
	Sodium azide (NaN_3)	0.1 g	Carl Roth
	PBS 1x	500 ml	Pan-Biotech
HEK 293T medium	Penicillin and streptomycin	1%	Thermo Fisher Scientific
	FBS Standard	10%	Pan-Biotech
	DMEM with glutamine and high glucose	500 ml	Thermo Fisher Scientific
HEPES buffered saline (HBS, 2X)	Sodium chloride (NaCl)	8.0 g	Sigma-Aldrich
	Potassium chloride (KCl)	0.38 g	Carl Roth
	Disodium phosphate (Na_2HPO_4)	0.1 g	Carl Roth
	HEPES	5.0 g	Sigma-Aldrich
	Glucose	1.0 g	Sigma-Aldrich
	ddH_2O	500 ml	Generated in house
Human T cell medium	Human serum, Type AB	5%	Capricorn Scientific
	Penicillin and streptomycin	1%	Thermo Fisher Scientific
	RPMI 1640 medium	500 ml	Pan-Biotech
Jurkat cell medium	FBS Standard	10%	Pan-Biotech
	Penicillin and streptomycin	1%	Thermo Fisher Scientific
	RPMI 1640 medium	500 ml	Pan-Biotech
LB medium	LB Broth Base	20 g	Invitrogen (Thermo Fisher Scientific)
	ddH_2O	1000 ml	Generated in house

MACS buffer	Bovine serum albumin (BSA)	0.5 %	Carl Roth
	EDTA	2 mM	Thermo Fisher Scientific
	PBS 1x	500 ml	Pan-Biotech
Mouse T cell medium	β-mercaptoethanol	0.01%	Sigma-Aldrich
	Fetal calf serum (FCS) (BC BW9645)	10%	Sigma-Aldrich
	Penicillin and streptomycin	1%	Thermo Fisher Scientific
	HEPES	1%	Thermo Fisher Scientific
	Non-essential amino acids (NEAA)	1%	Thermo Fisher Scientific
	Sodium pyruvate	1%	Thermo Fisher Scientific
	Glutamax	1%	Thermo Fisher Scientific
	RPMI 1640 medium	500 ml	Pan-Biotech
Pup-it assay medium	Recombinant FRB-PafA	1 µM	Generated in house
	Rapamycin	1 µM	Merck
	Recombinant bio-DE28	2 µM	Peptides & Elephants
	SEB peptide	4 ng/µl	Merck
	ATP	10 mM	Sigma-Aldrich
	$MgCl_2$	15 mM	Sigma-Aldrich
	Cell culture medium		Generated in house
THP-1 cells medium	β-mercaptoethanol	0.05 mM	Sigma-Aldrich
	FBS Standard	10%	Pan-Biotech
	Penicillin and streptomycin	1%	Thermo Fisher Scientific
	RPMI 1640 medium	500 ml	Pan-Biotech

2.1.7 Devices

Table 2.16: Devices

Device	**Supplier**
BD FACS Aria III cell sorter	BD Bioscience
BD FACS LSR II analyzer	BD Bioscience
BD FACSymphony A3 analyzer	BD Bioscience
Bench Top Micocentrifuge	Eppendorf
Centrifuge	Heraeus
Epifluorescence Microscope Eclipse	Nikon
Eppendorf® Thermomixer Compact	Eppendorf

FlexCycler2 (PCR cycler)	Analytik Jena
Gel documentary device	INTAS Science Imaging
Incucyte® S3 Live-Cell Analysis System	Sartorius
Light Microscope	Olympus
LSM700 confocal laser scanning microscope	Zeiss
MACS cell separators (magnets)	Miltenyi Biotec
NanoDrop™ 1000 Spectrophotometer	Thermo Fisher Scientific
SevenCompact pH-meter	Mettler-Toledo
Sterile hood	Thermo Fisher Scientific
Surgical instruments	FST Fine Scientific Tools

Table 2.17: BD FACS LSR II analyzer configuration.

Laser	Detector	Dichroic Mirror	Bandpass Filter	Primary Fluorochrome	Other Fluorochromes
488 nm	E	505 LP	530/30 513/17	FITC Alternative: GFP	Alexa Fluor 488, CFSE, YFP
	D	550 LP	575/26	PE	Cy3
	C	600 LP	610/20	PE-TxRed	PE-Dazzle594
	B	685 LP 635 LP	695/40 670/14	PerCP-Cy5.5 Alternative 1: PerCP	PerCP-eFluor710
	A	735 LP	780/60	PE-Cy7	PE-Vio770
405 nm	F		450/50	Pacific Blue	Alexa Fluor 405, Brilliant Violet 421, V450
	E	505 LP	525/50	AmCyan	V500, Brilliant Violet 510
	D	600 LP	610/20	BV605	
	C	630 LP	660/20	BV650	
	B	635 LP	710/50	BV711	
	A	735 LP	780/60	BV786	
633 nm	C		660/20	APC	Alexa Fluor 647, eFluor 660
	B	710 LP	730/45	Alexa700	
	A	755 LP	780/60	APC-Cy7	APC-eFluor780

Table 2.18: BD FACS Aria III cell sorter configuration.

Laser	Detector	Dichroic Mirror	Bandpass Filter	Primary Fluorochrome	Other Fluorochromes
488 nm	E	505 LP	530/30 513/17	FITC Alternative: GFP	Alexa Fluor 488, CFSE, YFP
	D	550 LP	575/26	PE	Cy3
	C	600 LP	610/20	PE-TxRed	PE-Dazzle594
	B	685 LP 635 LP	695/40 670/14	PerCP-Cy5.5 Alternative 1: PerCP	PerCP-eFluor710
	A	735 LP	780/60	PE-Cy7	PE-Vio770
405 nm	F		450/50	Pacific Blue	Alexa Fluor 405, Brilliant Violet 421, V450
	E	505 LP	525/50	AmCyan	V500, Brilliant Violet 510
	D	600 LP	610/20	BV605	
	C	630 LP	660/20	BV650	
	B	690 LP	710/50	BV711	
	A	750 LP	780/60	BV786	
633 nm	C		660/20	APC	Alexa Fluor 647, eFluor 660
	B	710 LP	730/45	Alexa700	
	A	755 LP	780/60	APC-Cy7	APC-eFluor780

Table 2.19: BD FACSymphony A3 analyzer configuration.

Laser	Detector	Dichroic Mirror	Bandpass Filter	Primary Fluorochrome	Other Fluorochromes
355 nm	G	370 LP	379/28	BUV395	
	F	410 LP	450/50	DAPI	Alexa 350
		490 LP	*515/30*	*Alternative: BUV496*	
	E	550 LP	580/20	BUV563	
	D	600 LP	610/20	BUV615	*PI*
	C	630 LP	670/20	BUV661	
	B	690 LP	735/30	BUV737	
	A	770 LP	810/40	BUV805	
405 nm	H	410 LP	431/28	BV421	Alexa 405, V450, Pacific blue
	G	505 LP	525/50	BV510	V500, AmCyan
	F	550 LP	585/15	BV570	
	E	595 LP	605/40	BV605	
	D	635 LP	677/20	BV650	
	C	685 LP	710/50	BV711	
	B	735 LP	750/30	BV750	
	A	770 LP	810/40	BV786	
488 nm	G		488/10	SSC	
	F	505 LP	530/30	Alexa 488	FITC, CFSE, YFP
			513/17	*Alternative: GFP*	
	E	600 LP	610/20	BB630	
	D	635 LP	670/30	BB660	
	C	685 LP	710/50	PerCP-Cy5.5	BB700
	B	735 LP	750/30	BB755	
	A	770 LP	810/40	BB790	
561 nm	D	570 LP	586/15	PE	RFP
	C	600 LP	610/20	PE-CF/Dazzle594	PE-TxRed, *PI*
	B	635 LP	670/30	PE-Cy5.5	7-AAD
	A	750 LP	780/60	PE-Cy7	
637 nm	C	655 LP	670/30	Alexa 647	APC, eFluor 660
	B	690 LP	730/45	Alexa700	APC-R700
	A	750 LP	780/60	APC-Cy7	APC-eFluor780, APC-H7

2.1.8 General consumables

Table 2.20: General consumables.

Consumable	Supplier
0.45 µm PES filter	Merck
CELLSTAR EASYstrainer (40 and 100 µm)	Greiner
Disposable hemocytometer	NanoEntek
FACS tubes (5 ml)	Sarstedt
Falcon tubes (15 and 50 ml)	Greiner
Liquid reservoir for multichannel pipettes	Integra
MACS® SmartStrainers (30, 70 and 100 µm)	Miltenyi Biotec
Micro tubes (0.5, 1.5, 2.5 ml)	Sarstedt
MS Columns	Miltenyi Biotec
Multiwell plates (96-well, 24-well, 12-well, 6-well)	Greiner
NucleoBond Xtra Midi kit	Macherey-Nagel

NucleoSpin Gel and PCR Clean-up	Macherey-Nagel
Nucleo Spin Plasmid easy pure kit	Macherey-Nagel
Parafilm N	Carl Roth
Pierce™ BCA reducing agent-compatible protein assay	Thermo Fisher Scientific
Pipette tips	Sarstedt
Pre-Separation Filters (30 µm)	Miltenyi Biotec
Reservoir for multichannel pipettes	Integra
Serological pipettes (2ml, 5ml, 10ml and 25ml)	Greiner, Sarstedt
Syringes and needles	Braun, BD Bioscience

2.1.9 Software

Table 2.21: Software.

Software	**Supplier**
Adobe Illustrator	Adobe Inc.
FACSDiva™	BD Bioscience
FlowJo v10	BD Bioscience
Graph Pad Prism v9	Graph Pad
Microsoft Office	Microsoft
TBase Client 4Dv12sql	MacKeeper
Zen black	Zeiss

2.2 Methods

2.2.1 GTEx analysis

Gene expression data of spleen samples from 87 women and 154 men was downloaded from the Genotype-Tissue Expression (GTEx) project at https://gtexportal.org (GTEx_Analysis_v8). Raw RNA-seq read counts were analyzed for differential expression between sexes using DESeq2_1.34.0. Genes with exclusive localization on one of the sex chromosomes were excluded. According to our cut off criteria (false discovery rate-adjusted *P* value < 0.05; absolute log2 fold change > 0.2), 408 differentially expressed genes were identified (153 higher in women, 255 higher in men; **Table 2.22**). To test for the influence of sex hormone levels on gene expression, premenopause samples (38 women, 63 men, age ≤ 49 years) were compared to postmenopause samples (49 women, 91 men, age ≥ 50 years) separately in sexes using DESeq2_1.34.0. Plotting of the gene expression data was performed using ggplot2_3.4.2 and tidyheatmaps_0.1.0 (**https://github.com/jbengler/tidyheatmaps**).

Table 2.22: Top 50 DEGs from the GTEx dataset sorted by adjusted *P* value.

ensembl_id	gene_symbol	chrom.[1]	baseMean[2]	log2fc[3]	stat[4]	pvalue[5]	padj[6]
ENSG00000002586.18	*CD99*	X & Y	9553,505	0,474	12,957	2,14E-38	1,34E-35
ENSG00000205611.4	*LINC01597*	20	69,988	1,227	10,436	1,70E-25	9,46E-23
ENSG00000237531.6	*RP11-309M23.1*	X & Y	4,759	-1,845	-9,050	1,43E-19	7,28E-17
ENSG00000278599.5	*TBC1D3E*	17	10,438	5,311	8,391	4,83E-17	2,37E-14
ENSG00000223773.7	*CD99P1*	X & Y	245,258	0,301	7,291	3,08E-13	1,40E-10
ENSG00000132204.13	*LINC00470*	18	14,320	1,933	7,249	4,19E-13	1,84E-10
ENSG00000169084.13	*DHRSX*	X & Y	772,088	0,241	6,690	2,24E-11	9,33E-09
ENSG00000167393.17	*PPP2R3B*	X & Y	1360,154	0,304	6,624	3,49E-11	1,43E-08
ENSG00000225972.1	*MTND1P23*	1	250,451	-1,753	-6,142	8,14E-10	3,23E-07
ENSG00000214717.11	*ZBED1*	X & Y	3316,289	0,205	6,023	1,71E-09	6,59E-07
ENSG00000080007.7	*DDX43*	6	85,671	0,731	6,014	1,81E-09	6,85E-07
ENSG00000167634.12	*NLRP7*	19	104,877	-0,760	-5,887	3,94E-09	1,47E-06
ENSG00000138075.11	*ABCG5*	2	32,774	1,208	5,875	4,24E-09	1,54E-06
ENSG00000105926.15	*MPP6*	7	452,297	-0,458	-5,664	1,48E-08	5,20E-06
ENSG00000273367.1	*RP5-827C21.6*	1	15,203	0,739	5,501	3,78E-08	1,28E-05
ENSG00000185291.11	*IL3RA*	X & Y	590,236	0,328	5,493	3,96E-08	1,32E-05
ENSG00000112812.15	*PRSS16*	6	82,426	-0,487	-5,435	5,47E-08	1,78E-05
ENSG00000110680.12	*CALCA*	11	114,627	1,456	5,420	5,97E-08	1,91E-05
ENSG00000253967.1	*RP11-333A23.4*	8	21,718	1,376	5,272	1,35E-07	4,22E-05
ENSG00000149531.15	*FRG1BP*	20	299,141	0,312	5,220	1,79E-07	5,47E-05
ENSG00000225411.2	*RP11-764K9.1*	9	90,490	0,561	5,171	2,33E-07	7,02E-05
ENSG00000282826.1	*FRG1CP*	20	520,101	0,304	5,167	2,38E-07	7,08E-05
ENSG00000203907.9	*OOEP*	6	8,038	0,931	5,148	2,63E-07	7,74E-05

ENSG00000258484.3	*SPESP1*	15	71,224	0,631	5,084	3,70E-07	1,06E-04
ENSG00000257219.5	*RP11-54A9.1*	12	28,078	0,778	4,970	6,69E-07	1,90E-04
ENSG00000232040.2	*ZBED9*	6	14,374	-0,623	-4,965	6,87E-07	1,93E-04
ENSG00000198353.7	*HOXC4*	12	152,271	-0,350	-4,957	7,16E-07	1,99E-04
ENSG00000225698.3	*IGHV3-72*	14	1511,372	-1,065	-4,941	7,77E-07	2,14E-04
ENSG00000240864.3	*IGKV1-16*	2	2874,573	-0,855	-4,913	8,98E-07	2,44E-04
ENSG00000100842.12	*EFS*	14	908,952	0,372	4,834	1,34E-06	3,56E-04
ENSG00000167941.2	*SOST*	17	5,711	1,505	4,822	1,42E-06	3,74E-04
ENSG00000086506.2	*HBQ1*	16	132,068	1,298	4,807	1,54E-06	4,00E-04
ENSG00000104290.10	*FZD3*	8	240,305	-0,334	-4,629	3,67E-06	9,47E-04
ENSG00000181408.3	*UTS2R*	17	29,257	-0,969	-4,572	4,82E-06	1,22E-03
ENSG00000255408.3	*PCDHA3*	5	12,671	-0,749	-4,562	5,06E-06	1,27E-03
ENSG00000272744.1	*RP11-367N14.3*	4	12,795	0,604	4,560	5,12E-06	1,27E-03
ENSG00000196565.13	*HBG2*	11	213,482	1,129	4,550	5,37E-06	1,32E-03
ENSG00000196433.12	*ASMT*	X & Y	27,296	-0,492	-4,533	5,82E-06	1,41E-03
ENSG00000184226.14	*PCDH9*	13	394,351	-0,543	-4,518	6,25E-06	1,50E-03
ENSG00000225476.1	*MTCO3P5*	2	6,244	1,076	4,509	6,50E-06	1,55E-03
ENSG00000101542.9	*CDH20*	18	12,743	0,567	4,483	7,35E-06	1,72E-03
ENSG00000125895.5	*TMEM74B*	20	204,321	0,473	4,484	7,32E-06	1,72E-03
ENSG00000022556.15	*NLRP2*	19	720,900	-0,537	-4,453	8,48E-06	1,95E-03
ENSG00000134545.13	*KLRC1*	12	215,855	0,473	4,433	9,30E-06	2,12E-03
ENSG00000102924.11	*CBLN1*	16	13,607	-0,809	-4,429	9,46E-06	2,13E-03
ENSG00000153822.13	*KCNJ16*	17	284,763	0,882	4,415	1,01E-05	2,24E-03
ENSG00000224106.1	*CYP4F25P*	9	6,724	0,669	4,410	1,04E-05	2,27E-03
ENSG00000124557.12	*BTN1A1*	6	49,183	-0,562	-4,404	1,06E-05	2,31E-03
ENSG00000237238.2	*BMS1P10*	9	73,848	-0,767	-4,382	1,18E-05	2,54E-03
ENSG00000234335.1	*RPS4XP11*	10	8,081	-0,593	-4,373	1,23E-05	2,62E-03

[1]chromosomal location; [2]baseMean: mean of normalized counts for all samples; [3]log2 fold change; [4]stat: Wald statistic; [5]DESeq2 Wald test p-value; [6]DESeq2 Benjamini-Hochberg adjusted *P* value.

2.2.2 PBMC isolation and cryopreservation

Blood was collected in EDTA coated tubes (Sarstedt) and processing of blood samples was started immediately upon receipt of blood samples in the laboratory. For MS patients, NND patients and healthy individuals PBMCs were isolated by a 30 min gradient centrifugation at 860 × g using Biocoll Separating Solution (Biochrom), followed by two washing steps. Cells were then cryopreserved in RPMI medium (Pan-Biotech) with 25% heat-inactivated fetal calf serum (FCS, Biochrom) and 10% (v/v) dimethyl sulfoxide (DMSO, AppliChem) and stored at -180°C in the gas phase of a liquid nitrogen tank until further analysis. For trans men, PBMCs were isolated by a 30 min gradient centrifugation at 500 × g using Lymphocyte Separation Media (Capricorn), followed by two washing steps. After lysis of erythrocytes with ACK Lysing Buffer (Lonza), cells were then cryopreserved in heat-inactivated fetal

bovine serum (FBS) supplemented with 10% (v/v) dimethyl sulfoxide (Sigma-Aldrich) and stored in liquid nitrogen until further analysis.

2.2.3 Flow cytometry

Surface staining: Staining of surface marker antigens was always performed at 4°C using fluorochrome labelled antibodies. In case of whole blood samples subsequently erythrocytes were lysed and lymphocytes fixed using BD FACS™ Lysing Solution. PBMCs and lymphocytes derived from CSF were fixed with BD Cytofix™ Fixation Buffer after staining prior to analysis. Surface marker antibodies used in this study are listed in **Table 2.4**.

Absolute cell quantification: Absolute cell counts were quantified using Precision Count Beads™ (BioLegend).

Sample analyses: All samples were acquired on a BD FACS LSR II analyzer or FACSymphony A3 analyzer (BD Bioscience). Flow cytometry-based cell sorting was performed on a FACSAria III cell sorter (BD Bioscience). Data was analyzed with FlowJo software (Version 10.8.1, BD Bioscience).

2.2.4 Human T cell proliferation

Cryopreserved PBMCs from healthy women and men were thawed and $CD3^+$ T cells were isolated from single-cell suspension using the Human Pan T Cell Isolation Kit (Miltenyi Biotec) according to the manufacturer's protocol and labelled with CFSE (CellTrace™ CFSE Cell Proliferation Kit, ThermoFisher) according to the manufacturer's protocol. $CD3^+$ T cells were seeded at a density of 25,000 cells per well in an anti-CD3 (0.5 µg/ml, clone OKT3, BioLegend) coated 96-well plate. Anti-CD28 (5 µg/ml, clone CD28.2, BioLegend) and anti-CD99 (5 µg/ml, clone HCD99, BioLegend) or respective isotype control (5 µg/ml, clone MOPC-173, BioLegend) were added in solution. Proliferation was tracked by cluster formation in the Incucyte® S3 Live-Cell Analysis System for 7 days.

2.2.5 Human T cell activation

Cryopreserved PBMCs from healthy women were thawed and seeded at a density of 2 x 10^5 cells per well in an anti-CD3 (10 µg/ml, clone OKT3, BioLegend) coated 96-well plate. Cells were supplemented with soluble anti-CD28 (2.5 µg/ml, clone CD28.2, BioLegend) and anti-CD99 (10 µg/ml, clone hec2, BioLegend) or respective isotype control (10 µg/ml, clone MOPC-21, BioLegend). Samples were incubated for 72 hours at 37°C and 5% CO_2, stained with antibodies listed in **Table 2.4** and analyzed by flow cytometry after 2, 24, 48 and 72 hours.

2.2.6 *In vitro* testosterone treatment

For testosterone treatment, we used RPMI 1640 Medium, without L-Glutamine (Capricorn) supplemented with 1% GlutaMAX™ Supplement (Gibco), 1% Pen Strep (Gibco) and 5% charcoal stripped FBS Standard (Pan-Biotech). For charcoal stripping of FBS, 2 g dextran-coated charcoal (DCC, Merck) were added to 100 ml FBS and incubated on a shaker overnight at 4°C followed by centrifugation and filtration. Cryopreserved PBMCs from male healthy individuals were thawed and seeded at a density of 2 x 10^5 cells per well in an anti-CD3 (10 µg/ml, clone OKT3, BioLegend) coated 96-well plate and supplemented with soluble anti-CD28 (2.5 µg/ml, clone CD28.2, BioLegend) or left unstimulated. Subsequently, testosterone (3, 30 and 300 ng/ml, Sigma-Aldrich) or 5α-dihydrotestosterone (0.3, 3 and 30 ng/ml, Sigma-Aldrich) was added. Samples were incubated for 48 hours at 37°C and 5% CO_2, stained with antibodies listed in **Table 2.4** and analyzed by flow cytometry after 2, 24 and 48 hours.

2.2.7 Generation of *Cd99*-deficient mice

To generate *Cd99*-deficient mice, the second coding exon was targeted by the CRISPR/Cas9 genome editing system. A single sgRNA was designed using the CRISPOR design tool (**http://crispor.tefor.net**)[311]. The template for transcription with the targeting sequence (GCGAGTGACGACTTCAACCT) was generated by fill-in reaction with Klenow DNA Polymerase (Thermo Fisher Scientific). Transcription was performed using the HiScribe™ *T7* High Yield RNA Synthesis Kit (#E2040S, New England Biolabs), with subsequent purification of the transcript with the MEGAClear™ Transcription Clean-Up Kit (#AM1908, Thermo Fisher Scientific), both according to the manufacturer's instructions. The sgRNA (600 ng/µL) and Cas9 protein (Alt-R® S.p. Cas9 Nuclease V3, #1,081,058, Integrated DNA Technologies (IDT)) (500 ng/µL) in Gibco™ Opti-MEM™ (Thermo Fisher Scientific) were electroporated into one-cell-stage embryos derived from superovulated C57BL/6 mice using the NEPA 21 electroporator (Nepa Gene)[312]. Embryos were implanted into F1 foster mothers (C57BL/6 × CBA) and the resulting offspring was analyzed by PCR amplification on genomic tail DNA using primers F (5'-CGGGGCCCGGATTGGATGTAAATGCTG-3') and R (5'-AGAGCCCCGGGTATGTAAATGACTC-3') and subsequent Sanger sequencing. For our experiments, we used animals with an insertion of 2 bp in exon 2, which resulted in CD99 protein deficiency. These offspring were analyzed by separate PCRs with either WT allele-specific forward primer (CCTCAGCGAGTGACGACTTCAACC) or mutant allele-specific forward primer (CCTCAGCGAGTGACGACTTCAAAACC) and common reverse primer (CCCAGAGCCCCGGGTATGTAAATGACTC). WT specific PCR resulted in a PCR product of 180 bp and mutant specific PCR resulted in a product of 182 bp.

2.2.8 Mouse T cell proliferation

Lymph nodes (axillary, brachial, inguinal) and spleen from homo- and heterozygous *Cd99*-deficient and C57BL/6 WT mice were collected in ice-cold PBS. $CD3^+$ T cells were isolated from single-cell suspension using the MojoSort™ Mouse CD3 T Cell Isolation Kit (BioLegend) according to the manufacturer's protocol and labelled with CFSE (CellTrace™ CFSE Cell Proliferation Kit, ThermoFisher) according to the manufacturer's protocol. $CD3^+$ T cells were seeded at a density of 3 x 10^5 cells per well in an anti-CD3 (1 µg/ml, clone 145-2CL11, BioLegend) coated 96-well plate. Cells were supplemented with soluble anti-CD28 (0.5 µg/ml, clone 37.51, BioLegend) and recombinant IL-2 (20 IU/ml, Peprotech). Samples were incubated for 72 hours at 37°C and 5% CO_2, stained with antibodies listed in **Table 2.4** and analyzed by flow cytometry.

2.2.9 EAE induction

Active Immunization: Mice were s.c. with 200 µg of $MOG_{35–55}$ peptide (Peptides & elephants) in CFA containing 2 mg/ml *Mycobacterium tuberculosis* (BD Bioscience). Additionally, 200 ng pertussis toxin (Merck Millipore) in PBS were injected intraperitoneally (i.p.) on the day of immunization and 48 hours later.

EAE scoring: Weight and clinical signs of disease were scored daily starting at day 7 by the following system: 0, no clinical deficits; 1, tail weakness; 2, hind limb paresis; 3, partial hind limb paralysis; 3.5, full hind limb paralysis; 4, full hind limb paralysis and forelimb paresis; 5, premorbid or dead. Animals reaching a clinical score of ≥ 4 or having more than 25% body weight loss (from starting weight) were sacrificed according to regulations of the local Animal Welfare Act. Scoring of EAE experiments was performed blinded for the genotype. Mice without any disease symptoms 20 dpi were excluded from the analyses. To minimize cage-specific effects, experimental groups were mixed within cages and littermates were used as control animals.

2.2.10 Immune cell isolation

Spleen and LN: Inguinal, brachial and axillary lymph nodes as well as spleen samples were homogenized through a 70 µm cell strainer and washed with PBS (300 × g, 10 min, 4°C). Splenic cells were resuspended in erythrocyte lysis buffer (10 mM potassium bicarbonate, Merck Millipore; 0.15 M ammoniochloride, Merck Millipore; 0.1 mM Na_2EDTA, Thermo Fisher Scientific; in ddH_2O; pH 7.4) and incubated for 5 min on ice to lyse red blood cells before it was stopped with PBS.

CNS: Before the CNS was taken, mice were intracardially perfused with 10 ml PBS. The CNS was minced with a razor blade, digested for 45 min at 37°C in a shaking water bath (1 mg/ml Collagenase A, Roche;

0.1 mg/ml DNaseI, Merck Millipore; in RPMI-1640 medium, Pan-Biotech) and subsequently homogenized through a 70 µm cell strainer. After washing with PBS, immune cells were isolated by percoll gradient centrifugation (30%/78% 1.13 g/ml, GE Healthcare) at 2500 rpm, 30 min, 4°C, w/o brake, harvested from the interphase and washed twice with PBS.

2.2.11 Jurkat cell proliferation

WT Jurkat cells, *CD99*-deficient Jurkat cells or transduced Jurkat cells were fluorescently labelled (CellTrace™ Violet Cell Proliferation Kit, ThermoFisher) according to the manufacturer's protocol. Cells were seeded at a density of 3 x 10^5 cells per well in a 12-well plate. Samples were incubated for 96 hours at 37°C and 5% CO_2 and analyzed by flow cytometry after 0, 24, 48, 72 and 96 hours. Jurkat cells are derived from a male donor and harbor X and Y chromosomes.

2.2.12 Vector construction

CD99 overexpression: To insert human CD99 (hCD99) into a lentiviral vector harboring a CMV promoter and C-terminal P2A-eGFP domain, we first performed PCR using Primer_f_1 and Primer_r_1 from a human CD99 gene ORF cDNA clone expression plasmid (Biozol). Restriction and ligation were performed using BamHI and XbaI restriction sites.

CD99 CRISPR-KO: To generate hCD99 CRISPR-KO cells, we used four guide RNAs (Oligo_f/r_1, Oligo_f/r_2, Oligo_f/r_3, Oligo_f/r_4) targeting different protein coding exonic regions of hCD99 that were annealed and inserted using Esp3I restriction sites into the Lenti-Cas9-gRNA-GFP. Lenti-Cas9-gRNA-GFP was a gift from Jason Sheltzer (Addgene #124770; http://n2t.net/addgene:124770; RRID: Addgene_124770).

CD99 pupylation constructs: To generate L21C-CD99-PafA-P2A-eGFP constructs, we inserted the PafA domain from the original pEF6a-CD28-PafA vector into a lentiviral vector harboring a CMV promoter and C-terminal P2A-eGFP domain. Restriction and ligation were performed using BsiWI and XbaI restriction sites. pEF6a-CD28-PafA was a gift from Min Zhuang (Addgene plasmid # 113400 ; http://n2t.net/addgene:113400 ; RRID:Addgene_113400). To insert hCD99, we first performed PCR using Primer_f_2 and Primer_r_2 from a human CD99 gene ORF cDNA clone expression plasmid (Biozol). Restriction and ligation were performed using AgeI and BsiWI restriction sites.

To facilitate lentiviral production, we inserted the CD28-PafA domain from the original pEF6a-CD28-PafA vector into a lentiviral vector harboring a CMV promotor and C-terminal P2A-eGFP domain. Restriction and ligation were performed using NheI and Eco32I restriction sites.

To generate L21C-FKBP-CD99-P2A-eGFP constructs, we inserted the FKBP domain from the original pEF6a-FKBP-CD28 vector into a lentiviral vector harboring a CMV promoter and C-terminal P2A-eGFP domain. Restriction and ligation were performed using AgeI and BamHI restriction sites. pEF6a-FKBP-CD28 was a gift from Min Zhuang (Addgene plasmid # 113401 ; http://n2t.net/addgene:113401 ; RRID:Addgene_113401). To insert hCD99 without its signal peptide, which needs to be cloned upstream of the FKBP domain to ensure extracellular expression, we first performed PCR using Primer_f_3 and Primer_r_3 from a human CD99 gene ORF cDNA clone expression plasmid (Biozol). Restriction and ligation were performed using BamHI and XbaI restriction sites. Previous to insertion of the CD99 signal peptide, we removed an AgeI restriction site, which was located in the original FKBP domain by recombinant PCR using Primer_f_4, Primer_r_4, Primer_f_5 and Primer_r_5. Restriction and ligation were performed using AgeI and BamHI restriction sites. Next, we inserted CD99 signal peptide and FLAG tag by Oligo annealing using the oligonucleotides CD99-SP-FLAG-for and CD99-SP-FLAG-rev. Restriction and ligation were performed using AgeI and BsiWI restriction sites.

Primers, oligonucleotides, and the respective restriction sites are listed in

Table 2.6.

2.2.13 Generation of stable cell lines

CD99-deficient Jurkat cells were transfected by Lipofectamine 2000 (ThermoFisher Scientific) according to the standard protocol. CD99-FKBP Jurkat and mScarlet THP-1 cells were generated by lentiviral transduction. 5×10^5 cells per 500 µL each were incubated with 500 µL of transfected HEK293T cell supernatant containing lentiviruses. In case of THP-1 cells, polybrene (Sigma-Aldrich, 8 µg/ml) was added and cells were spinoculated (800 × g, 60 min, 32°C) afterwards. GFP-/mScarlet-expressing cells were identified and sorted by flow cytometry using a FACSAria III cell sorter (BD Bioscience). Genetic KO was confirmed using flow cytometry and Sanger sequencing.

2.2.14 Lentiviral production

To produce lentiviruses, we first transfected HEK293T cells with 10 µg expression plasmid, 10 µg pMDLg/pRRE, 5 µg pRSV-Re, 2 µg pMD2.G. pMDLg/pRRE was a gift from Didier Trono (Addgene #12251; http://n2t.net/addgene:12251; RRID: Addgene_12251). pRSV-Rev was a gift from Didier Trono (Addgene #12253; http://n2t.net/addgene:12253; RRID:Addgene_12253). pMD2.G was a gift from Didier Trono (Addgene #12259; http://n2t.net/addgene:12259; RRID: Addgene_12259). Briefly, HEK293T cells were seeded out with an 80% confluency in DMEM with glutamine and high glucose (ThermoFisher), the next day the plasmids were mixed in 1× HEPES buffered saline (HBS) and 125 mM

$CaCl_2$ and were applied to the HEK293T cells for 6 hours. Subsequently, medium was changed and after 48 hours the supernatant was filtered through a 0.45 µm PES filter, immediately snap frozen and stored at -80°C. Transfer plasmids used to generate lentiviruses included L21C-CD99-P2A-eGFP, L21C-mScarlet, L21C-CD99-PafA-P2A-eGFP, L21C-CD28-PafA-P2A-eGFP, L21C-FKBP-CD99-P2A-eGFP and pLVX-TRE3G-BCCP-PupE-IRES-BFP. pLVX-TRE3G-BCCP-PupE-IRES-BFP was a gift from Min Zhuang (Addgene plasmid # 113405 ; http://n2t.net/addgene:113405 ; RRID:Addgene_113405).

2.2.15 Recombinant protein expression and purification

Recombinant protein expression and purification was performed as previously described in the original publication with minor changes[313]. Cells were grown in LB media supplemented with 100 µg/ml ampicillin at 37 °C until the OD_{600} reached 0.8. Protein expression was induced with 0.2 mM IPTG and cells continued to grow at 18 °C overnight. Cells were collected by centrifugation, aliquoted and stored at -80°C. Plasmids pGEX6p-1-FRB-PafA and pGEX6p-1-BCCP-PupE encoding FRB-PafA and bio-PupE were transformed into *E. coli* BL21. pGEX6p-1-BCCP-PupE was a gift from Min Zhuang (Addgene plasmid # 113403 ; http://n2t.net/addgene:113403 ; RRID:Addgene_113403) pGEX6p-1-FRB-PafA was a gift from Min Zhuang (Addgene plasmid # 113404 ; http://n2t.net/addgene:113404 ; RRID:Addgene_113404).

For purification of GST-tagged proteins, bacterial suspension aliquots were thawed on ice, resuspended in lysis buffer (3% Triton X-100 in PBS) and lysed by sonification with subsequent incubation on an overhead shaker (4°C, 30 min). The supernatant was isolated by centrifugation (20,000 x g, 4°C, 10 min) and GST-tagged proteins were purified with Glutathione-Sepharose™ 4B beads (GE Healthcare) on an overhead shaker (60 min, 4°C). After beads precipitation (500 x g, 3 min, 4°C) and extensive washing with 1% Triton X-100 in PBS and cleavage buffer (50 mM Tris, pH 7.0, 150 mM NaCl, 1 mM EDTA and 1 mM DTT), proteins were eluted by incubating with precision protease (PreScission™, Cytiva) at a ratio of 1:100 (V/V) on an overhead shaker at 4°C overnight. Protein purity and quantity was analyzed by standard SDS-PAGE with subsequent coomassie staining and Pierce™ BCA reducing agent-compatible protein assay (Thermofisher) according to the manufacturer's protocol.

2.2.16 Cell surface pupylation assay

Pupylation assay for the detection of cell surface ligands was performed as previously described in the original publication with minor changes[313]. After optimization, 2.5×10^5 CD99-FKBP Jurkat cells were incubated (60 min, 37°C, 5% CO_2) with 2.5×10^5 mScarlet-THP-1 cells or previously $CD45^+$ labelled

PBMCs in the presence of 1 µM FRB–PafA, 1 µM rapamycin, 2 µM bio-DE28, 4 ng/µl SEB peptide, 10 mM ATP, and 15 mM $MgCl_2$ in cell culture medium. After washing twice with PBS, the cells were incubated for 30 min with strepatvidin-APC (Thermofisher) and analyzed by immunofluorescent staining or flow cytometry.

2.2.17 Immunofluorescent staining and confocal microscopy

WT Jurkat cells or CD99-FKBP transfected Jurkat cells in PBS were added onto a cover slip in the bottom of a 24-well cell culture plate. After resting (30 min, room temperature (RT)) to enable cells to attach, non-adherent cells were slowly aspirated and cells were fixed with 4 % PFA for 10 min at RT. After incubation time, cells were washed two times with PBS and permeabilized with PBS containing 0.25 % Triton-X-100. After washing with PBS for 5 min, cells were incubated with PBS containing 10 % normal donkey serum (NDS) for blocking of unspecific binding for 30 min at RT. Next, primary antibodies (anti-CD99, BioLegend) or Streptavidin-Allophycocyanin (Thermo Fisher Scientific) were added for 60 min at RT. Cells were washed with PBS and mounted with ROTI®Mount FluorCare. Immunostainings were analyzed with a 40× or 63× objective on a Zeiss LSM 700 confocal microscope. Images were analyzed with Fiji software (ImageJ).

2.2.18 Statistical analysis

Bar graphs represent mean ± standard error of the mean (SEM). Statistical analyses were performed using Prism 9 software (GraphPad Software). Normal distribution was tested using Kolmogorov-Smirnov or Shapiro-Wilk test. Significant results are indicated by $*P < 0.05$, $**P < 0.01$, $***P < 0.001$.

3 Results

3.1 Increased CD99 expression by male immune cells

To identify genes that are differentially regulated in women and men and might contribute to sex-specific differences in autoimmunity, we conducted an unsupervised and systematic gene expression analysis. We made use of a publicly available dataset compiled by the GTEx project[314], that includes information about the donor's sex, and analyzed mRNA expression in the spleen. Of note, we focused on genes, which are not exclusively located on the X or Y chromosome, thus mainly focusing on (pseudo)autosomal differences. With our cut-off criteria (absolute log2 fold change > 0.2; *padj* < 0.05), we identified 408 differentially expressed genes (DEGs) between women and men in the spleen, of which 153 were higher in women and 255 were higher in men (**Figure 3.1A; Figure 3.2A,B**). These DEGs included protein-coding genes (e.g., *TBC1D3E*, *DHRSX* and *ZBED1*) as well as pseudogenes (e.g., *CD99P1* and *MTND1P23*), long non-coding RNAs (e.g., *LINC01597* and *LINC00470*) and unspecific transcripts (e.g., *RP11-309M23.1*). Protein-coding genes that were increased in males included *TBC1D3E*, *DHRSX* and *ZBED1*, whereas *NLRP7*, *MPP6* and *PRSS16* were increased in women. However, the candidate with the highest significance according to the adjusted *P* value was *CD99* (absolute log2 fold change = 0.47; *padj* = 1.34×10^{-35}), showing an increased expression in males (**Figure 3.1B**). As internal validation of the dataset, we detected *XIST* expression only in women and *SRY* only in males (**Figure 3.1C**). *XIST* encodes for the X inactive specific transcript and should therefore only be expressed in women, while *SRY* encodes for the sex-determining region Y, which is located on the Y chromosome. In order to investigate, whether sex-specific expression differences of CD99 on mRNA level translate to differential expression on protein level and in particular on functionally relevant surface expression level, we performed flow cytometry analyses of cryoconserved PBMCs from healthy individuals (HI) with *n* = 30 individuals per group. Indeed, surface expression of CD99 was significantly higher in male HI on $CD4^+$ and $CD8^+$ memory and naïve T cells as well as on pDCs and NK cells (**Figure 3.1D; Figure 3.3A–C**). We did not observe any significant differences in cDCs, B cells and monocytes. Together, we detected CD99 to be markedly higher expressed in male spleens on transcript level and on $CD4^+$ and $CD8^+$ memory and naïve T cells, pDCs and NK cells on surface protein level.

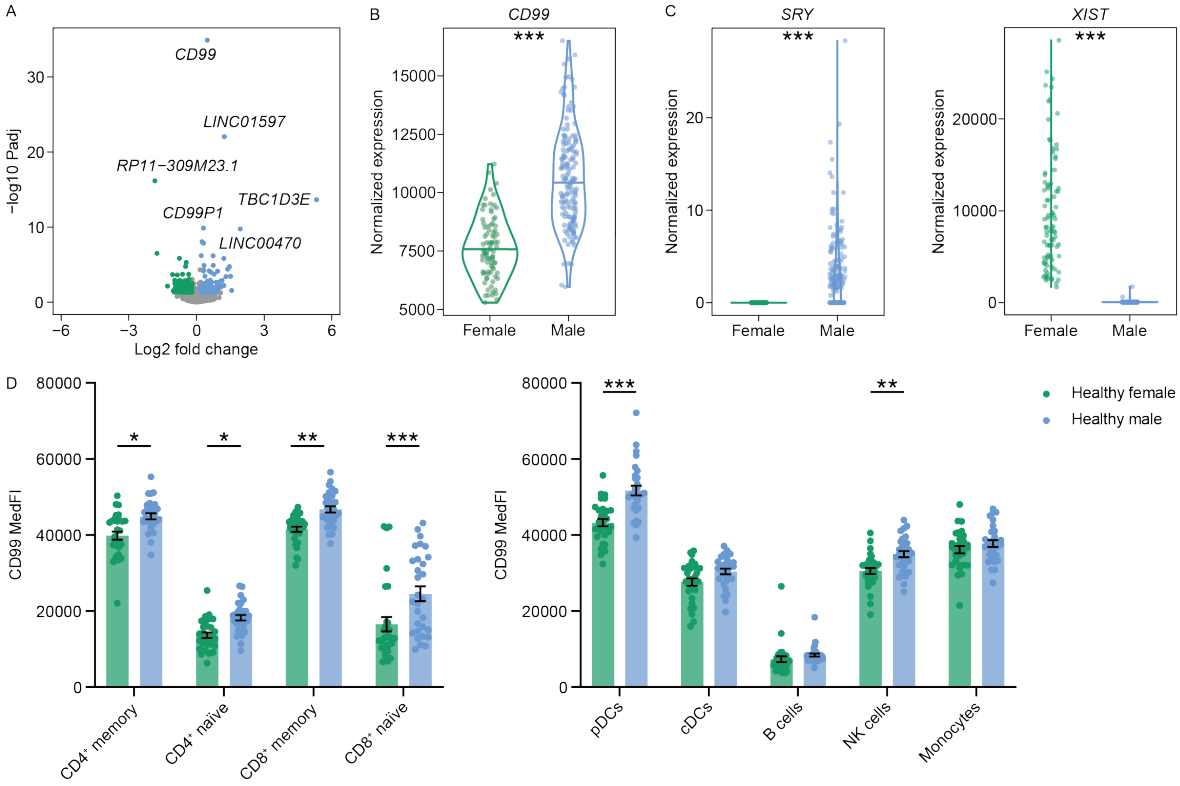

Figure 3.1: Increased CD99 expression in immune cells from men. (**A**) Sex-specific differentially expressed (pseudo)autosomal genes in spleen samples (*n* = 87 women and 154 men) from the Genotype-Tissue Expression (GTEx) dataset. (**B, C**) Corresponding mRNA expression levels of CD99, SRY and XIST in spleen. (**D**) CD99 surface protein expression on subsets of cryoconserved peripheral blood mononuclear cells (PBMCs) from male (*n* = 30) and female (*n* = 30) healthy individuals as analyzed by flow cytometry. Cell subsets were identified as following: $CD4^+$ and $CD8^+$ memory (gated as living $CD3^+$-$CD4^+$/$CD8^+$-$CD45RA^-$ cells) and naïve (gated as living $CD3^+$-$CD4^+$/$CD8^+$-$CD45RA^+$ cells) T cells; pDCs (gated as living $CD45^+$-Lineage(CD3, CD14, CD19, CD20, CD56)$^-$-$HLA\text{-}DR^+$-$CD11c^-$-$CD123^+$-$CD304^+$ cells); cDCs (gated as living $CD45^+$-Lineage(CD3, CD14, CD19, CD20, CD56)$^-$-$HLA\text{-}DR^+$-$CD11c^+$ cells); B cells (gated as living $CD45^+$-$CD19^+$-$CD20^+$ cells); NK cells (gated as living $CD45^+$- $CD19^-$-$CD20^-$-$CD3^-$-$CD14^-$-$CD56^+$ cells) and monocytes (gated as living $CD45^+$-$CD19^-$-$CD20^-$-$CD3^-$-$CD14^+$ cells). Data are shown as violin plots including median. Statistics: (A–C) DESeq2 false discovery rate-adjusted P value; (D) two-way ANOVA with Tukey post-hoc; *P < 0.05; **P < 0.01; ***P < 0.001.

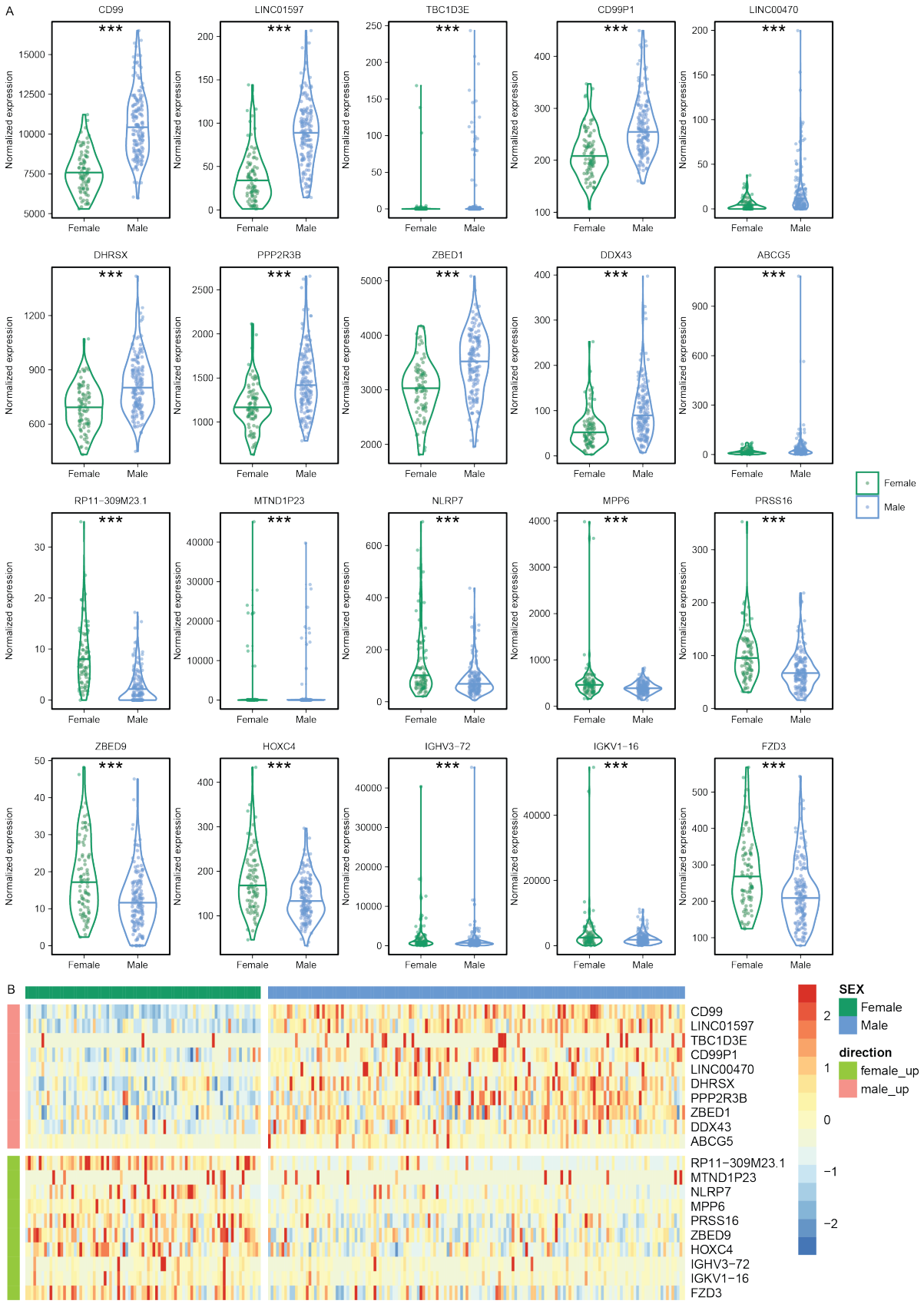

Figure 3.2: Differentially expressed genes in females and males. (**A**) mRNA expression levels of top 20 sex-specific genes in spleen samples (*n* = 87 women and 154 men) from the GTEx dataset. (**B**) Individual gene expression levels from the same dataset as shown in a heatmap. Data are shown as violin plots including median. Statistics: DESeq2 false discovery rate-adjusted *P* value; **P* < 0.05; ***P* < 0.01; ****P* < 0.001.

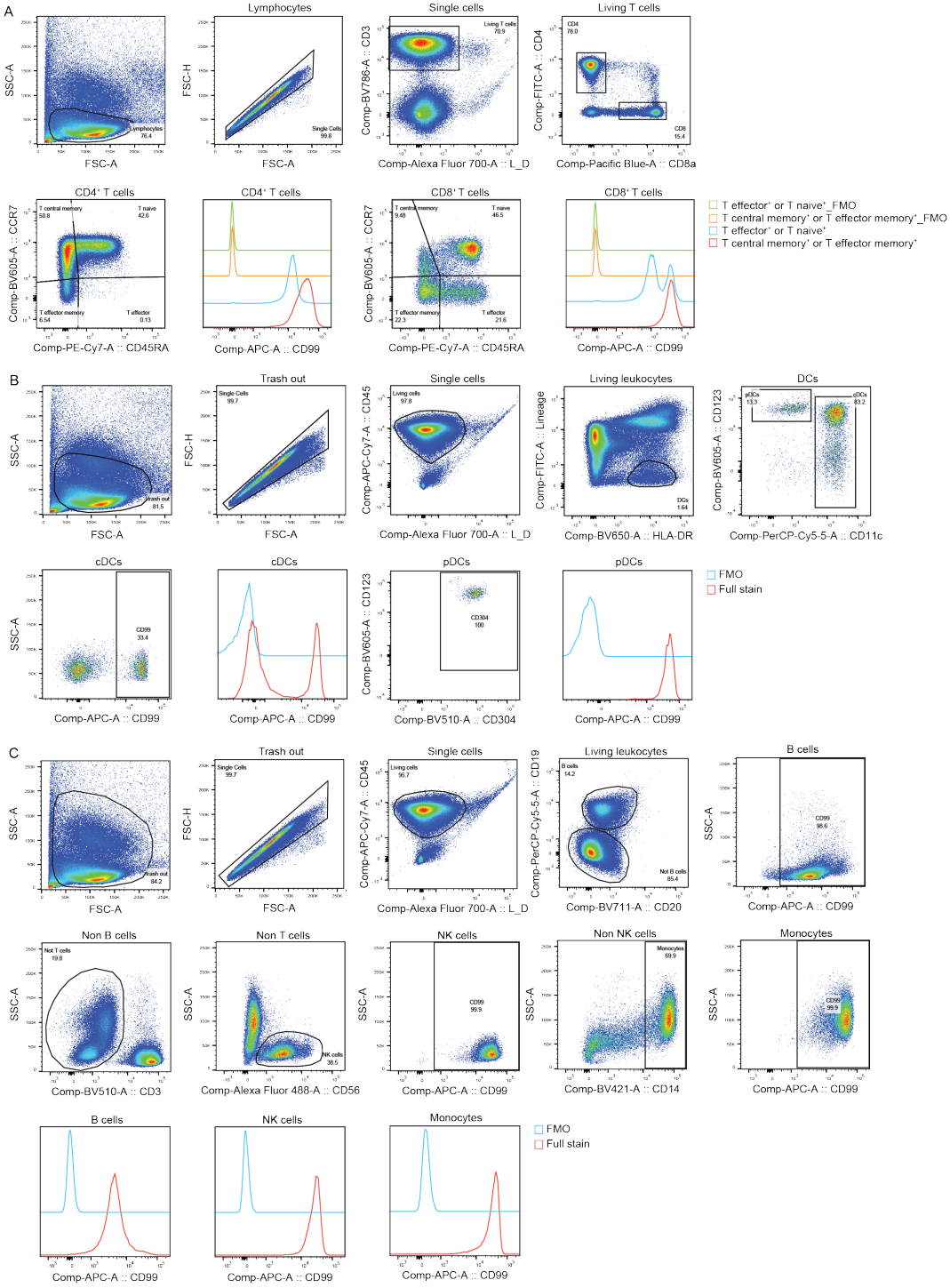

Figure 3.3: Identification of immune cell subsets in PBMC cohort. Representative gating strategy for identification of (**A**) T cells, (**B**) DCs as well as (**C**) B cells, NK cells and monocytes.

3.2 Testosterone does not regulate CD99 expression

Although CD99 expression is genetically regulated by its localization on both sex chromosomes and the ability to escape XCI, we next tested whether CD99 surface expression could additionally be regulated by sex hormones[152,163]. To probe whether increased CD99 levels in men could be attributed to the

influence of testosterone, we first treated TCR-stimulated and unstimulated PBMCs with different concentrations of testosterone and dihydrotestosterone, its most potent bioactive form, for 48 hours. Neither testosterone nor dihydrotestosterone had an influence on CD99 surface expression in this *in vitro* setting (**Figure 3.4A; Figure 3.5A,B**). Second, to corroborate these findings *ex vivo*, we analyzed CD99 surface expression of cryoconserved PBMCs from trans men, who received intramuscular (i.m.) testosterone treatment. When comparing baseline levels (month 0, M0) to protein levels after 6 months (M6) or 12 months (M12) of treatment, we did not observe changes of CD99 surface expression upon testosterone treatment in any immune cell subset (T cells, DCs, B cells and NK cells) but in monocytes, where we saw a decrease after 6 and 12 months (**Figure 3.4B, Figure 3.6A,B**). Third, we re-analyzed our GTEx dataset separating samples into pre- (≤ 49 years) and postmenopausal (≥ 50 years) to ask whether sex hormone level decline with age is associated with changes in CD99 expression levels. While there was no change in expression levels for *CD99*, other representative genes like *GPR158* or *PODXL2* were regulated, showing overall analysis validity (**Figure 3.4C**). In addition, we were able to reproduce previous findings about *CD99* escaping XCI[193] on single cell level in pDCs of a female donor harboring a SNP (rs1136447) in the *CD99* locus of one X-chromosomal allele. By analyzing mRNA transcripts with different probes[315], we detected 41.9% biallelic CD99 expression and 30.2% expression from one allele and 27.9% expression from the other allele (data not shown). Taken together, these data demonstrate that human CD99 expression levels are not regulated by testosterone *in vitro* and *in vivo*, indicating that incomplete XCI accounts for sex-specific expression patterns of CD99. Thus, Y-encoded transcription is insufficiently compensated by transcription from the Xi.

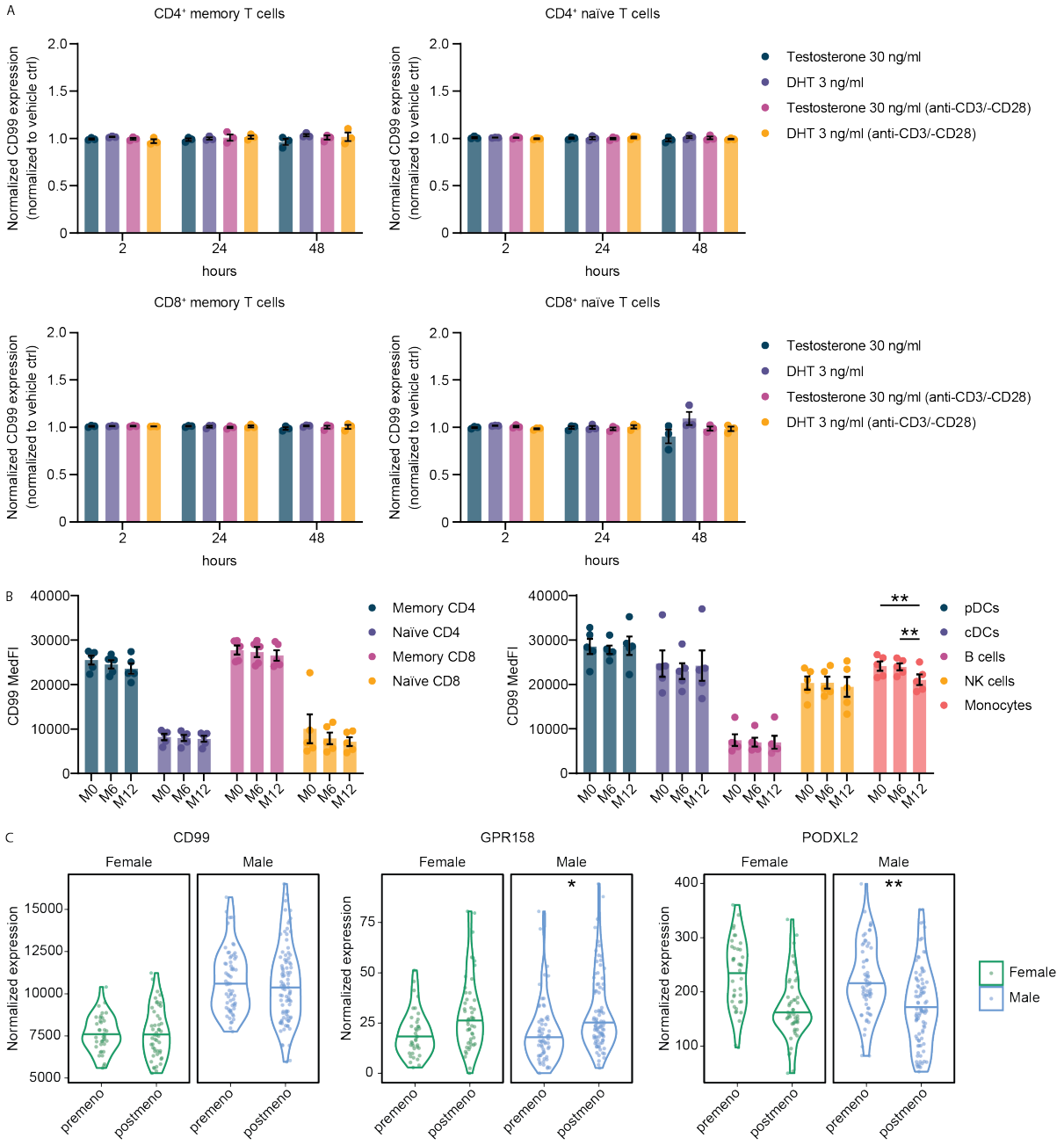

Figure 3.4: CD99 expression is independent of sex hormones. (**A**) CD99 surface expression of T cells (*n* = 3 men). Cryopreserved PBMCs were either stimulated with anit-CD3 and anti-CD28 mAbs or left unstimulated and treated with either testosterone (30 ng/ml) or dihydrotestosterone (DHT; 3 ng/ml). (**B**) CD99 surface protein expression on subsets of cryoconserved peripheral blood mononuclear cells (PBMCs) from trans men individuals (*n* = 5) receiving testosterone treatment as analyzed by flow cytometry. Cell subsets were identified as following: $CD4^+$ and $CD8^+$ memory (gated as living $CD3^+$-$CD4^+$/$CD8^+$-$CD45RA^-$ cells) and naïve (gated as living $CD3^+$-$CD4^+$/$CD8^+$-$CD45RA^+$ cells) T cells; pDCs (gated as living $CD45^+$-Lineage(CD3, CD14, CD19, CD20)$^-$-$HLA\text{-}DR^+$-$CD11c^-$-$CD123^+$ cells); cDCs (gated as living $CD45^+$-Lineage(CD3, CD14, CD19, CD20)$^-$-$HLA\text{-}DR^+$-$CD11c^+$ cells); B cells (gated as living $CD45^+$-$CD19^+$-$CD20^+$ cells); NK cells (gated as living $CD45^+$-$CD19^-$-$CD20^-$-$CD3^-$-$CD14^-$-$HLA\text{-}DR^-$-$CD56^+$ cells) and monocytes (gated as living $CD45^+$-$CD19^-$-$CD20^-$-$CD3^-$-$CD14^+$ cells). (**C**) mRNA expression levels of CD99, GPR158 and PODXL2 in pre- or postmenopausal samples of previously analyzed GTEx dataset in females and males. Data are shown as mean ± SEM (A, B) and violin plots including median (C). Statistics: (A, B) two-way ANOVA with Tukey post-hoc; (C) DESeq2 false discovery rate-adjusted P value; *P < 0.05; **P < 0.01; ***P < 0.001.

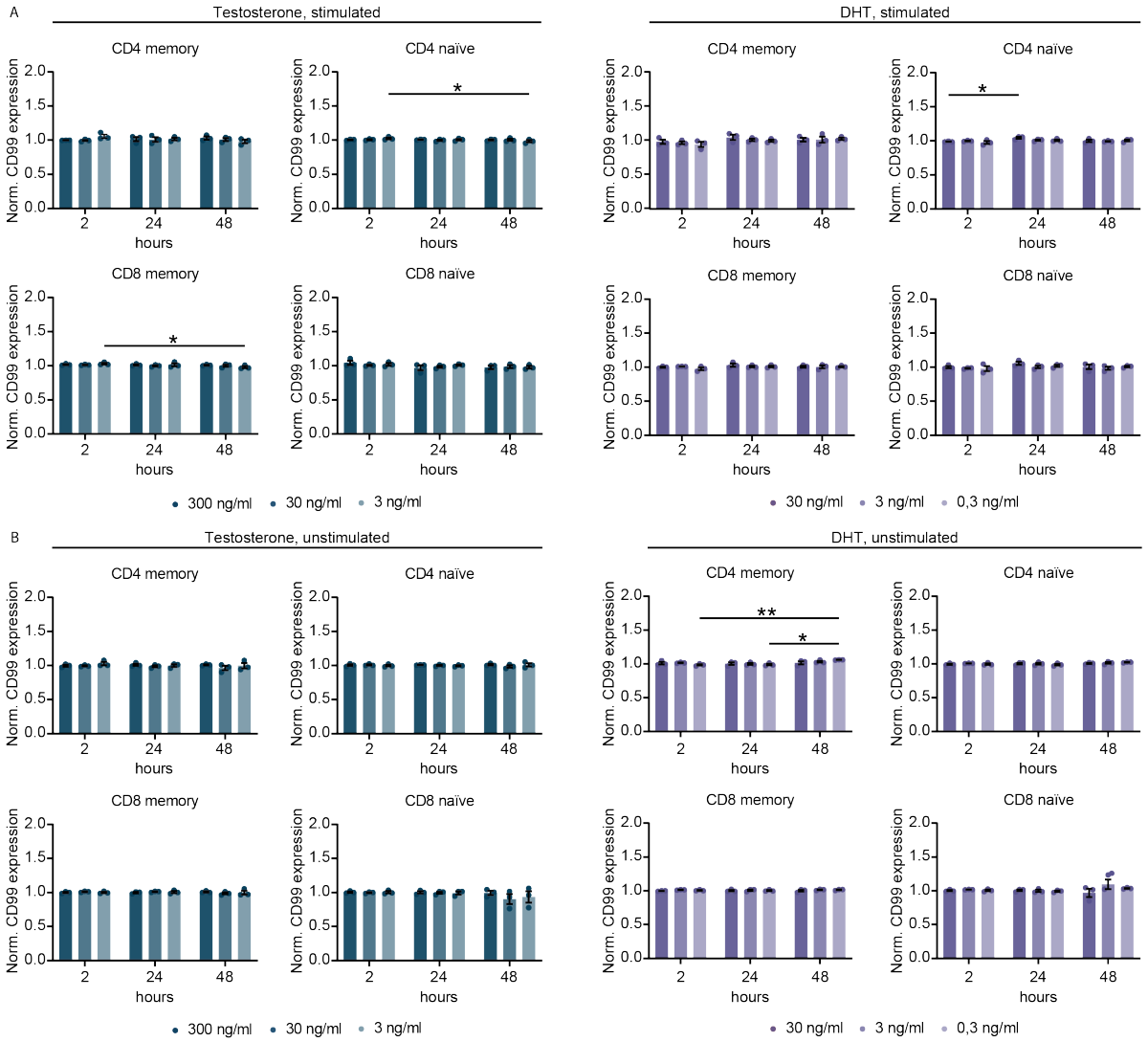

Figure 3.5: Testosterone or DHT treatment of human T cells. (**A**) CD99 surface expression on T cells of anti-CD3 and anti-CD28 stimulated cryopreserved PBMCs (*n* = 3 males) treated with different concentrations of testosterone or dihydrotestosterone. (**B**) CD99 surface expression on T cells of unstimulated cryopreserved PBMCs (*n* = 3 males) treated with different concentrations of testosterone or dihydrotestosterone. Expression values are normalized to the individual vehicle control for every time point. Data are shown as mean ± SEM. Statistics: two-way ANOVA with Tukey post-hoc; **P* < 0.05; ***P* < 0.01; ****P* < 0.001.

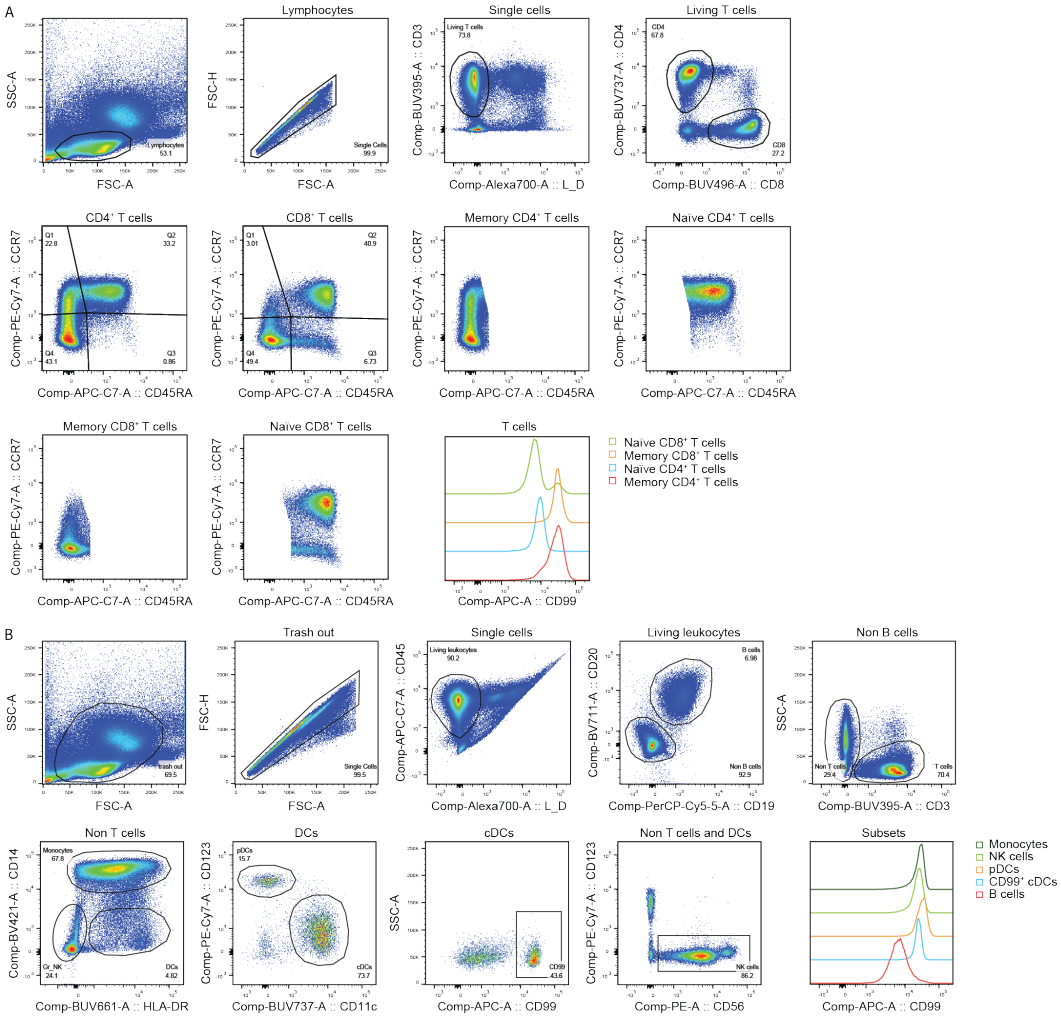

Figure 3.6: Identification of immune cell subsets in trans men cohort. Representative gating strategy for identification of (**A**) T cells, (**B**) DCs, B cells, NK cells and monocytes.

3.3 CD99 increase in the CSF and loss of sex differences driven by male MS patients

Sex-specific differential surface expression of CD99 on T cells and pDCs could possibly contribute to higher female preponderance in autoimmune diseases. To probe whether surface expression changes were altered in autoimmunity, we performed flow cytometry analyses of cryoconserved PBMCs from MS patients (MS) with *n* = 30 individuals per group. Notably, the sex-specific expression pattern observed in healthy individuals (HI) was equally detectable in $CD4^+$ memory and naïve T cells, $CD8^+$ naïve T cells and pDCs in MS patients and there were no expression differences between HI and MS patients (**Figure 3.7A, Figure 3.8**). Hence, differential CD99 expression is not regulated in this autoimmune disease in the peripheral blood, but could still mediate functional differences of T cells and pDCs with relevance for the disease pathogenesis and perpetuation. Such as, CD99 has been proposed to be involved in blood-brain barrier transmigration[279,316]. Therefore, we next analyzed CD99 surface protein expression on T cells from the CSF of MS patients (*n* = 24 females, 9 males) and of

patients with non-neuroinflammatory diseases (NND patients; *n* = 11 females, 5 males). As CD99 is mainly expressed on memory T cells (**Figure 3.1D; Figure 3.7A; Figure 3.9A,B**) and as naïve T cells are basically absent from the CSF (**Figure 3.10**), we quantified CD99 expression on non-naïve T cells and compared expression levels in the CSF to the blood of the same donor drawn at the same day. Indeed, CD99 expression was markedly increased on non-naïve $CD4^+$ T cells and $CD8^+$ T cells in the CSF compared to the peripheral blood in both patient cohorts (**Figure 3.7B**), likely due to the increased ability of CD99 high expressing T cells to transmigrate to the CNS. Of note, we detected an overall lower CD99 surface expression on non-naïve $CD4^+$ T cells in the CSF of MS patients compared to NND patients (**Figure 3.7C).** Stratifying CD99 expression on CSF T cells by sex revealed that lower CD99 expression levels in the MS cohort were solely driven by lower expression in male MS patients, while in women there was no difference between MS and NND patients (**Figure 3.7D**). This lower CD99 expression on T cells in male MS patients led to a loss of the sex-specific expression pattern in the CSF on $CD4^+$ T cells and to a lesser pronounced sex-specific difference in $CD8^+$ T cells in disease context.

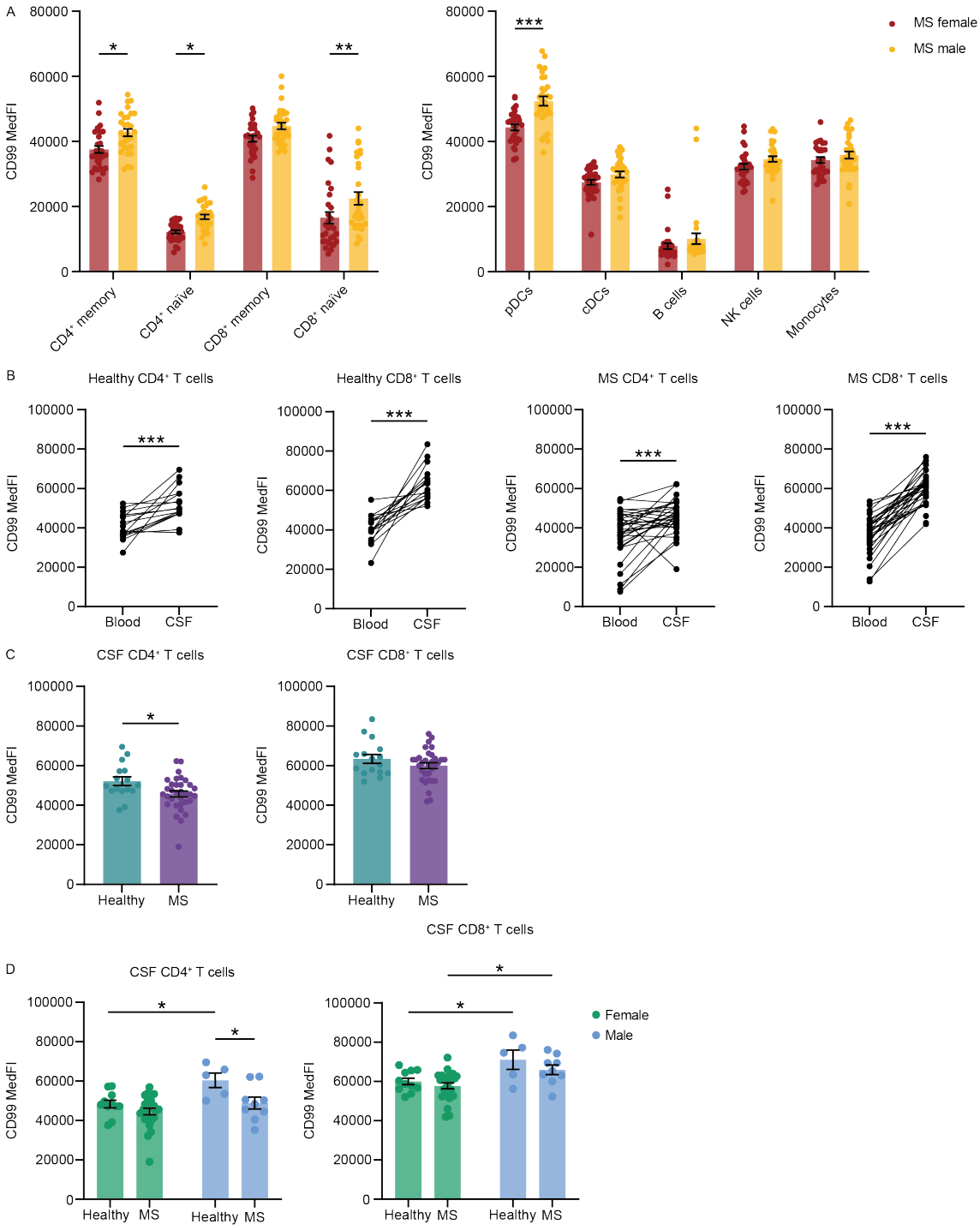

Figure 3.7: CD99 reduction on T cells in the CSF of male MS patients. (**A**) CD99 surface protein expression on subsets of cryoconserved peripheral blood mononuclear cells (PBMCs) from male (*n* = 30) and female (*n* = 30) MS patients as analyzed by flow cytometry. Cell subsets were identified as following: $CD4^+$ and $CD8^+$ memory (gated as living $CD3^+$-$CD4^+$/$CD8^+$-$CD45RA^-$ cells) and naïve (gated as living $CD3^+$-$CD4^+$/$CD8^+$-$CD45RA^+$ cells) T cells; pDCs (gated as living $CD45^+$-Lineage(CD3, CD14, CD19, CD20, CD56)$^-$-$HLA\text{-}DR^+$-$CD11c^-$-$CD123^+$-$CD304^+$ cells); cDCs (gated as living $CD45^+$-Lineage(CD3, CD14, CD19, CD20, CD56)$^-$-$HLA\text{-}DR^+$-$CD11c^+$ cells); B cells (gated as living $CD45^+$-$CD19^+$-$CD20^+$ cells); NK cells (gated as living $CD45^+$-$CD19^-$-$CD20^-$-$CD3^-$-$CD14^-$-$CD56^+$ cells) and monocytes (gated as living $CD45^+$-$CD19^-$-$CD20^-$-$CD3^-$-$CD14^+$ cells). (**B**) CD99 surface expression on freshly isolated T cells in peripheral blood and CSF of non-neuroinflammatory controls (*n* = 16) and MS patients (*n* = 33) as analyzed by flow cytometry. (**C**) Comparison of CD99 expression levels in the same set of non-inflammatory controls and MS patients. (**D**) Sex-specific analysis of CD99 surface expression in the same set of healthy individuals (*n* = 11 females, 5 males) and MS patients (*n* = 24 females, 9 males). Data are shown as mean ± SEM. Statistics: (A) two-

way ANOVA with Tukey post-hoc; (B) Wilcoxon matched-pairs signed rank test; (C) Mann Whitney test; (D) two-way ANOVA with Sidak's post-hoc; *P < 0.05; **P < 0.01; ***P < 0.001.

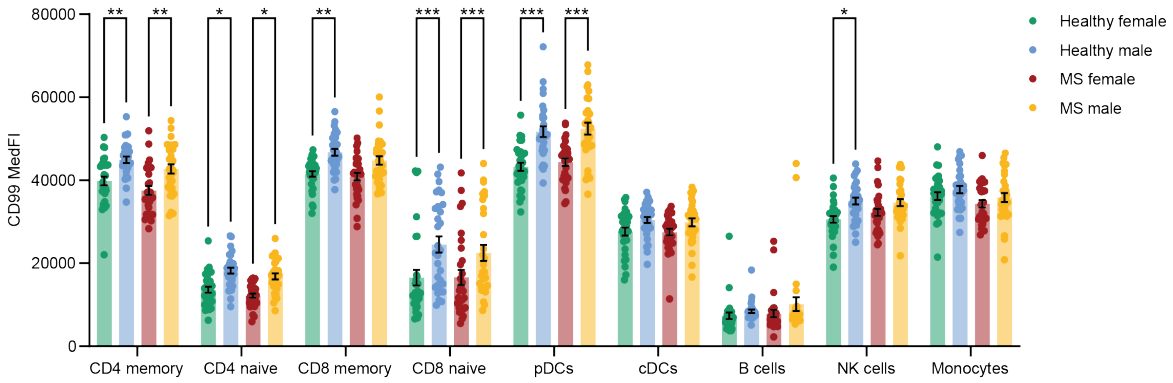

Figure 3.8: CD99 expression in immune cells from healthy individuals and MS patients. CD99 surface protein expression on subsets of cryoconserved peripheral blood mononuclear cells (PBMCs) from male (*n* = 30) and female (*n* = 30) healthy individuals and MS patients as analyzed by flow cytometry. Data are shown as mean ± SEM. Statistics: two-way ANOVA with Tukey post-hoc; *P < 0.05; **P < 0.01; ***P < 0.001.

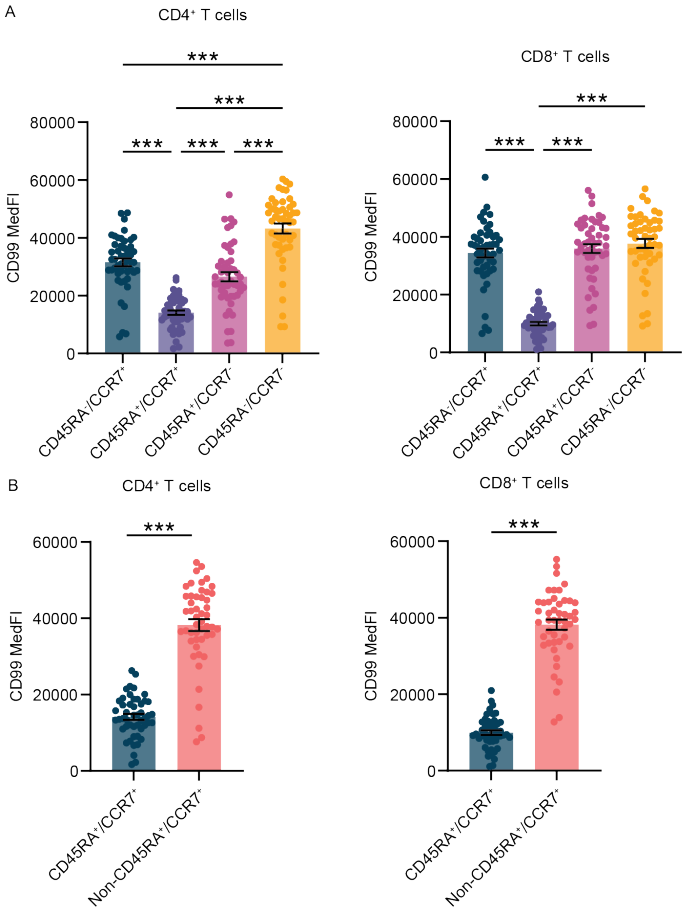

Figure 3.9: CD99 surface expression of memory and naïve T cell subsets. (**A**) CD99 expression levels on freshly isolated $CD4^+$/$CD8^+$ central memory T cells (Q1: $CD45RA^-CCR7^+$), naïve T cells (Q2: $CD45RA^+CCR7^+$), effector T cells (Q3: $CD45RA^+CCR7^-$) and effector memory T cells (Q4: $CD45RA^-CCR7^-$) in a representative individual as analyzed by flow cytometry. (**B**) Comparison of CD99 expression levels of the same individual on freshly isolated naïve T cells (Q2: $CD45RA^+CCR7^+$) and "non-naïve" T cells (Q1: $CD45RA^-CCR7^+$, Q3: $CD45RA^+CCR7^-$ and Q4: $CD45RA^-CCR7^-$ combined). Data are shown as mean ± SEM. Statistics: (A) Friedman test with Dunn post-hoc; (B) Wilcoxon matched-pairs signed rank test; *P < 0.05; **P < 0.01; ***P < 0.001.

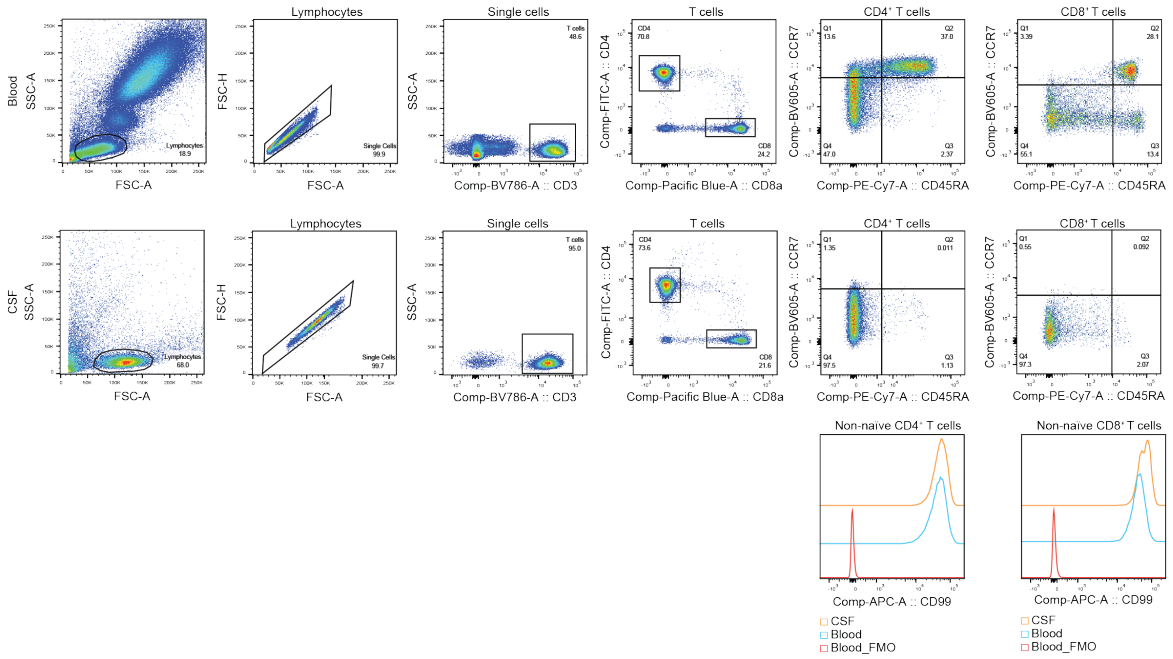

Figure 3.10: Identification of memory and naïve T cell subsets. Representative gating strategy for the characterization of T cell subsets in freshly isolated blood or CSF samples.

3.4 *Cd99*-deficient mice are insufficient to reproduce sex-dosage phenotype in humans

The cause of reduced CD99 expression on T cells in the CSF in male MS patients is difficult to infer and functional consequences are challenging to address in the absence of experimental manipulation in humans. Therefore, we next set out to establish a mouse model to investigate functional consequences of CD99 expression in the CNS. As a first step, we analyzed CD99 surface expression on immune cell subsets in C57BL/6 WT mice. While CD99 levels were increased in B cells and Ly-6C high monocytes of male mice, all other subsets including T cells did not display sex-specific expression patterns and thus failed to reproduce results from human PBMCs **(Figure 3.11A)**. Given the solely genetic and not hormonal regulation of sex-specific CD99 expression patterns in humans and the fact that in mice CD99 is encoded on an autosomal chromosome, this result is not surprising and corroborates our previous findings. To still use mice to address functional consequences of altered CD99 expression, we generated *Cd99*-deficient mice with the idea that the heterozygous knockout mice would show lower CD99 expression, thus reflecting decreased levels that we observed in women. Indeed, we confirmed the absence of CD99 in T cells from the spleen, lymph nodes and from the CNS of homozygous knockout mice and a decreased expression in heterozygous knockout mice **(Figure 3.11B)**. Since CD99 has been shown to participate in T cell proliferation[298], we performed a dye-based cell proliferation assay with T cells from these three genotypes, but did not see any difference in cell proliferation **(Figure 3.11C)**. To probe whether differential CD99 expression could still be of relevance in the animal model

of MS, for example by influencing BBB transmigration, we performed an EAE by active immunization against MOG_{35-55} peptide with these animals for 30 days. Neither did we observe a difference in the clinical course, nor a change in body weight or the day of onset depending on the genotype **(Figure 3.11D)**. Furthermore, we analyzed immune cell infiltration in the CNS in the acute (day 15) and chronic phase (day 30) of EAE. Apart from macrophages, which were more abundant in the homozygous knockout mice compared to the WT littermates at day 15, none of the other immune cell subsets showed a difference **(Figure 3.12)**. To probe whether upregulation of other adhesion molecules could compensate for the loss of CD99 in BBB transmigration, we analyzed surface expression of CD99L2, VLA-4α, VLA-β and LFA-1α of $\alpha\beta$ T cells isolated from the CNS, spleen and lymph nodes of WT, heterozygous or homozygous knockout mice (*n* = 6 per group), but did not detect any differences (**Figure 3.13**). Taken together, these findings demonstrate that although CD99 surface expression levels are stepwise decreased in the three genotypes of our newly generated mouse line and thus might reflect the expression pattern in humans, we did not detect an impact on T cell function *in vitro* and EAE *in vivo*. Sex-specific surface expression pattern of CD99 and its functional consequences seem to be a species-specific trait in humans and can therefore not be analyzed further in the genetic C57BL/6 mouse model.

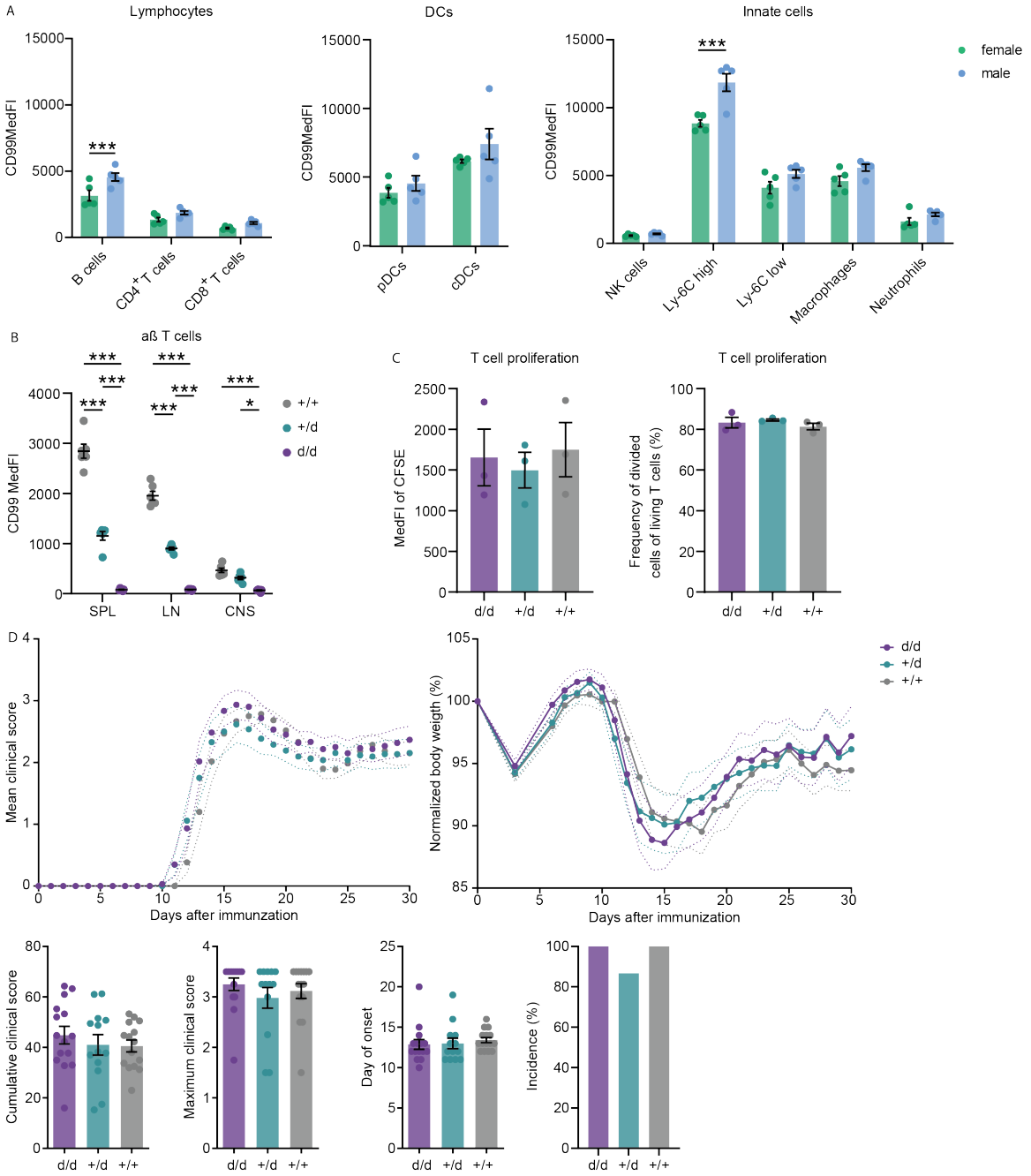

Figure 3.11: *Cd99*-deficient mice show no difference in immune cell function. (**A**) CD99 surface expression of immune cells in C57BL/6 WT mice (*n* = 5 females, *n* = 5 males). (**B**) CD99 surface expression of T cells in homozygous *Cd99*$^{-/-}$, heterozygous *Cd99*$^{-/-}$ and WT littermates (*n* = 4 female d/d, *n* = 2 male d/d, *n* = 3 female +/d, *n* = 3 male +/d, *n* = 3 female +/+, *n* = 3 male +/+). (**C**) Cell proliferation assay with isolated T cells from homozygous *Cd99*$^{-/-}$, heterozygous *Cd99*$^{-/-}$ and WT littermates (*n* = 2 females and 1 male per group). (**D**) EAE course in homozygous *Cd99*$^{-/-}$, heterozygous *Cd99*$^{-/-}$ and WT littermates after active immunization against MOG_{35-55} peptide (*n* = 8 female d/d, *n* = 7 male d/d, *n* = 6 female +/d, *n* = 7 male +/d, *n* = 8 female +/+, *n* = 7 male +/+). Data are shown as mean ± SEM. Statistics: (A) two-way ANOVA with Sidak post-hoc; (B) two-way ANOVA with Tukey post-hoc; (C) Kruskal-Wallis test with Dunn post-hoc; (D) Mann-Whitney U test; *P < 0.05; **P < 0.01; ***P < 0.001.

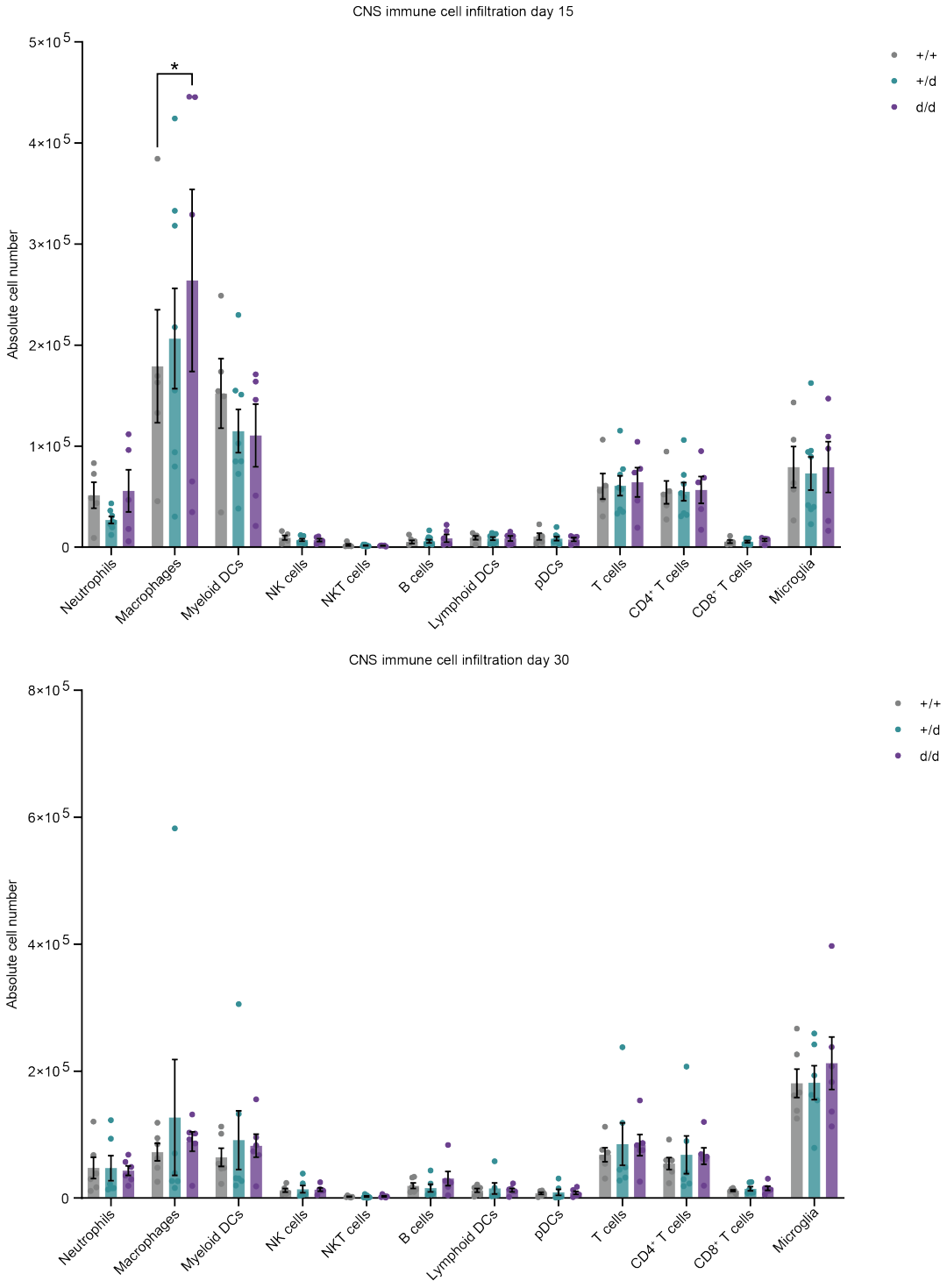

Figure 3.12: Immune cell infiltration of the CNS during EAE. Immune cell infiltration during EAE at acute phase (upper panel, day 15; *n* = 5 male d/d, *n* = 2 female +/d, *n* = 6 male +/d, *n* = 5 male +/+) and chronic phase (lower panel, day 30; *n* = 3 females and 3 males per group). Data are shown as mean ± SEM. Statistics: two-way ANOVA with Tukey post-hoc; *P < 0.05; **P < 0.01; ***P < 0.001.

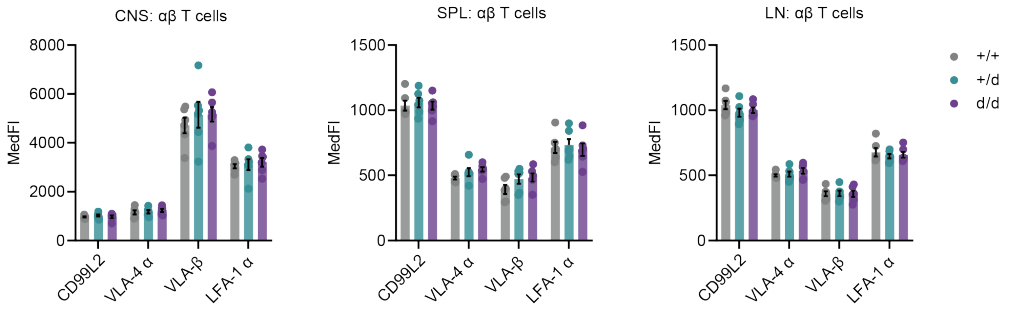

Figure 3.13: Adhesion molecules surface expression of αβ T cells. Surface expression of CD99L2, VLA-4α, VLA-β and LFA-1α of αβ T cells isolated from the CNS, spleen and lymph nodes of WT, heterozygous or homozygous knockout mice (*n* = 4 female d/d, *n* = 2 male d/d, *n* = 3 female +/d, *n* = 3 male +/d, *n* = 3 female +/+, *n* = 3 male +/+) as analyzed by flow cytometry. Data are shown as mean ± SEM. Statistics: two-way ANOVA with Tukey post-hoc; *P < 0.05; **P < 0.01; ***P < 0.001.

3.5 CD99 is induced in primary human naïve T cells upon stimulation

Having shown that the mouse is not a suitable model organism to study sex-specific CD99 function, we focused on human T cell function in *in vitro* assays. While some studies describe CD99 to be involved in T cell activation[296,299] and other studies attribute an inhibitory role[317], the regulation of CD99 itself upon T cell stimulation has not been investigated. To further explore the role of CD99 in human T cell regulation, we first analyzed CD99 dynamics upon T cell stimulation. We detected an induction of CD99 in naïve $CD4^+$ and $CD8^+$ T cells in a time-dependent manner over 72 hours. However, in memory $CD4^+$ and $CD8^+$ T cells, CD99 levels remained stable for 48 hours and were even slightly decreased after 72 hours (**Figure 3.14; Figure 3.15A)**, while upregulation of CD69 on naïve and memory T cells confirmed proper T cell activation of both subsets. We further used a blocking anti-CD99 antibody (mAb; clone hec2) in these assays to probe whether this could have an influence on T cell activation. However, we did not observe altered CD69 expression levels in these conditions **(Figure 3.15B)**, while it has previously been shown that T cell proliferation can be inhibited by CD99 blockade. Together, these results indicate a rapid induction of CD99 on the cell surface of naïve T cells after primary activation until eventually they become memory T cells with no further regulation of CD99 upon re-activation. This suggests CD99 levels to rather reflect a trait of memory T cells than a state.

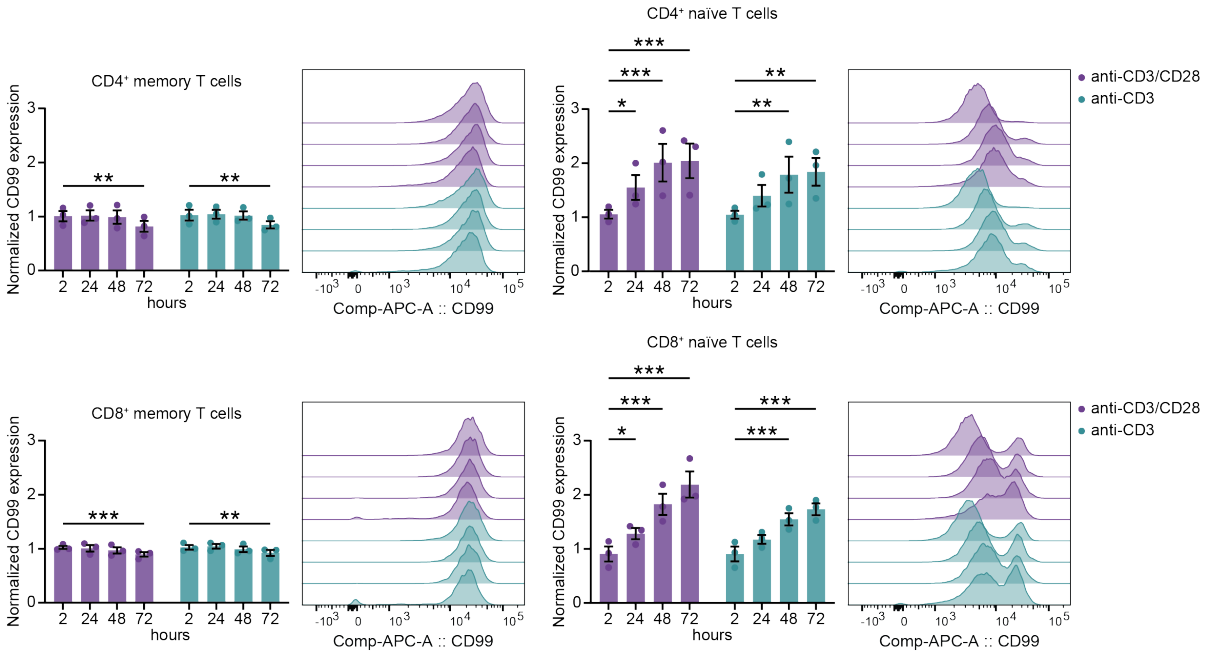

Figure 3.14: CD99 induction in human naïve T cells upon stimulation. Cryopreserved PBMCs from healthy controls (*n* = 3 females) were treated with anti-CD3 and anti-CD28 mAbs and cultured for 72 hours. CD99 surface protein expression of memory and naïve $CD4^+$ T cells (upper row) and $CD8^+$ T cells (lower row) was analyzed by flow cytometry. Expression levels are normalized to the individual uncultured control. Data are shown as mean ± SEM. Statistics: two-way ANOVA with Dunnett post-hoc; *P < 0.05; **P < 0.01; ***P < 0.001.

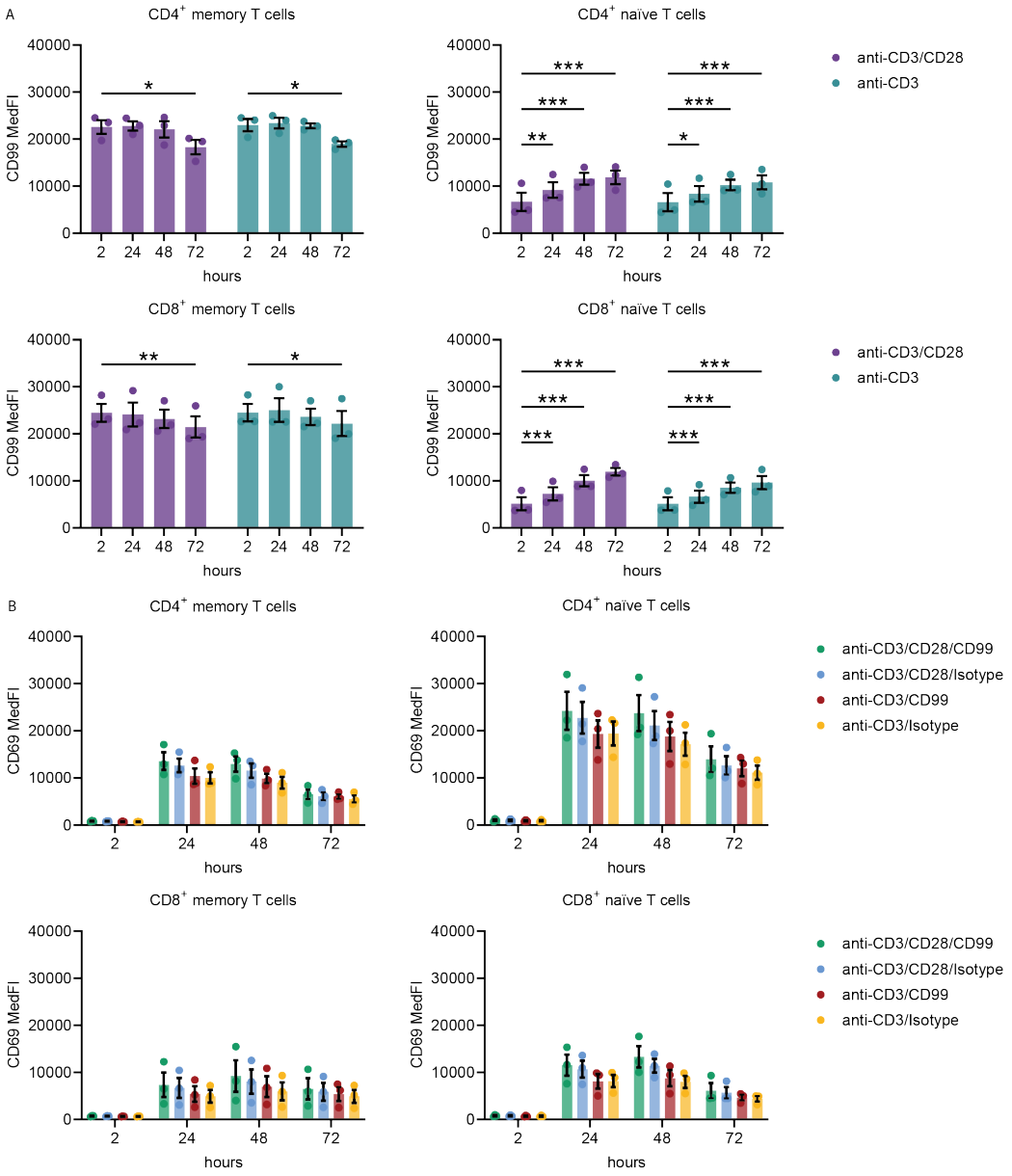

Figure 3.15: CD99 dynamics in human T cells upon stimulation. Cryopreserved PBMCs from healthy controls (*n* = 3 females) were treated with anti-CD3 and anti-CD28 mAbs and cultured for 72 hours. (**A**) Raw CD99 expression values of memory and naïve T cells was analyzed by flow cytometry. (**B**) Raw CD69 expression values of memory and naïve T cells as a marker for T cell activation analyzed by flow cytometry. Data are shown as mean ± SEM. Statistics: (A) two-way ANOVA with Dunnett post-hoc; (B) two-way ANOVA with Tukey post-hoc; *P < 0.05; **P < 0.01; ***P < 0.001.

3.6 CD99 blockade inhibits cell proliferation in primary human T cell monocultures

It has previously been shown that anti-CD99 (mAb clone MT99/3) treatment inhibits T cell proliferation, but this inhibitory effect requires cell-to-cell contact between monocytes and lymphocytes, while soluble mediators produced by monocytes were insufficient to mediate hypo-responsiveness in T cells[298]. To probe whether this inhibition of proliferation by CD99 blockade can be mediated solely to CD99 signaling in T cells, we performed a proliferation assay with T cells in a

monoculture. We stimulated freshly isolated T cells with anti-CD3/anti-CD28, added an anti-CD99 mAb (clone HCD99) and monitored proliferation by cluster formation for seven days. T cell clusters started to form at day two with a steady increase of their cluster size until eventually almost 40% of the analyzed area was covered by clusters at day seven. Notably, CD99 blockade led to an inhibition of T cell proliferation compared to isotype control-treated T cells (**Figure 3.16**). Next, we asked whether expression differences in female and male T cells have a functional impact and analyzed the same samples by sex, but no significant difference in inhibition of proliferation by anti-CD99 treatment was observed (**Figure 3.17**). Together, these data show that specific blockade of CD99 in T cell monocultures is sufficient to inhibit cluster formation and proliferation, but that the effect of CD99 blockade is not different in a small sample size of women and men.

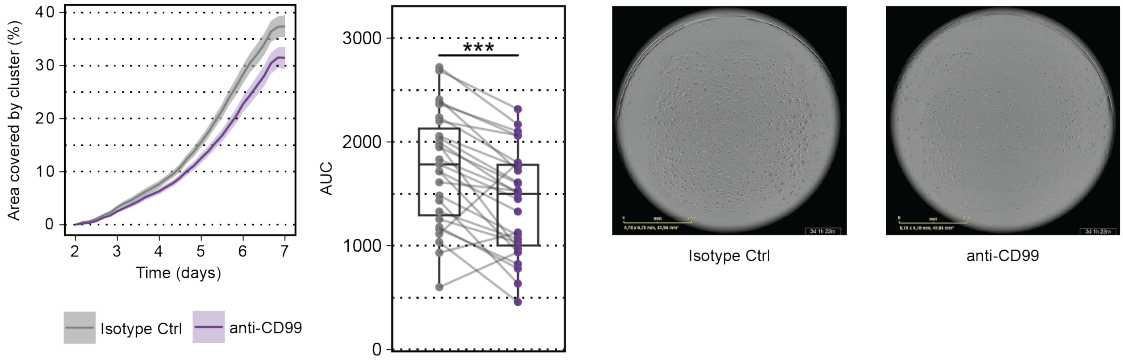

Figure 3.16: CD99 blockade inhibits proliferation in human T cells. Anti-CD3 and anti-CD28 stimulated cryopreserved T cells from 27 healthy controls (*n* = 12 females and *n* = 15 males) were treated with anti-CD99 mAb (clone HCD99) or the respective isotype control antibody and proliferation was tracked by cluster formation in the IncuCyte® S3 for 7 days. Data are shown as mean ± SEM. Statistics: Wilcoxon matched-pairs signed rank test; *P < 0.05; **P < 0.01; ***P < 0.001.

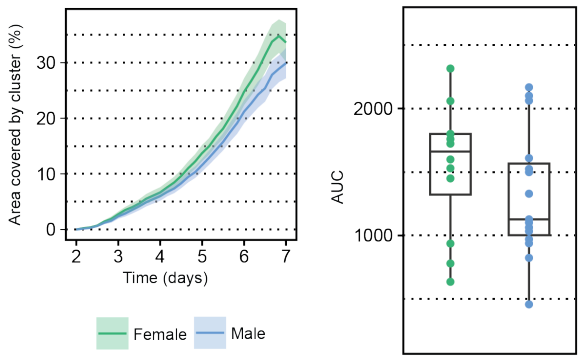

Figure 3.17: Sex-specific analysis of anti-CD99 treatment on proliferation in human T cells. Anti-CD3 and anti-CD28 stimulated cryopreserved T cells from 27 healthy controls (*n* = 12 women and *n* = 15 men) were treated with anti-CD99 mAb (clone HCD99) or the respective isotype control antibody and proliferation was tracked by cluster formation in the IncuCyte® S3 for 7 days. Data are shown as mean ± SEM. Statistics: Wilcoxon matched-pairs signed rank test; *P < 0.05; **P < 0.01; ***P < 0.001.

3.7 Rescue of proliferation inhibition by CD99 reintroduction in T cells *in vitro*

To mechanistically decipher our observation of specific T cell proliferation inhibition by CD99 blockade, we next generated *CD99*-deficient Jurkat cells. With this model we further aimed to probe the reported role of homophilic interaction in cell aggregation[277,318]. Indeed, *CD99* deficiency in Jurkat cells led to diminished cell aggregation and cluster formation compared to WT Jurkat cells (**Figure 3.18A**). To corroborate that reduced cluster formation has an impact on proliferation, we performed proliferation assays with fluorescently labelled dyes and detected a reduction of cell proliferation of *CD99*-deficient Jurkat cells compared to WT Jurkat cells in a time-dependent manner for four days (**Figure 3.18B**). Moreover, this phenotype could be rescued by reintroduction of CD99 by lentiviral transduction with cell proliferation almost reaching the level of WT Jurkat cells (**Figure 3.18B**). As CD99 expression in transduced Jurkat cells did not reach the same level as in WT cells (**Figure 3.18C**), we hypothesized that there is a threshold of CD99 expression that is sufficient for the initiation of cell aggregation and thus proliferation, but not sufficient to maintain the same extent of proliferation as in WT cells over time. Notably, increasing CD99 surface expression levels in WT Jurkat cells by lentiviral transduction even enhanced cell proliferation in those cells compared to unmodified WT Jurkat cells (**Figure 3.18B,C**). Together, these findings demonstrate a crucial role of homotypic CD99 interaction in cell aggregation and proliferation.

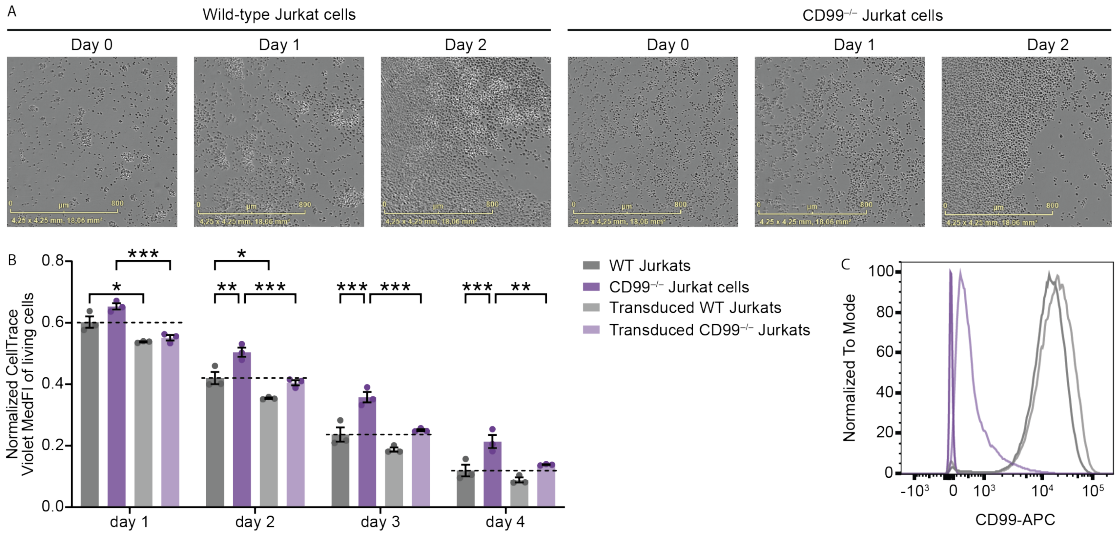

Figure 3.18: Rescue of proliferation inhibition by CD99 reintroduction in Jurkat cells. (**A**) WT or *CD99*-deficient Jurkat cells were tracked by cluster formation in the IncuCyte® S3 for 2 days. (**B**) Cell proliferation in WT Jurkat cells, *CD99*-deficient Jurkat cell clone and its rescued phenotype by lentiviral reintroduction of CD99 (n = 3 biological replicates with 3 technical replicates each). (**C**) CD99 surface expression of WT Jurkat cells, *CD99*-deficient Jurkat cells and their rescued phenotype as analyzed by flow cytometry. Data are shown as mean ± SEM. Statistics: (B) two-way ANOVA with Tukey post-hoc; *P < 0.05; **P < 0.01; ***P < 0.001.

3.8 Identification of novel CD99 ligands and downstream signaling pathways

Although communication between cells is often mediated by membrane protein interactions, the detection of these direct protein-protein interactions (PPIs) remains challenging. Recently, *Liu et al.* developed a proximity-based tagging system, which they call PUP-IT (pupylation-based interaction tagging) that allows deciphering of membrane protein interactions[313]. A small protein tag, Pup, is ligated to proteins, which interact with PafA-fused bait proteins, allowing interactions to be enriched by pull-down methods and profiled by mass spectrometry (**Figure 3.19A**). Pup is a small bacterial protein with 64 amino acids, which can be phosphorylated by PafA, a Pup ligase, and then conjugated to a target protein. This process resembles the ubiquitination process in eukaryotes. We aimed to establish this method to identify undescribed extracellular ligands of CD99 on the surface of other immune cells (**Figure 3.19B**) and intracellular interaction partner (**Figure 3.19C**).

For the extracellular ligand approach, we first cloned a FK506-binding protein (FKBP)-fused CD99 construct, which enables a rapamycin-inducible system to avoid prolonged exposure of PafA on the cell surface (**Figure 3.19B,D**). Rapamycin treatment induces FKBP binding to purified FRB-PafA, resulting in the reassembly of the CD99-PafA protein complex. We transduced *CD99*-deficient Jurkat cells with the FKBP-CD99 vector to ensure that all potential ligands will exclusively bind to PafA-CD99 since Jurkat cells endogenously express CD99 on their surface membrane, which we confirmed by immunofluorescent staining (**Figure 3.19E**). An eGFP domain included in this construct allowed to select and establish a stable polyclonal CD99-FKBP expressing Jurkat cell line, in which we confirmed surface expression (**Figure 3.19F, Figure 3.20A,B**). We then co-cultured rapamycin-treated FKBP-CD99 Jurkat cells in the presence of FRB-PafA and the Pup substrate with CD99-deficient Jurkat cells and analyzed biotin surface expression by immunofluorescent staining and flow cytometry (**Figure 3.19G,H**). Biotin detection was enabled since the Pup substrate was fused to a bacteria-derived biotin-carboxylase domain, termed bio-PupE substrate, so that pupylated proteins on the cell surface can be visualized or purified via biotin-binding strepavidin conjugates. This would allow a streptavidin pulldown followed by mass spectrometry characterization. We were able to detect biotin signal in the condition supplemented with rapamycin, while it was mostly absent in the control setting without rapamycin. However, localization of the biotin signal as well as quantification in flow cytometry indicated that most of the signal was located on the surface of CD99-FKBP cells, whereas CD99-deficient cells were mostly unbiotinylated meaning little interaction between both cell types. To improve cell-cell-interaction, we next incubated CD99-FKBP Jurkat cells with previously labelled $CD45^+$ PBMCs or mScarlet-transfected THP-1 cells (**Figure 3.20C,D**) and quantified biotin signal by flow cytometry. However, the overall biotin signal was very low in both settings (**Figure 3.19I**) suggesting low cell-cell interaction and possible malfunction of purified recombinant FRB-PafA and Pup proteins.

In addition to use only newly purified proteins subsequently, we prolonged incubation time and added Staphylococcal enterotoxin B (SEB) to our culture system. SEB as a so called superantigen can bind to the MHC of APCs and the TCR independent of the displayed antigen on the MHC thus bringing both molecules together. Indeed, these measures increased the biotin signal on $CD45^-$ CD99-FKBP Jurkat cells showing overall functionality of the assay (**Figure 3.19J**). However, the biotin signal on $CD45^+$ PBMCs remained very low compared to control conditions indicating further necessity of improving cell-cell contact. Of note, we also tested another generated monoclonal CD99-FKBP Jurkat cell line, which was derived from the polyclonal CD99-FKBP Jurkat cells by sorting for high eGFP and thus high CD99-FKBP expressing individual cell clones (**Figure 3.20E,F**). Indeed, monoclonal CD99-FKBP Jurkat cells display increased biotin signal and less background staining compared to polyclonal cells. To further optimize culture conditions, we probed different incubation times as well as increased cell numbers and additionally used a different commercially available Pup substrate (bio-DE28), which is already fused to biotin instead of the biotin carboxylase, making it less dependent of endogenous biotin and carboxylase activity. However, these conditions showed almost no biotin signal compared to control conditions and increased background biotin signal compared to previous settings (**Figure 3.19K**). As also subsequent conditions with newly purified FRB-PafA and mScarlet-transfected THP-1 cells failed, assay conditions are still being optimized as ongoing work.

In addition to identify CD99 ligands, we aimed to use this technique in a related fashion to decipher binding proteins involved in the signaling cascade by fusing the PafA protein to the intracellular C-terminus of CD99 in *CD99*-deficient Jurkat cells **(Figure 3.19C)**. Similar to the previous approach, proteins involved in CD99 signaling will be pupylated in the presence of the bio-PupE substrate, which allows us to perform a streptavidin pulldown followed by mass spectrometry. Beside already described proteins like sAC or PKA, we expected to identify unknown signaling partners with possible sex-specific expression and downstream regulation, which can be further analyzed after identification. However, as we focused on extracellular ligand identification, we successfully cloned the corresponding CD99-PafA, control CD28-PafA as well as the inducible intracellular PupE constructs and generated lentiviruses carrying these constructs (**Figure 3.20G**), but did not perform any pupylation assay until submission of this thesis.

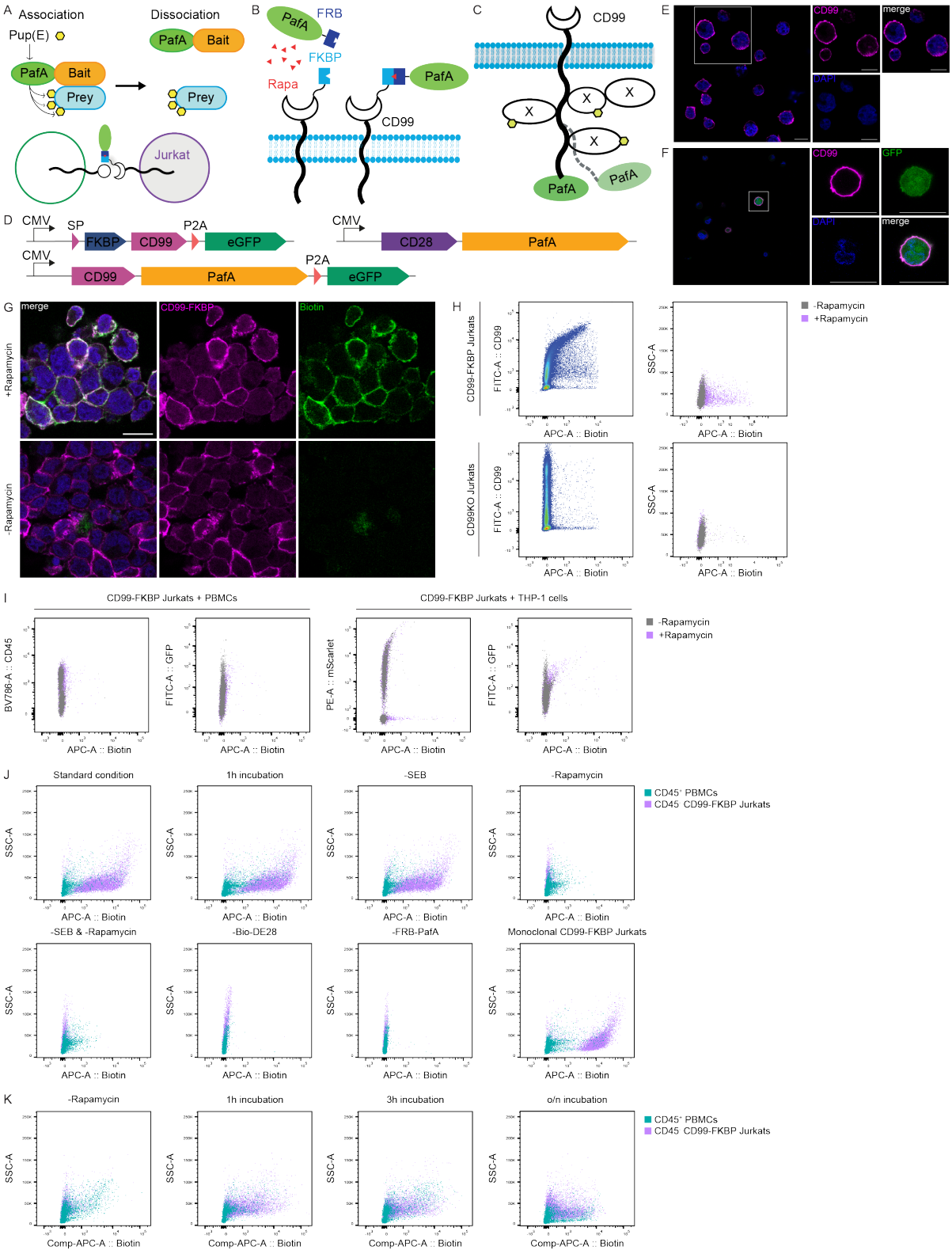

Figure 3.19: CD99 ligand identification via proximity-tagging. (**A**) Schematic design of the PUP-IT proximity-tagging system, in which PafA is fused to a bait protein facilitating PupE modification of prey proteins in close vicinity. (**B**) Inducible PUP-IT system to label extracellular surface proteins. (**C**) Intracellular PUP-IT system to label cytosolic interacting proteins of membrane receptors. (**D**) Schematic overview of CD99 pupylation constructs. (**E, F**) Immunofluorescent staining of CD99 in (E) WT Jurkat cells or (F) CD99-FKBP Jurkat cells. Scale bars: 10 µm. (**G**) Immunofluorescent staining of biotin in pupylated CD99-FKBP Jurkat cells. Costaining for CD99. Scale bars: 10 µm. (**H-K**) Optimization of cell-cell interaction for trans-pupylation as quantified by flow cytometry. *Figure A-C modified from Liu Q et al. Nat Methods. 2018 Sep;15(9):715-722*[313].

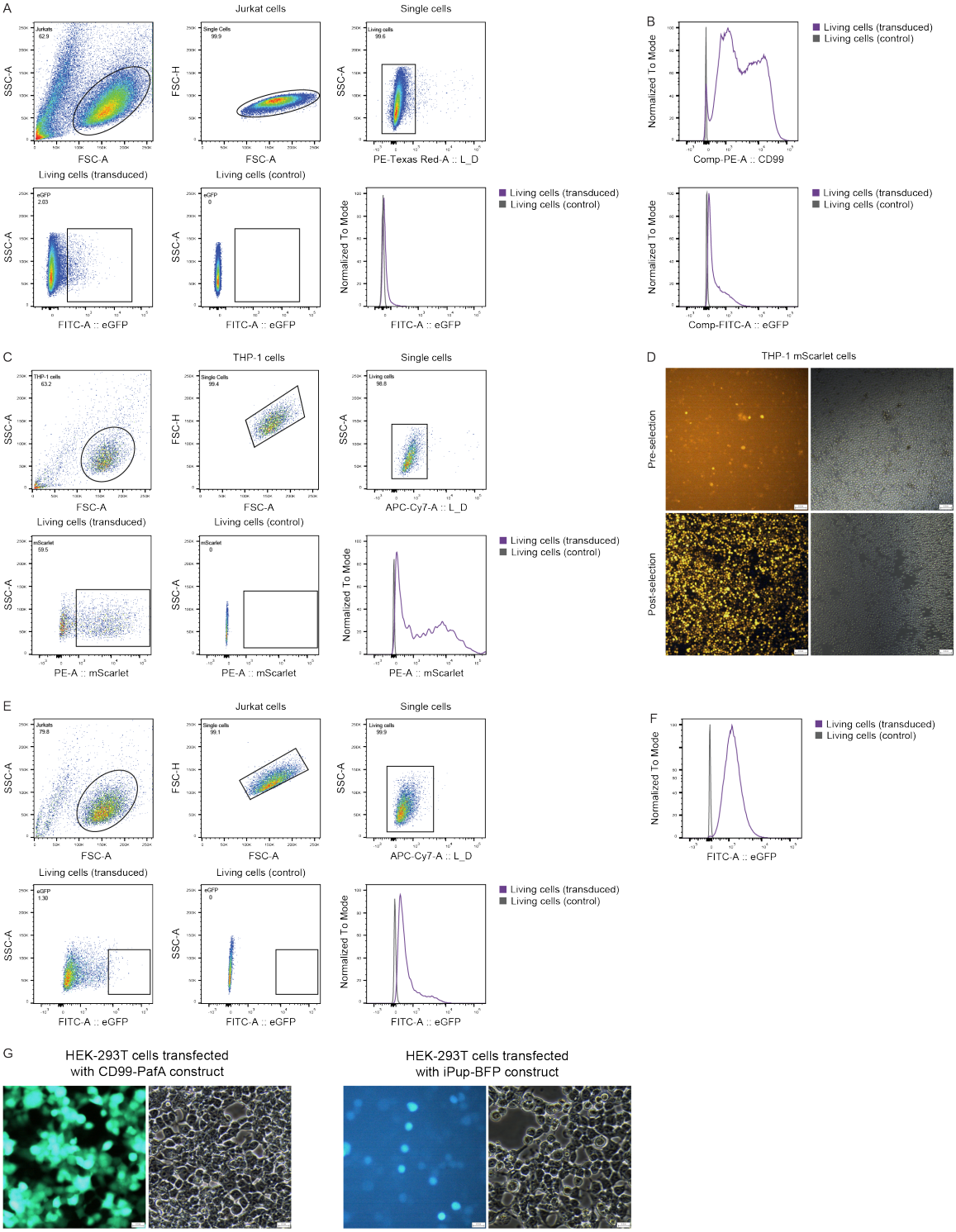

Figure 3.20: Stable cell line generation. (**A**) Generation and (**B**) validation of stable polyclonal CD99-FKBP Jurkat cells as analyzed by flow cytometry. (**C**) Generation and (**D**) validation of stable polyclonal THP-1 mScarlet cells as analyzed by flow cytometry and epifluorescence microscopy. (**E**) Generation and (**F**) validation of stable monoclonal CD99-FKBP Jurkat cells as analyzed by flow cytometry. (**G**) Lentivirus generation by HEK293T cell transfection with respective CD99-PafA or iPup-BFP constructs as analyzed by epifluorescence microscopy.

4 Discussion

Sex is a critical biological variable in development and pathogenesis of autoimmune diseases including MS[152,163,186,187]. Here, we show that transcriptional regulation by both sex chromosomes, but not hormonal regulation, leads to sex-specific CD99 surface expression on immune cells, which is partially lost in the CSF of MS patients. However, these sex differences are human-specific as we do not see sexually dimorphic regulation in mice. Considering CD99 impact on T cell activation, proliferation and migration, our findings pronounce the necessity of including sex as an important factor influencing the phenotypical outcome of immune responses in women and men.

4.1 Insufficient Xi allelic transcription as main driver of sexually dimorphic CD99 expression

We found that *CD99* mRNA expression in the spleen and CD99 protein levels on the surface of T cells, pDCs and NK cells were higher in men. This sexual dimorphism is most likely explained by full CD99 expression from the PAR of both, the X and Y chromosome in men, while in women CD99 expression from one X chromosome is reduced due to XCI as it has been shown for the majority of genes in the PAR1[193]. Although *CD99* can escape XCI, it appears that transcription from the Xi cannot compensate for the Y-encoded expression. This is supported by our data about XCI escape of *CD99* in pDCs of a female donor with 41.9% biallelic expression. However, this needs to be analyzed comprehensively in a similar approach using an adequate sample size of female and male donors and with different probes for X- and Y-encoded transcription. This would also allow inclusion of T cells among other cell types.

A possible reason why we do not see a sexual dimorphism of CD99 expression in other immune cell subsets like cDCs, B cells and monocytes could be cell-type-specific regulation of XCI. This was recently shown for B cell-specific *XIST* complexes driving cell-type-specific diversification[319]. While it has been previously assumed that *XIST* is only required for the initiation but not for the maintenance of the Xi, the authors identified a subset of X-linked genes, including *TLR7*, which require constant *XIST* RNA expression to maintain gene expression dosage in B cells[320]. Loss of *XIST* resulted in overexpression of *XIST*-dependent genes in a subset of $CD11c^+$ atypical B cells, often found in SLE patients. Therefore, general analysis of these atypical B cells in MS patients as well as assessment of *CD99* expression behavior in B cells and other immune cells with loss of *XIST* would be worth investigating. In general, XCI escapees can be classified as ‘constitutive’ or ‘facultative’[192]. Constitutive escapees are expressed in most cell types, whereas facultative escapees appear to be silenced and then reactivated and can be lineage specific and differ between individuals, developmental stages or ages.

4.2 Androgens are dispensable for CD99 regulation

Supporting the hypothesis of incomplete XCI as driver of the sexual dimorphism in CD99 expression, we could not find evidence for hormonal regulation. Besides non-genomical signaling, the classical perspective of androgen action on gene regulation is that testosterone is intracellularly converted into its more potent bioactive form DHT, which binds to the AR with high affinity[321]. This results in removal of the heat-shock protein and binding to importin-α to translocate into the nucleus, where receptor dimers bind to androgen response elements (AREs) in promoter regions of target genes to enhance or repress transcription. Analysis of AREs in *CD99* promoter regions needs further investigation. However, our *in vitro* as well as *ex vivo* human data propose no interaction between androgen signaling and CD99 surface expression levels in T cells.

Since we observed higher CD99 levels in men, we assessed the induction of CD99 upon androgen signaling, but suppression of CD99 by estrogens could be an additional mechanism driving sex disparity. Estrogens include estrone (E1), estradiol (E2) and estriol (E3) with estradiol being the primary biologically active estrogen exerting its pleiotropic effects in immune cells through nuclear ERα and ERβ as well as through the membrane-bound G-protein-coupled estrogen receptor (GPER)[322]. Similar to testosterone, E2 binds to genomic ERs, which translocate to the nucleus, where they bind to estrogen response elements (EREs) and cause transcriptional changes including EREs in immune-related genes such as *IL10* and *TLR7*[322]. Thus, assessing E2 effects on CD99 expression in immune cells and T cells in particular could reveal specific regulation pathways in females, which has not been explored yet.

4.3 Genetical differences prohibit sexual disparity of CD99 in mice

Studying sex differences in humans is challenging. To investigate functional consequences of sexually dimorphic CD99 expression in more detail, we aimed to transfer our findings into the mouse model. Though, CD99 surface expression was not different in female and male T cells in C57BL/6 mice. This discrepancy in mice and humans could at least be partially attributed to the unique genetical features of *CD99*. In humans, together with *Xga* and CD99 antigen-like 2 (*CD99L2*), which are also located in the PAR, CD99 composes a family of proteins, for which no homology to any other known family is reported[323]. Additionally, CD99 homologs were only found in primates and the mouse ortholog (D4) shows only 46% protein homology with human CD99 and is located on chromosome 4[324]. It is thought that the *CD99* orthologous genes of carnivores and artiodactyls should be located in the PAR and that human and mouse *CD99* developed differently with the translocation of mouse *Cd99* to an autosome after the divergence of rodents and other non-primate eutherians[324]. With mouse *Cd99* located on an

autosome, the absence of sexual dimorphism of CD99 expression in mice is plausible and further corroborates differential expression from the Xa or Xi and/or the Y chromosome as driver of the sexual dimorphism in CD99 expression in humans instead of hormonal regulation. Unique genetic properties of murine *Cd99* resulted in missing annotation in many datasets including ImmGen and Tabula Muris and its missing representation in sex-specific analysis of such datasets[325,326].

4.4 Compensatory mechanisms and mouse strain differences as potential cause of absent functional consequences after genetic *Cd99* ablation

To circumvent the absence of sexual dimorphism in mice, but still use a mouse model for mechanistic analyses of consequences of differential CD99 expression, we newly generated *Cd99*-deficient mice and used heterozygous littermates as female mimics. However, we did not observe any differences in T cell proliferation between WT, homozygous or heterozygous knockout mice, which suggests that CD99 is not involved in mouse T cell activation or that in the knockout condition compensatory mechanisms are able to fully restore T cell function. Additionally, although anti-CD99 treatment was shown to ameliorate the disease course in EAE[279], we did not observe any impact of genetic ablation of CD99 on clinical symptoms or body weight change in EAE. This discrepancy might be at least partially explained by compensatory mechanisms, such as upregulation of other cell adhesion molecules. However, we detected no differences in the expression of other adhesion molecules, such as LFA-1, VLA-4 or CD99L2, another CD99 paralog in mice, that could compensate for the loss of CD99. As these are only three adhesion molecules among a huge variety, RNA sequencing of *Cd99*-deficient T cells would enable a more comprehensive analysis and could reveal additional compensatory mechanisms.

Moreover, the reported anti-mouse CD99 mAb (clone 3F11) for the treatment of EAE animals was generated in-house. Its mode of action might include activating or blocking capacities of CD99. Thus, reproducing these findings with different anti-CD99 mAbs, for which the mode of action has been defined, such as the blocking clone hec2, would contribute to the understanding of the opposing effects of pharmacological inhibition and genetic inhibition in EAE. In addition, the EAE showing an effect of antibody treatment was carried out in female SJL mice, while we executed EAE in female and male CD99-deficient C57BL/6 mice, which might be another reason for different disease course as strain differences in EAE severity and outcome depending on mouse strain and sex are well known. As such, serum testosterone levels are elevated in male SJL mice compared to C57BL/6 mice impacting immune cell funtion[101]. Although we did not observe CD99 regulation by androgens in human T cells *in vitro*, strain differences could nevertheless impact EAE outcome. Hence, backcrossing *Cd99*-deficient C57BL/6 mice to the SJL strain would enable to investigate effects of *Cd99*-deficiency in SJL mice. Even

though we did not detect compensatory developmental effects on expression of adhesion molecules LFA-1, VLA-4 or CD99L2 on T cells, global *Cd99* knockout might influence cell function across all tissues as it is expressed in almost any human cell types with particularly high levels in immune cells, thymocytes and endothelial cells[287]. To prevent this, generation of a conditional Lck-Cre or Tie-2-Cre driven gene inactivation would allow investigation of cell-specific *Cd99* loss in T cells or endothelial cells. Alternatively, adoptive transfer EAE of MOG-reactivated *Cd99*-deficient T cells into Rag1-deficient mice, which lack mature T and B cells, facilitates examination of CD99-specific effects on T cell function during EAE. While transfer of MOG-reactivated *Cd99*-deficient T cells into *Rag1*-deficient recipient mice would enable to analyze *Cd99*-deficiency of T cells in particular, transfer of MOG-reactivated WT T cells into *Rag1-/Cd99*-deficient mice would allow to probe the relevance of *Cd99*-deficiency in other cells but T cells, such as endothelial cells. Furthermore, to examine the importance of homotypic CD99-CD99 interaction of T cells with other cells, transfer of MOG-reactivated *Cd99*-deficient T cells into *Rag1-/Cd99*-deficient recipient mice could be performed. Transfer of MOG-reactivated WT T cells into *Rag1*-deficient recipient mice would serve as a control. Analysis of EAE severity as well as immune cell infiltration into the CNS during the acute phase would disentangle mechanisms of *Cd99*-deficiency beyond a global knockout.

Although *Cd99l2* shares 45% homology with the human *CD99* gene and 81% homology with human *CD99L2* gene, there is only limited overlap in function[323]. Nevertheless, expanding the analysis of CD99L2 and its potential compensatory role in *Cd99*-deficient mice might be worthwhile as an interaction between these two molecules has been shown[327]. Moreover, anti-CD99L2 antibodies blocked neutrophil recruitment into the inflamed peritoneum and cremaster[286,328,329] and genetic inactivation of the *Cd99l2* gene revealed its importance for the entry of lymphocytes and neutrophils into inflamed tissues[330]. Of note, it has been shown that conditional Tie-2-Cre driven gene inactivation of *Cd99l2* inhibits leukocyte entry into the CNS during MOG_{35-55}-induced EAE and alleviates severity of the disease[331].

4.5 Relevance of sex-specific CD99 expression in MS

Similar to human healthy individuals, we observed increased CD99 expression in male MS patients. Because of its association with T cell activation and transmigration, we initially hypothesized increased CD99 expression in MS patients, which could be a driver of an overall higher inflammatory state, but we did not find any significant differences between MS patients and healthy individuals in the peripheral blood. However, in CSF samples we detected increased CD99 levels on T cells compared to peripheral blood in every individual regardless of disease state. This is in accordance with a recent single-cell analysis of blood and CSF leukocytes that revealed *CD99* to be more abundant on $CD4^+$ and

$CD8^+$ T cells in the CSF[77] as well as on CSF-resident $CD4^+$ T cells[332] of non-inflammatory controls and MS patients. In another study, transcriptomic profiling of T cells from the peripheral blood and CSF of healthy individuals and MS patients by scRNAseq revealed *CD99* to be moderately upregulated in the blood and CSF of MS patients compared to healthy individuals[333], which is contrary to our data of CD99 protein expression. Furthermore, the authors examined two additional datasets of T cells in brain parenchyma. One was generated by performing single-nucleus RNA sequencing (snRNAseq) from post-mortem (*n* = 2 donors) and normal-appearing tissue during epilepsy surgery (*n* = 1 donor) and the other was an existing scRNAseq dataset from freshly processed normal-appearing brain tissue during epilepsy surgery (*n* = 3 donors). In both datasets, T cells display higher CD99 expression compared to non-T cells in brain parenchyma (snRNAseq: 37% T cells vs 3% non-T cells; scRNAseq: 52% T cells vs 21% non-T cells) with overall increased mean expression as indicated by log2 fold change. In addition, candidate pathways of communication between T cells and parenchymal cells within the brain were identified using the CellPhoneDB software, which enables to study cell-cell communication from single-cell transcriptomics data[334]. Of note, an interaction between *CD99* and *PILRA* has been described, although further validation on protein level needs to be executed.

Of note, in our cohorts male MS patients showed lower CD99 levels on $CD4^+$ T and $CD8^+$ T cells in the CSF in comparison to male patients with non-neuroinflammatory diseases. This could be explained by a suppression or lack of induction of CD99 through inflammatory processes in the CNS to prevent hyper-inflammation. However, we could not detect regulation of CD99 expression in response to TCR activation in memory cells *in vitro*. Alternatively, CD99 decrease in the CSF of MS patients could also be due to CD99 downregulation after recognition of its ligand resulting in a residency of activated T cells at the site of inflammation. Another explanation for reduced CD99 expression in the CSF in MS could be that during CNS inflammation, $CD4^+$ T cells with lower CD99 expression are able to transmigrate from the periphery to the CNS compartment leading to an overall lower CD99 expression in the CNS due to a leakier BBB. CD99 involvement in T cell transmigration has been extensively studied[286-290,292,293], but none of these studies took sex-specific differences into account. We focused on effects of CD99 blockade and genetic ablation on T cell activation and in turn proliferation, but studying the role of CD99 in transmigration in a sex-specific manner would shed light on further consequences of the sexual dimorphism in CD99 expression.

4.6 Possible implications of CD99 ligands and downstream signaling for homeostatic equilibrium in sexes

In the context of altered CD99 expression on T cells in the CSF, differential expression of CD99 ligands could be an additional factor contributing to functional differences between females and males as it influences the homeostatic equilibrium. Besides its homophilic interaction[277], the existence of other CD99 ligands has been proposed[298-300], such as the GDF6 prodomain, which maintains EWS growth[294] or the PILRs, capable of binding mouse CD99[301,302]. However, there is currently not much known about their sex-specific differential expression in males and females as well as their expression in different organs and cell types. In our GTEx analysis, neither *GDF6*, nor *PILRA* (encoding PILRα) or *PILRB* (encoding PILRβ) showed sex-specific regulation.

Here, we modified a pupylation based proximity labeling assay to identify possible additional CD99 ligands in PBMCs as a heterophilic cell population to broaden the interaction spectrum. Indeed, we were able to detect an adequate biotin signal on CD99-FKBP Jurkat cells itself demonstrating overall assay functionality. However, cell-cell interactions remained sparse as detected by little biotin signal on interacting cells showing necessity for further assay optimization. One essential difficulty could be implicated in PafA itself as it is a rather large enzyme of 55 kDa, which could interfere with bait protein function. To circumvent this, the same group developed an advanced PUP-IT2 system, in which only a small 7 kDa protein is used achieving equal labeling efficiency[335]. Moreover, in this approach bio-PupE is directly fused to the bait protein with addition of recombinant PafA resulting in less labeling background from self-labeling.

In the same manner, sex-specific regulation of CD99 downstream signaling could mediate differences in protein function and thus impacting differential T cell properties in females and males. A more efficient amplifying of effector signaling molecules in women could compensate for less surface protein expression. Hence, identifying interacting downstream molecules by finalizing the adaptation of the intracellular pupylation approach to our model system would shed light onto these aspects. In addition, this would provide further molecules, which could serve as readouts in immunological assays as assessment of phosphorylation of extracellular signal-regulated protein kinase1/2 (ERK1/2) and cAMP response element-binding protein (CREB) phosphorylation, as it has been shown in EWS cells[336], did not deliver reliable results in our hands (data not shown).

In EWS cells, clofarabine, which is an FDA approved drug for the treatment of acute lymphoblastic leukemia has been demonstrated to directly interact with CD99 and to induce ERK1/2, mitogen and stress activated kinases 1/2 (MSK1/2) and CREB activation[336]. As also cladribine, a similar purine analogue to treat leukemia, directly interacts with CD99[337] and has been repurposed for the treatment

of multiple sclerosis, we tested these two compounds in our T cell proliferation assays. Although utilized in very low doses, viability of T cells was very low, since both drugs eliminate lymphocytes as a mode of action. However, recently the same group designed and validated new nucleosidic CD99 inhibitors, BK50164 and BK60106, derived from clofarabine and cladribine by modifying the chemical structure[338]. Both compounds caused cell death in EWS cells due to inhibition of CD99, which is not mediated via inhibition of DNA synthesis allowing their application in our T cell assays.

4.7 CD99-dependent cell clustering as a prerequisite for T cell proliferation and activation

We found that CD99 expression is induced in naïve T cells upon TCR activation, while memory T cells did not regulate CD99 expression in response to activation. Induction of CD99 upon T cell activation stresses its importance in T cell regulation and indicates that CD99 acts as a co-stimulatory factor in T cell activation[287,296]. Engagement of CD99 and suboptimal anti-CD3-induced T cell activation was comparable to that obtained with anti-CD3/anti-CD28[296] and enhanced the expression of several T cell activation markers and cytokines on anti-CD3-stimulated T cells[299,339]. Additionally, we observed inhibition of homotypic T cell clustering by anti-CD99 mAb, which indicates a crucial role of CD99 for T cell clustering as a prerequisite for T cell activation. CD99 might be essential in maintaining T cell clusters via its homophilic interaction as it has been described for LFA-1/ICAM-1[340]. Along that line, CD99 has been reported to form complexes with MHC-I, MHC-II and tetraspanin CD81 and is associated to the formation of the immunologic synapse[297,317] as well as translocation of TCR complexes to the lipid raft[296]. Our data showing inhibition of T cell proliferation in primary human T cells by anti-CD99 treatment *in vitro* complements previous findings. While agonistic mAb treatment (clone 3B2/TA8) has been shown to induce proliferation in resting peripheral blood T cells[295], other studies found an inhibition of T cell proliferation with anti-CD99 mAb (clone MT99/3) in PBMCs[317] or in a co-culture of T cells and monocytes[298]. Additionally, by CD99 reintroduction and subsequent rescue, we could attribute these findings to CD99 properties. Considering all these findings, one can speculate that a lower expression of CD99 in women is a counterregulatory mechanism to compensate for an overall lower activation threshold of female T cell activation[163].

4.8 CD99 function in other immune cells

Apart from T cells, a very recent study explored CD99 engagement in macrophages in context of EWS pathogenesis[341]. It was shown that *in vivo* anti-CD99 diabody treatment reduced EWS growth in mice and ligation of CD99 on EWS cells induced their phagocytosis by macrophages *in vitro* by upregulation

of phosphatidylserine, an ‘eat me‘ signal, and a downregulation of CD47, a ‘don’t eat me‘ signal, on EWS cells. Intriguingly, ligation of CD99 on murine macrophages induced their polarization towards an inflammatory M1-like phenotype. Although we did not specifically include macrophages in our flow cytometric analyses, we observed high CD99 expression on human monocytes as well as on murine monocytes and macrophages. In mice, Ly6C-high monocytes even display highest and sex-specific expression in our analysis. As macrophages are the most abundant immune cells in acute inflammatory MS lesions, exploring CD99 in human macrophages as well as sex-specific regulations in murine macrophages could be one opportunity to expand our analysis to other immune cells.

4.9 Conclusion and remarks

Taken together, we were able to show that CD99 is regulated on a genetic level in a sex- and species-specific manner and functionally contributes to T cell costimulation in humans. These findings stress the relevance for stratification of immunological data by sex and for taking species differences into account. While exploring human properties is a reasonable starting point to begin research, we aimed to investigate these findings more in depth and mechanistically in mice, but were unable to transfer these findings to our Cd99-deficient C57BL/6 model. To overcome the absence of sexually dimorphic CD99 expression in mice and the missing phenotype in EAE, further refinement of our mouse models by passive immunization protocols, usage of different mouse strains or treatment with different anti-CD99 antibodies would be the next steps. Differential regulation of CD99 on CSF T cells in female and male MS patients might hint to a functional sex-specific involvement of CD99 in MS pathogenesis, but warrants further investigation. Higher CD99 expression levels in men are difficult to interpret given the higher incidence of MS in women and its involvement in T cell regulation. Taking an accelerated disease progression in male MS patients into consideration, exploring different mechanisms of CD99 in immune cell regulation is crucial in understanding its role in autoimmunity. Another important step to get a comprehensive understanding of CD99 contribution to disease pathogenesis will be the identification of CD99 ligands as well as downstream signaling molecules as important variables in a diverse interplay. All in all, considering sex differences in basic research and clinical studies will pave the way for sex-specific personalized treatment.

5 Summary

Differences in immune responses between women and men are leading to a strong sex bias in the incidence of autoimmune diseases that predominantly affect women, such as MS. MS manifests in more than twice as many women, making sex one of the most important risk factors. However, it is incompletely understood which genes contribute to sex differences in autoimmune incidence. To address that, we conducted a gene expression analysis in female and male human spleen using the GTEx project dataset to identify differentially expressed genes between women and men. We identified the transmembrane protein CD99 as one of the most significantly differentially expressed genes with marked increase in men. CD99 has been reported to participate in immune cell transmigration and T cell regulation, but sex-specific implications have not been comprehensively investigated.

Here, we found higher *CD99* gene expression in male human spleens compared to females and confirmed this expression difference on protein level on the surface of T cells and pDCs. Hormones were ruled out as the cause by *in vitro* assays and *ex vivo* analysis of trans men samples. In CSF, CD99 was higher on T cells compared to blood. Of note, male MS patients had lower CD99 levels on $CD4^+$ T cells in the CSF, unlike controls. By contrast, female and male mice had similar CD99 expression and *Cd99*-deficient mice showed equal susceptibility to EAE compared to WTs. Functionally, CD99 increased upon human T cell activation and inhibited T cell proliferation after blockade. Accordingly, *CD99*-deficient Jurkat cells showed decreased cell proliferation and cluster formation, rescued by CD99 reintroduction.

Our results demonstrate that CD99 is sex-specifically regulated in healthy individuals and MS patients and that it is involved in T cell costimulation in humans but not in mice. CD99 could potentially contribute to MS incidence and susceptibility in a sex-specific manner.

6 Zusammenfassung

Unterschiede im Immunsystem von Frauen und Männern führen zu einer starken geschlechtsspezifischen Verteilung beim Auftreten bestimmter Autoimmunerkrankungen, die vorwiegend Frauen betreffen, wie z. B. die Multiple Sklerose (MS). MS tritt bei mehr als doppelt so vielen Frauen auf, was das Geschlecht zu einem der wichtigsten Risikofaktoren macht. Es ist jedoch nicht vollständig geklärt, welche Gene zu den Geschlechtsunterschieden der unterschiedlichen Häufigkeitsverteilung von Autoimmunerkrankungen beitragen. Um dies zu untersuchen, haben wir unter Verwendung des Genotype-Tissue Expression (GTEx)-Projektdatensatzes eine Genexpressionsanalyse in weiblicher und männlicher menschlicher Milz durchgeführt, um Gene zu identifizieren, die bei Frauen und Männern unterschiedlich exprimiert sind. Wir identifizierten das Transmembranprotein CD99 als eines der am stärksten unterschiedlich exprimierten Gene, welches bei Männern deutlich erhöht ist. Aus der Literatur ist bekannt, dass CD99 an der Transmigration von Immunzellen und der Regulation von T-Zellen beteiligt ist, wobei die geschlechtsspezifischen Implikationen noch nicht umfassend untersucht wurden.

In dieser Arbeit haben wir eine höhere *CD99*-Genexpression in der Milz von Männern im Vergleich zu Frauen festgestellt und diesen Expressionsunterschied auf Proteinebene auf der Oberfläche von T-Zellen und pDCs bestätigt. Geschlechtshormone konnten durch *in vitro* Tests und *ex vivo* Analysen von Blutproben von trans Männern als Ursache ausgeschlossen werden. In der Cerebrospinalflüssigkeit (CSF) war CD99 auf T-Zellen höher als im Blut. Interessanterweise wiesen männliche MS-Patienten im Gegensatz zu Kontrollpersonen niedrigere CD99-Werte auf $CD4^+$ T-Zellen im CSF auf. Im Gegensatz dazu hatten weibliche und männliche Mäuse eine ähnliche CD99-Expression. Zusätzlich zeigten *Cd99*-defiziente Mäuse im Vergleich zu Wildtypen die gleiche Anfälligkeit im MS Tiermodell Experimentelle autoimmune Enzephalomyelitis. Funktionell stieg CD99 bei der Aktivierung menschlicher T-Zellen an und eine CD99-Blockade hemmte die T-Zellproliferation. Dementsprechend zeigten CD99-defiziente Jurkat-Zellen eine verringerte Zellproliferation und Clusterbildung, die durch Wiedereinführung von CD99 rückgängig gemacht wurde.

Unsere Ergebnisse zeigen, dass CD99 bei gesunden Menschen und MS-Patient:innen geschlechtsspezifisch reguliert wird und dass es bei Menschen, nicht aber bei Mäusen, an der T-Zell-Costimulation beteiligt ist. CD99 könnte somit möglicherweise auf geschlechtsspezifische Weise zum Auftreten und zur Anfälligkeit für MS beitragen.

IV. Bibliography

1 Attfield, K. E., Jensen, L. T., Kaufmann, M., Friese, M. A. & Fugger, L. The immunology of multiple sclerosis. *Nat Rev Immunol* **22**, 734-750 (2022). **https://doi.org/10.1038/s41577-022-00718-z**

2 Bierhansl, L. *et al.* Thinking outside the box: non-canonical targets in multiple sclerosis. *Nat Rev Drug Discov* **21**, 578-600 (2022). **https://doi.org/10.1038/s41573-022-00477-5**

3 Walton, C. *et al.* Rising prevalence of multiple sclerosis worldwide: Insights from the Atlas of MS, third edition. *Mult Scler* **26**, 1816-1821 (2020). **https://doi.org/10.1177/1352458520970841**

4 Dendrou, C. A., Fugger, L. & Friese, M. A. Immunopathology of multiple sclerosis. *Nat Rev Immunol* **15**, 545-558 (2015). **https://doi.org/10.1038/nri3871**

5 Rodríguez Murúa, S., Farez, M. F. & Quintana, F. J. The Immune Response in Multiple Sclerosis. *Annu Rev Pathol* **17**, 121-139 (2022). **https://doi.org/10.1146/annurev-pathol-052920-040318**

6 Leray, E. *et al.* Evidence for a two-stage disability progression in multiple sclerosis. *Brain* **133**, 1900-1913 (2010). **https://doi.org/10.1093/brain/awq076**

7 Cree, B. A. C. *et al.* Secondary Progressive Multiple Sclerosis: New Insights. *Neurology* **97**, 378-388 (2021). **https://doi.org/10.1212/wnl.0000000000012323**

8 Kuhlmann, T. *et al.* Multiple sclerosis progression: time for a new mechanism-driven framework. *Lancet Neurol* **22**, 78-88 (2023). **https://doi.org/10.1016/s1474-4422(22)00289-7**

9 Magliozzi, R. *et al.* Inflammatory intrathecal profiles and cortical damage in multiple sclerosis. *Ann Neurol* **83**, 739-755 (2018). **https://doi.org/10.1002/ana.25197**

10 Moccia, M. *et al.* Pathologic correlates of the magnetization transfer ratio in multiple sclerosis. *Neurology* **95**, e2965-e2976 (2020). **https://doi.org/10.1212/wnl.0000000000010909**

11 Kappos, L. *et al.* Contribution of Relapse-Independent Progression vs Relapse-Associated Worsening to Overall Confirmed Disability Accumulation in Typical Relapsing Multiple Sclerosis in a Pooled Analysis of 2 Randomized Clinical Trials. *JAMA Neurol* **77**, 1132-1140 (2020). **https://doi.org/10.1001/jamaneurol.2020.1568**

12 Consortium, I. M. S. G. Multiple sclerosis genomic map implicates peripheral immune cells and microglia in susceptibility. *Science* **365** (2019). **https://doi.org/10.1126/science.aav7188**

13 Alfredsson, L. & Olsson, T. Lifestyle and Environmental Factors in Multiple Sclerosis. *Cold Spring Harb Perspect Med* **9** (2019). **https://doi.org/10.1101/cshperspect.a028944**

14 Dean, G. & Kurtzke, J. F. On the risk of multiple sclerosis according to age at immigration to South Africa. *Br Med J* **3**, 725-729 (1971). **https://doi.org/10.1136/bmj.3.5777.725**

15 Ebers, G. C., Sadovnick, A. D. & Risch, N. J. A genetic basis for familial aggregation in multiple sclerosis. Canadian Collaborative Study Group. *Nature* **377**, 150-151 (1995). **https://doi.org/10.1038/377150a0**

16 Ascherio, A., Munger, K. L. & Lünemann, J. D. The initiation and prevention of multiple sclerosis. *Nat Rev Neurol* **8**, 602-612 (2012). **https://doi.org/10.1038/nrneurol.2012.198**

17 Compston, A. & Coles, A. Multiple sclerosis. *Lancet* **372**, 1502-1517 (2008). **https://doi.org/10.1016/s0140-6736(08)61620-7**

18 Munger, K. L. *et al.* Childhood body mass index and multiple sclerosis risk: a long-term cohort study. *Mult Scler* **19**, 1323-1329 (2013). **https://doi.org/10.1177/1352458513483889**

19 Hawkes, C. H. Smoking is a risk factor for multiple sclerosis: a metanalysis. *Mult Scler* **13**, 610-615 (2007). **https://doi.org/10.1177/1352458506073501**

20 Kampman, M. T., Wilsgaard, T. & Mellgren, S. I. Outdoor activities and diet in childhood and adolescence relate to MS risk above the Arctic Circle. *J Neurol* **254**, 471-477 (2007). **https://doi.org/10.1007/s00415-006-0395-5**

21 Bäärnhielm, M. *et al.* Sunlight is associated with decreased multiple sclerosis risk: no interaction with human leukocyte antigen-DRB1*15. *Eur J Neurol* **19**, 955-962 (2012). **https://doi.org/10.1111/j.1468-1331.2011.03650.x**

22 Berer, K. *et al.* Commensal microbiota and myelin autoantigen cooperate to trigger autoimmune demyelination. *Nature* **479**, 538-541 (2011). **https://doi.org/10.1038/nature10554**

23 Sundqvist, E. *et al.* Epstein-Barr virus and multiple sclerosis: interaction with HLA. *Genes Immun* **13**, 14-20 (2012). **https://doi.org/10.1038/gene.2011.42**

24 Engdahl, E. *et al.* Increased Serological Response Against Human Herpesvirus 6A Is Associated With Risk for Multiple Sclerosis. *Front Immunol* **10**, 2715 (2019). **https://doi.org/10.3389/fimmu.2019.02715**

25 Moutsianas, L. *et al.* Class II HLA interactions modulate genetic risk for multiple sclerosis. *Nat Genet* **47**, 1107-1113 (2015). **https://doi.org/10.1038/ng.3395**

26 van Oosten, B. W. *et al.* Treatment of multiple sclerosis with the monoclonal anti-CD4 antibody cM-T412: results of a randomized, double-blind, placebo-controlled, MR-monitored phase II trial. *Neurology* **49**, 351-357 (1997). **https://doi.org/10.1212/wnl.49.2.351**

27 Kaur, G., Trowsdale, J. & Fugger, L. Natural killer cells and their receptors in multiple sclerosis. *Brain* **136**, 2657-2676 (2013). **https://doi.org/10.1093/brain/aws159**

28 Hafler, D. A. *et al.* Risk alleles for multiple sclerosis identified by a genomewide study. *N Engl J Med* **357**, 851-862 (2007). **https://doi.org/10.1056/NEJMoa073493**

29 Sawcer, S., Franklin, R. J. & Ban, M. Multiple sclerosis genetics. *Lancet Neurol* **13**, 700-709 (2014). **https://doi.org/10.1016/s1474-4422(14)70041-9**

30 Dendrou, C. A. *et al.* Resolving TYK2 locus genotype-to-phenotype differences in autoimmunity. *Sci Transl Med* **8**, 363ra149 (2016). **https://doi.org/10.1126/scitranslmed.aag1974**

31 Locus for severity implicates CNS resilience in progression of multiple sclerosis. *Nature* **619**, 323-331 (2023). **https://doi.org/10.1038/s41586-023-06250-x**

32 Bjornevik, K. *et al.* Longitudinal analysis reveals high prevalence of Epstein-Barr virus associated with multiple sclerosis. *Science* **375**, 296-301 (2022). **https://doi.org/10.1126/science.abj8222**

33 Handel, A. E. *et al.* An updated meta-analysis of risk of multiple sclerosis following infectious mononucleosis. *PLoS One* **5** (2010). **https://doi.org/10.1371/journal.pone.0012496**

34 Endriz, J., Ho, P. P. & Steinman, L. Time correlation between mononucleosis and initial symptoms of MS. *Neurol Neuroimmunol Neuroinflamm* **4**, e308 (2017). **https://doi.org/10.1212/nxi.0000000000000308**

35 Robinson, W. H. & Steinman, L. Epstein-Barr virus and multiple sclerosis. *Science* **375**, 264-265 (2022). **https://doi.org/10.1126/science.abm7930**

36 Jog, N. R. *et al.* Epstein Barr virus nuclear antigen 1 (EBNA-1) peptides recognized by adult multiple sclerosis patient sera induce neurologic symptoms in a murine model. *J Autoimmun* **106**, 102332 (2020). **https://doi.org/10.1016/j.jaut.2019.102332**

37 Tengvall, K. *et al.* Molecular mimicry between Anoctamin 2 and Epstein-Barr virus nuclear antigen 1 associates with multiple sclerosis risk. *Proc Natl Acad Sci U S A* **116**, 16955-16960 (2019). **https://doi.org/10.1073/pnas.1902623116**

38 Lanz, T. V. *et al.* Clonally expanded B cells in multiple sclerosis bind EBV EBNA1 and GlialCAM. *Nature* **603**, 321-327 (2022). **https://doi.org/10.1038/s41586-022-04432-7**

39 Vietzen, H. *et al.* Ineffective control of Epstein-Barr-virus-induced autoimmunity increases the risk for multiple sclerosis. *Cell* (2023). **https://doi.org/10.1016/j.cell.2023.11.015**

40 Kunkl, M., Frascolla, S., Amormino, C., Volpe, E. & Tuosto, L. T Helper Cells: The Modulators of Inflammation in Multiple Sclerosis. *Cells* **9** (2020). **https://doi.org/10.3390/cells9020482**

41 Hu, D. *et al.* Transcriptional signature of human pro-inflammatory T(H)17 cells identifies reduced IL10 gene expression in multiple sclerosis. *Nat Commun* **8**, 1600 (2017). **https://doi.org/10.1038/s41467-017-01571-8**

42 Murphy, A. C., Lalor, S. J., Lynch, M. A. & Mills, K. H. Infiltration of Th1 and Th17 cells and activation of microglia in the CNS during the course of experimental autoimmune

encephalomyelitis. *Brain Behav Immun* **24**, 641-651 (2010). **https://doi.org/10.1016/j.bbi.2010.01.014**

43 Tahmasebinia, F. & Pourgholaminejad, A. The role of Th17 cells in auto-inflammatory neurological disorders. *Prog Neuropsychopharmacol Biol Psychiatry* **79**, 408-416 (2017). **https://doi.org/10.1016/j.pnpbp.2017.07.023**

44 Cruciani, C. *et al.* T-Cell Specificity Influences Disease Heterogeneity in Multiple Sclerosis. *Neurol Neuroimmunol Neuroinflamm* **8** (2021). **https://doi.org/10.1212/nxi.0000000000001075**

45 Wekerle, H., Kojima, K., Lannes-Vieira, J., Lassmann, H. & Linington, C. Animal models. *Ann Neurol* **36 Suppl**, S47-53 (1994). **https://doi.org/10.1002/ana.410360714**

46 Lodygin, D. *et al.* β-Synuclein-reactive T cells induce autoimmune CNS grey matter degeneration. *Nature* **566**, 503-508 (2019). **https://doi.org/10.1038/s41586-019-0964-2**

47 Hiltensperger, M. *et al.* Skin and gut imprinted helper T cell subsets exhibit distinct functional phenotypes in central nervous system autoimmunity. *Nat Immunol* **22**, 880-892 (2021). **https://doi.org/10.1038/s41590-021-00948-8**

48 Kondělková, K. *et al.* Regulatory T cells (TREG) and their roles in immune system with respect to immunopathological disorders. *Acta Medica (Hradec Kralove)* **53**, 73-77 (2010). **https://doi.org/10.14712/18059694.2016.63**

49 Yu, N. *et al.* CD4(+)CD25 (+)CD127 (low/-) T cells: a more specific Treg population in human peripheral blood. *Inflammation* **35**, 1773-1780 (2012). **https://doi.org/10.1007/s10753-012-9496-8**

50 Feger, U. *et al.* Increased frequency of CD4+ CD25+ regulatory T cells in the cerebrospinal fluid but not in the blood of multiple sclerosis patients. *Clin Exp Immunol* **147**, 412-418 (2007). **https://doi.org/10.1111/j.1365-2249.2006.03271.x**

51 Venken, K. *et al.* Compromised CD4+ CD25(high) regulatory T-cell function in patients with relapsing-remitting multiple sclerosis is correlated with a reduced frequency of FOXP3-positive cells and reduced FOXP3 expression at the single-cell level. *Immunology* **123**, 79-89 (2008). **https://doi.org/10.1111/j.1365-2567.2007.02690.x**

52 Verma, N. D. *et al.* Multiple sclerosis patients have reduced resting and increased activated CD4(+)CD25(+)FOXP3(+)T regulatory cells. *Sci Rep* **11**, 10476 (2021). **https://doi.org/10.1038/s41598-021-88448-5**

53 Piconese, S., Walker, L. S. K. & Dominguez-Villar, M. Editorial: Control of Regulatory T Cell Stability, Plasticity, and Function in Health and Disease. *Front Immunol* **11**, 611591 (2020). **https://doi.org/10.3389/fimmu.2020.611591**

54 Zhao, H., Liao, X. & Kang, Y. Tregs: Where We Are and What Comes Next? *Front Immunol* **8**, 1578 (2017). **https://doi.org/10.3389/fimmu.2017.01578**

55 Frischer, J. M. *et al.* The relation between inflammation and neurodegeneration in multiple sclerosis brains. *Brain* **132**, 1175-1189 (2009). **https://doi.org/10.1093/brain/awp070**

56 Babbe, H. *et al.* Clonal expansions of CD8(+) T cells dominate the T cell infiltrate in active multiple sclerosis lesions as shown by micromanipulation and single cell polymerase chain reaction. *J Exp Med* **192**, 393-404 (2000). **https://doi.org/10.1084/jem.192.3.393**

57 Machado-Santos, J. *et al.* The compartmentalized inflammatory response in the multiple sclerosis brain is composed of tissue-resident CD8+ T lymphocytes and B cells. *Brain* **141**, 2066-2082 (2018). **https://doi.org/10.1093/brain/awy151**

58 Fransen, N. L. *et al.* Tissue-resident memory T cells invade the brain parenchyma in multiple sclerosis white matter lesions. *Brain* **143**, 1714-1730 (2020). **https://doi.org/10.1093/brain/awaa117**

59 Vincenti, I. *et al.* Tissue-resident memory CD8(+) T cells cooperate with CD4(+) T cells to drive compartmentalized immunopathology in the CNS. *Sci Transl Med* **14**, eabl6058 (2022). **https://doi.org/10.1126/scitranslmed.abl6058**

60 Biddison, W. E. *et al.* CD8+ myelin peptide-specific T cells can chemoattract CD4+ myelin peptide-specific T cells: importance of IFN-inducible protein 10. *J Immunol* **160**, 444-448 (1998).

61 Hauser, S. L. & Oksenberg, J. R. The neurobiology of multiple sclerosis: genes, inflammation, and neurodegeneration. *Neuron* **52**, 61-76 (2006). **https://doi.org/10.1016/j.neuron.2006.09.011**

62 Jurewicz, A., Biddison, W. E. & Antel, J. P. MHC class I-restricted lysis of human oligodendrocytes by myelin basic protein peptide-specific CD8 T lymphocytes. *J Immunol* **160**, 3056-3059 (1998).

63 Medana, I. M. *et al.* MHC class I-restricted killing of neurons by virus-specific CD8+ T lymphocytes is effected through the Fas/FasL, but not the perforin pathway. *Eur J Immunol* **30**, 3623-3633 (2000). **https://doi.org/10.1002/1521-4141(200012)30:12**<3623::Aid-immu3623>3.0.Co;2-f

64 Giuliani, F., Goodyer, C. G., Antel, J. P. & Yong, V. W. Vulnerability of human neurons to T cell-mediated cytotoxicity. *J Immunol* **171**, 368-379 (2003). **https://doi.org/10.4049/jimmunol.171.1.368**

65 van Nierop, G. P. *et al.* Phenotypic and functional characterization of T cells in white matter lesions of multiple sclerosis patients. *Acta Neuropathol* **134**, 383-401 (2017). **https://doi.org/10.1007/s00401-017-1744-4**

66 Veroni, C., Serafini, B., Rosicarelli, B., Fagnani, C. & Aloisi, F. Transcriptional profile and Epstein-Barr virus infection status of laser-cut immune infiltrates from the brain of patients with progressive multiple sclerosis. *J Neuroinflammation* **15**, 18 (2018). **https://doi.org/10.1186/s12974-017-1049-5**

67 Konjevic Sabolek, M. *et al.* Communication of CD8(+) T cells with mononuclear phagocytes in multiple sclerosis. *Ann Clin Transl Neurol* **6**, 1151-1164 (2019). **https://doi.org/10.1002/acn3.783**

68 Baughman, E. J. *et al.* Neuroantigen-specific CD8+ regulatory T-cell function is deficient during acute exacerbation of multiple sclerosis. *J Autoimmun* **36**, 115-124 (2011). **https://doi.org/10.1016/j.jaut.2010.12.003**

69 Cunnusamy, K. *et al.* Disease exacerbation of multiple sclerosis is characterized by loss of terminally differentiated autoregulatory CD8+ T cells. *Clin Immunol* **152**, 115-126 (2014). **https://doi.org/10.1016/j.clim.2014.03.005**

70 Saligrama, N. *et al.* Opposing T cell responses in experimental autoimmune encephalomyelitis. *Nature* **572**, 481-487 (2019). **https://doi.org/10.1038/s41586-019-1467-x**

71 Cencioni, M. T., Mattoscio, M., Magliozzi, R., Bar-Or, A. & Muraro, P. A. B cells in multiple sclerosis - from targeted depletion to immune reconstitution therapies. *Nat Rev Neurol* **17**, 399-414 (2021). **https://doi.org/10.1038/s41582-021-00498-5**

72 Florou, D., Katsara, M., Feehan, J., Dardiotis, E. & Apostolopoulos, V. Anti-CD20 Agents for Multiple Sclerosis: Spotlight on Ocrelizumab and Ofatumumab. *Brain Sci* **10** (2020). **https://doi.org/10.3390/brainsci10100758**

73 Kuenz, B. *et al.* Cerebrospinal fluid B cells correlate with early brain inflammation in multiple sclerosis. *PLoS One* **3**, e2559 (2008). **https://doi.org/10.1371/journal.pone.0002559**

74 Villar, L. M. *et al.* Immunoglobulin M oligoclonal bands: biomarker of targetable inflammation in primary progressive multiple sclerosis. *Ann Neurol* **76**, 231-240 (2014). **https://doi.org/10.1002/ana.24190**

75 Lisak, R. P. *et al.* Secretory products of multiple sclerosis B cells are cytotoxic to oligodendroglia in vitro. *J Neuroimmunol* **246**, 85-95 (2012). **https://doi.org/10.1016/j.jneuroim.2012.02.015**

76 Lisak, R. P. *et al.* B cells from patients with multiple sclerosis induce cell death via apoptosis in neurons in vitro. *J Neuroimmunol* **309**, 88-99 (2017). **https://doi.org/10.1016/j.jneuroim.2017.05.004**

77 Schafflick, D. *et al.* Integrated single cell analysis of blood and cerebrospinal fluid leukocytes in multiple sclerosis. *Nat Commun* **11**, 247 (2020). **https://doi.org/10.1038/s41467-019-14118-w**

78 von Büdingen, H. C. *et al.* B cell exchange across the blood-brain barrier in multiple sclerosis. *J Clin Invest* **122**, 4533-4543 (2012). **https://doi.org/10.1172/jci63842**

79 Palanichamy, A. *et al.* Immunoglobulin class-switched B cells form an active immune axis between CNS and periphery in multiple sclerosis. *Sci Transl Med* **6**, 248ra106 (2014). **https://doi.org/10.1126/scitranslmed.3008930**

80 Stern, J. N. *et al.* B cells populating the multiple sclerosis brain mature in the draining cervical lymph nodes. *Sci Transl Med* **6**, 248ra107 (2014). **https://doi.org/10.1126/scitranslmed.3008879**

81 Brioschi, S. *et al.* Heterogeneity of meningeal B cells reveals a lymphopoietic niche at the CNS borders. *Science* **373** (2021). **https://doi.org/10.1126/science.abf9277**

82 Mitsdoerffer, M. *et al.* Formation and immunomodulatory function of meningeal B cell aggregates in progressive CNS autoimmunity. *Brain* **144**, 1697-1710 (2021). **https://doi.org/10.1093/brain/awab093**

83 McKenzie, D. R. *et al.* IL-17-producing γδ T cells switch migratory patterns between resting and activated states. *Nat Commun* **8**, 15632 (2017). **https://doi.org/10.1038/ncomms15632**

84 Ammitzbøll, C. *et al.* MAIT cell subtypes in multiple sclerosis. *J Neuroimmunol* **339**, 577117 (2020). **https://doi.org/10.1016/j.jneuroim.2019.577117**

85 De Biasi, S. *et al.* iNKT Cells in Secondary Progressive Multiple Sclerosis Patients Display Pro-inflammatory Profiles. *Front Immunol* **7**, 555 (2016). **https://doi.org/10.3389/fimmu.2016.00555**

86 Stinissen, P. *et al.* Increased frequency of gamma delta T cells in cerebrospinal fluid and peripheral blood of patients with multiple sclerosis. Reactivity, cytotoxicity, and T cell receptor V gene rearrangements. *J Immunol* **154**, 4883-4894 (1995).

87 Zeine, R. *et al.* Mechanism of gammadelta T cell-induced human oligodendrocyte cytotoxicity: relevance to multiple sclerosis. *J Neuroimmunol* **87**, 49-61 (1998). **https://doi.org/10.1016/s0165-5728(98)00047-2**

88 Schirmer, L., Rothhammer, V., Hemmer, B. & Korn, T. Enriched CD161high CCR6+ γδ T cells in the cerebrospinal fluid of patients with multiple sclerosis. *JAMA Neurol* **70**, 345-351 (2013). **https://doi.org/10.1001/2013.jamaneurol.409**

89 Willing, A. *et al.* $CD8^+$ MAIT cells infiltrate into the CNS and alterations in their blood frequencies correlate with IL-18 serum levels in multiple sclerosis. *Eur J Immunol* **44**, 3119-3128 (2014). **https://doi.org/10.1002/eji.201344160**

90 Held, K. *et al.* αβ T-cell receptors from multiple sclerosis brain lesions show MAIT cell-related features. *Neurol Neuroimmunol Neuroinflamm* **2**, e107 (2015). **https://doi.org/10.1212/nxi.0000000000000107**

91 Willing, A., Jäger, J., Reinhardt, S., Kursawe, N. & Friese, M. A. Production of IL-17 by MAIT Cells Is Increased in Multiple Sclerosis and Is Associated with IL-7 Receptor Expression. *J Immunol* **200**, 974-982 (2018). **https://doi.org/10.4049/jimmunol.1701213**

92 Lamichhane, R. *et al.* TCR- or Cytokine-Activated CD8(+) Mucosal-Associated Invariant T Cells Are Rapid Polyfunctional Effectors That Can Coordinate Immune Responses. *Cell Rep* **28**, 3061-3076.e3065 (2019). **https://doi.org/10.1016/j.celrep.2019.08.054**

93 Leng, T. *et al.* TCR and Inflammatory Signals Tune Human MAIT Cells to Exert Specific Tissue Repair and Effector Functions. *Cell Rep* **28**, 3077-3091.e3075 (2019). **https://doi.org/10.1016/j.celrep.2019.08.050**

94 Hinks, T. S. C. *et al.* Activation and In Vivo Evolution of the MAIT Cell Transcriptome in Mice and Humans Reveals Tissue Repair Functionality. *Cell Rep* **28**, 3249-3262.e3245 (2019). **https://doi.org/10.1016/j.celrep.2019.07.039**

95 van Wilgenburg, B. *et al.* MAIT cells are activated during human viral infections. *Nat Commun* **7**, 11653 (2016). **https://doi.org/10.1038/ncomms11653**

96 Leeansyah, E. *et al.* Arming of MAIT Cell Cytolytic Antimicrobial Activity Is Induced by IL-7 and Defective in HIV-1 Infection. *PLoS Pathog* **11**, e1005072 (2015). **https://doi.org/10.1371/journal.ppat.1005072**

97 Croxford, J. L., Miyake, S., Huang, Y. Y., Shimamura, M. & Yamamura, T. Invariant V(alpha)19i T cells regulate autoimmune inflammation. *Nat Immunol* **7**, 987-994 (2006). **https://doi.org/10.1038/ni1370**

98 Vivier, E. *et al.* Innate Lymphoid Cells: 10 Years On. *Cell* **174**, 1054-1066 (2018). **https://doi.org/10.1016/j.cell.2018.07.017**

99 Kwong, B. *et al.* T-bet-dependent NKp46(+) innate lymphoid cells regulate the onset of T(H)17-induced neuroinflammation. *Nat Immunol* **18**, 1117-1127 (2017). **https://doi.org/10.1038/ni.3816**

100 Grigg, J. B. *et al.* Antigen-presenting innate lymphoid cells orchestrate neuroinflammation. *Nature* **600**, 707-712 (2021). **https://doi.org/10.1038/s41586-021-04136-4**

101 Russi, A. E., Ebel, M. E., Yang, Y. & Brown, M. A. Male-specific IL-33 expression regulates sex-dimorphic EAE susceptibility. *Proc Natl Acad Sci U S A* **115**, E1520-e1529 (2018). **https://doi.org/10.1073/pnas.1710401115**

102 Gross, C. C. *et al.* Impaired NK-mediated regulation of T-cell activity in multiple sclerosis is reconstituted by IL-2 receptor modulation. *Proc Natl Acad Sci U S A* **113**, E2973-2982 (2016). **https://doi.org/10.1073/pnas.1524924113**

103 Han, S. *et al.* Comprehensive immunophenotyping of cerebrospinal fluid cells in patients with neuroimmunological diseases. *J Immunol* **192**, 2551-2563 (2014). **https://doi.org/10.4049/jimmunol.1302884**

104 Rodríguez-Martín, E. *et al.* Natural killer cell subsets in cerebrospinal fluid of patients with multiple sclerosis. *Clin Exp Immunol* **180**, 243-249 (2015). **https://doi.org/10.1111/cei.12580**

105 Nielsen, N., Ødum, N., Ursø, B., Lanier, L. L. & Spee, P. Cytotoxicity of CD56(bright) NK cells towards autologous activated CD4+ T cells is mediated through NKG2D, LFA-1 and TRAIL and dampened via CD94/NKG2A. *PLoS One* **7**, e31959 (2012). **https://doi.org/10.1371/journal.pone.0031959**

106 Plantone, D. *et al.* Circulating CD56dim NK cells expressing perforin are increased in progressive multiple sclerosis. *J Neuroimmunol* **265**, 124-127 (2013). **https://doi.org/10.1016/j.jneuroim.2013.10.004**

107 Guilliams, M., Mildner, A. & Yona, S. Developmental and Functional Heterogeneity of Monocytes. *Immunity* **49**, 595-613 (2018). **https://doi.org/10.1016/j.immuni.2018.10.005**

108 Akaishi, T., Takahashi, T. & Nakashima, I. Peripheral blood monocyte count at onset may affect the prognosis in multiple sclerosis. *J Neuroimmunol* **319**, 37-40 (2018). **https://doi.org/10.1016/j.jneuroim.2018.03.016**

109 Kouwenhoven, M., Teleshova, N., Ozenci, V., Press, R. & Link, H. Monocytes in multiple sclerosis: phenotype and cytokine profile. *J Neuroimmunol* **112**, 197-205 (2001). **https://doi.org/10.1016/s0165-5728(00)00396-9**

110 Mishra, M. K., Wang, J., Silva, C., Mack, M. & Yong, V. W. Kinetics of proinflammatory monocytes in a model of multiple sclerosis and its perturbation by laquinimod. *Am J Pathol* **181**, 642-651 (2012). **https://doi.org/10.1016/j.ajpath.2012.05.011**

111 Cugurra, A. *et al.* Skull and vertebral bone marrow are myeloid cell reservoirs for the meninges and CNS parenchyma. *Science* **373** (2021). **https://doi.org/10.1126/science.abf7844**

112 Locatelli, G. *et al.* Mononuclear phagocytes locally specify and adapt their phenotype in a multiple sclerosis model. *Nat Neurosci* **21**, 1196-1208 (2018). **https://doi.org/10.1038/s41593-018-0212-3**

113 Blecher-Gonen, R. *et al.* Single-Cell Analysis of Diverse Pathogen Responses Defines a Molecular Roadmap for Generating Antigen-Specific Immunity. *Cell Syst* **8**, 109-121.e106 (2019). **https://doi.org/10.1016/j.cels.2019.01.001**

114 King, I. L., Dickendesher, T. L. & Segal, B. M. Circulating Ly-6C+ myeloid precursors migrate to the CNS and play a pathogenic role during autoimmune demyelinating disease. *Blood* **113**, 3190-3197 (2009). **https://doi.org/10.1182/blood-2008-07-168575**

115 White, M. P. J., Webster, G., Leonard, F. & La Flamme, A. C. Innate IFN-γ ameliorates experimental autoimmune encephalomyelitis and promotes myeloid expansion and PDL-1 expression. *Sci Rep* **8**, 259 (2018). **https://doi.org/10.1038/s41598-017-18543-z**

116 Smith, B. C., Sinyuk, M., Jenkins, J. E., 3rd, Psenicka, M. W. & Williams, J. L. The impact of regional astrocyte interferon-γ signaling during chronic autoimmunity: a novel role for the immunoproteasome. *J Neuroinflammation* **17**, 184 (2020). **https://doi.org/10.1186/s12974-020-01861-x**

117 Lotfi, N., Zhang, G. X., Esmaeil, N. & Rostami, A. Evaluation of the effect of GM-CSF blocking on the phenotype and function of human monocytes. *Sci Rep* **10**, 1567 (2020). **https://doi.org/10.1038/s41598-020-58131-2**

118 Villani, A. C. *et al.* Single-cell RNA-seq reveals new types of human blood dendritic cells, monocytes, and progenitors. *Science* **356** (2017). **https://doi.org/10.1126/science.aah4573**

119 Schwab, N., Zozulya, A. L., Kieseier, B. C., Toyka, K. V. & Wiendl, H. An imbalance of two functionally and phenotypically different subsets of plasmacytoid dendritic cells characterizes the dysfunctional immune regulation in multiple sclerosis. *J Immunol* **184**, 5368-5374 (2010). **https://doi.org/10.4049/jimmunol.0903662**

120 Haas, J., Schwarz, A., Korporal-Kuhnke, M., Jarius, S. & Wildemann, B. Myeloid dendritic cells exhibit defects in activation and function in patients with multiple sclerosis. *J Neuroimmunol* **301**, 53-60 (2016). **https://doi.org/10.1016/j.jneuroim.2016.10.007**

121 Thewissen, K. *et al.* Circulating dendritic cells of multiple sclerosis patients are proinflammatory and their frequency is correlated with MS-associated genetic risk factors. *Mult Scler* **20**, 548-557 (2014). **https://doi.org/10.1177/1352458513505352**

122 Segal, B. M. *et al.* Repeated subcutaneous injections of IL12/23 p40 neutralising antibody, ustekinumab, in patients with relapsing-remitting multiple sclerosis: a phase II, double-blind, placebo-controlled, randomised, dose-ranging study. *Lancet Neurol* **7**, 796-804 (2008). **https://doi.org/10.1016/s1474-4422(08)70173-x**

123 Huang, Y. *et al.* Repopulated microglia are solely derived from the proliferation of residual microglia after acute depletion. *Nat Neurosci* **21**, 530-540 (2018). **https://doi.org/10.1038/s41593-018-0090-8**

124 Krogsgaard, M. *et al.* Visualization of myelin basic protein (MBP) T cell epitopes in multiple sclerosis lesions using a monoclonal antibody specific for the human histocompatibility leukocyte antigen (HLA)-DR2-MBP 85-99 complex. *J Exp Med* **191**, 1395-1412 (2000). **https://doi.org/10.1084/jem.191.8.1395**

125 Wolf, Y. *et al.* Microglial MHC class II is dispensable for experimental autoimmune encephalomyelitis and cuprizone-induced demyelination. *Eur J Immunol* **48**, 1308-1318 (2018). **https://doi.org/10.1002/eji.201847540**

126 Prinz, M., Jung, S. & Priller, J. Microglia Biology: One Century of Evolving Concepts. *Cell* **179**, 292-311 (2019). **https://doi.org/10.1016/j.cell.2019.08.053**

127 Masuda, T. *et al.* Spatial and temporal heterogeneity of mouse and human microglia at single-cell resolution. *Nature* **566**, 388-392 (2019). **https://doi.org/10.1038/s41586-019-0924-x**

128 Tozaki-Saitoh, H. *et al.* Transcription factor MafB contributes to the activation of spinal microglia underlying neuropathic pain development. *Glia* **67**, 729-740 (2019). **https://doi.org/10.1002/glia.23570**

129 Liddelow, S. A. *et al.* Neurotoxic reactive astrocytes are induced by activated microglia. *Nature* **541**, 481-487 (2017). **https://doi.org/10.1038/nature21029**

130 Procaccini, C., De Rosa, V., Pucino, V., Formisano, L. & Matarese, G. Animal models of Multiple Sclerosis. *Eur J Pharmacol* **759**, 182-191 (2015). **https://doi.org/10.1016/j.ejphar.2015.03.042**

131 Tsunoda, I. & Fujinami, R. S. Neuropathogenesis of Theiler's murine encephalomyelitis virus infection, an animal model for multiple sclerosis. *J Neuroimmune Pharmacol* **5**, 355-369 (2010). **https://doi.org/10.1007/s11481-009-9179-x**

132 Matsushima, G. K. & Morell, P. The neurotoxicant, cuprizone, as a model to study demyelination and remyelination in the central nervous system. *Brain Pathol* **11**, 107-116 (2001). **https://doi.org/10.1111/j.1750-3639.2001.tb00385.x**

133 Kipp, M., Clarner, T., Dang, J., Copray, S. & Beyer, C. The cuprizone animal model: new insights into an old story. *Acta Neuropathol* **118**, 723-736 (2009). **https://doi.org/10.1007/s00401-009-0591-3**

134 Rivers, T. M., Sprunt, D. H. & Berry, G. P. OBSERVATIONS ON ATTEMPTS TO PRODUCE ACUTE DISSEMINATED ENCEPHALOMYELITIS IN MONKEYS. *J Exp Med* **58**, 39-53 (1933). **https://doi.org/10.1084/jem.58.1.39**

135 Stromnes, I. M. & Goverman, J. M. Active induction of experimental allergic encephalomyelitis. *Nat Protoc* **1**, 1810-1819 (2006). **https://doi.org/10.1038/nprot.2006.285**

136 Levine, S. & Sowinski, R. Experimental allergic encephalomyelitis in inbred and outbred mice. *J Immunol* **110**, 139-143 (1973).

137 Linthicum, D. S., Munoz, J. J. & Blaskett, A. Acute experimental autoimmune encephalomyelitis in mice. I. Adjuvant action of Bordetella pertussis is due to vasoactive amine sensitization and increased vascular permeability of the central nervous system. *Cell Immunol* **73**, 299-310 (1982). **https://doi.org/10.1016/0008-8749(82)90457-9**

138 Simmons, S. B., Pierson, E. R., Lee, S. Y. & Goverman, J. M. Modeling the heterogeneity of multiple sclerosis in animals. *Trends Immunol* **34**, 410-422 (2013). **https://doi.org/10.1016/j.it.2013.04.006**

139 Yednock, T. A. *et al.* Prevention of experimental autoimmune encephalomyelitis by antibodies against alpha 4 beta 1 integrin. *Nature* **356**, 63-66 (1992). **https://doi.org/10.1038/356063a0**

140 Kawakami, N. *et al.* The activation status of neuroantigen-specific T cells in the target organ determines the clinical outcome of autoimmune encephalomyelitis. *J Exp Med* **199**, 185-197 (2004). **https://doi.org/10.1084/jem.20031064**

141 Lees, J. R., Golumbek, P. T., Sim, J., Dorsey, D. & Russell, J. H. Regional CNS responses to IFN-gamma determine lesion localization patterns during EAE pathogenesis. *J Exp Med* **205**, 2633-2642 (2008). **https://doi.org/10.1084/jem.20080155**

142 Kroenke, M. A., Carlson, T. J., Andjelkovic, A. V. & Segal, B. M. IL-12- and IL-23-modulated T cells induce distinct types of EAE based on histology, CNS chemokine profile, and response to cytokine inhibition. *J Exp Med* **205**, 1535-1541 (2008). **https://doi.org/10.1084/jem.20080159**

143 Stromnes, I. M. & Goverman, J. M. Passive induction of experimental allergic encephalomyelitis. *Nat Protoc* **1**, 1952-1960 (2006). **https://doi.org/10.1038/nprot.2006.284**

144 Krishnamoorthy, G., Lassmann, H., Wekerle, H. & Holz, A. Spontaneous opticospinal encephalomyelitis in a double-transgenic mouse model of autoimmune T cell/B cell cooperation. *J Clin Invest* **116**, 2385-2392 (2006). **https://doi.org/10.1172/jci28330**

145 Bettelli, E., Baeten, D., Jäger, A., Sobel, R. A. & Kuchroo, V. K. Myelin oligodendrocyte glycoprotein-specific T and B cells cooperate to induce a Devic-like disease in mice. *J Clin Invest* **116**, 2393-2402 (2006). **https://doi.org/10.1172/jci28334**

146 Ransohoff, R. M. A mighty mouse: building a better model of multiple sclerosis. *J Clin Invest* **116**, 2313-2316 (2006). **https://doi.org/10.1172/jci29834**

147 Litzenburger, T. *et al.* B lymphocytes producing demyelinating autoantibodies: development and function in gene-targeted transgenic mice. *J Exp Med* **188**, 169-180 (1998). **https://doi.org/10.1084/jem.188.1.169**

148 Mestas, J. & Hughes, C. C. Of mice and not men: differences between mouse and human immunology. *J Immunol* **172**, 2731-2738 (2004). **https://doi.org/10.4049/jimmunol.172.5.2731**

149 Ransohoff, R. M. Animal models of multiple sclerosis: the good, the bad and the bottom line. *Nat Neurosci* **15**, 1074-1077 (2012). **https://doi.org/10.1038/nn.3168**

150 Mauvais-Jarvis, F. *et al.* Sex and gender: modifiers of health, disease, and medicine. *Lancet* **396**, 565-582 (2020). **https://doi.org/10.1016/s0140-6736(20)31561-0**

151 Clayton, J. A. Studying both sexes: a guiding principle for biomedicine. *Faseb j* **30**, 519-524 (2016). **https://doi.org/10.1096/fj.15-279554**

152 Wilkinson, N. M., Chen, H. C., Lechner, M. G. & Su, M. A. Sex Differences in Immunity. *Annu Rev Immunol* **40**, 75-94 (2022). **https://doi.org/10.1146/annurev-immunol-101320-125133**

153 GAO, U. Most drugs withdrawn in recent years had greater health risks for women. *Government Accountability Office.[View Article]* (2001).

154 Clayton, J. A. & Collins, F. S. Policy: NIH to balance sex in cell and animal studies. *Nature* **509**, 282-283 (2014). **https://doi.org/10.1038/509282a**

155 Franconi, F., Brunelleschi, S., Steardo, L. & Cuomo, V. Gender differences in drug responses. *Pharmacol Res* **55**, 81-95 (2007). **https://doi.org/10.1016/j.phrs.2006.11.001**

156 Yoon, S. *et al.* Effect of CYP3A4 metabolism on sex differences in the pharmacokinetics and pharmacodynamics of zolpidem. *Scientific Reports* **11**, 19150 (2021). **https://doi.org/10.1038/s41598-021-98689-z**

157 Mayer, A. T. *et al.* A tissue atlas of ulcerative colitis revealing evidence of sex-dependent differences in disease-driving inflammatory cell types and resistance to TNF inhibitor therapy. *Science Advances* **9**, eadd1166 (2023). **https://doi.org/doi:10.1126/sciadv.add1166**

158 Klein, S. L., Jedlicka, A. & Pekosz, A. The Xs and Y of immune responses to viral vaccines. *Lancet Infect Dis* **10**, 338-349 (2010). **https://doi.org/10.1016/s1473-3099(10)70049-9**

159 Prendergast, B. J., Onishi, K. G. & Zucker, I. Female mice liberated for inclusion in neuroscience and biomedical research. *Neurosci Biobehav Rev* **40**, 1-5 (2014). **https://doi.org/10.1016/j.neubiorev.2014.01.001**

160 50/50, G. H. *Towards gender equality in global health*, <**https://globalhealth5050.org/glossary/**> (access date: 10th October 2023).

161 Regitz-Zagrosek, V. *et al.* Gender in cardiovascular diseases: impact on clinical manifestations, management, and outcomes. *Eur Heart J* **37**, 24-34 (2016). **https://doi.org/10.1093/eurheartj/ehv598**

162 Pelletier, R., Ditto, B. & Pilote, L. A composite measure of gender and its association with risk factors in patients with premature acute coronary syndrome. *Psychosom Med* **77**, 517-526 (2015). **https://doi.org/10.1097/psy.0000000000000186**

163 Klein, S. L. & Flanagan, K. L. Sex differences in immune responses. *Nat Rev Immunol* **16**, 626-638 (2016). **https://doi.org/10.1038/nri.2016.90**

164 Zuk, M. The sicker sex. *PLoS Pathog* **5**, e1000267 (2009). **https://doi.org/10.1371/journal.ppat.1000267**

165 Mondal, S. & Rai, U. Sexual dimorphism in phagocytic activity of wall lizard's splenic macrophages and its control by sex steroids. *Gen Comp Endocrinol* **116**, 291-298 (1999). **https://doi.org/10.1006/gcen.1999.7370**

166 Pap, P. L., Czirják, G. A., Vágási, C. I., Barta, Z. & Hasselquist, D. Sexual dimorphism in immune function changes during the annual cycle in house sparrows. *Naturwissenschaften* **97**, 891-901 (2010). **https://doi.org/10.1007/s00114-010-0706-7**

167 Hill-Burns, E. M. & Clark, A. G. X-linked variation in immune response in Drosophila melanogaster. *Genetics* **183**, 1477-1491 (2009). **https://doi.org/10.1534/genetics.108.093971**

168 Taylor, K. & Kimbrell, D. Host immune response and differential survival of the sexes in Drosophila. *Fly* **1**, 197-204 (2007).

169 Abdullah, M. *et al.* Gender effect on in vitro lymphocyte subset levels of healthy individuals. *Cell Immunol* **272**, 214-219 (2012). **https://doi.org/10.1016/j.cellimm.2011.10.009**

170 Huang, Z. *et al.* Effects of sex and aging on the immune cell landscape as assessed by single-cell transcriptomic analysis. *Proc Natl Acad Sci U S A* **118** (2021). **https://doi.org/10.1073/pnas.2023216118**

171 Lee, B. W. *et al.* Age- and sex-related changes in lymphocyte subpopulations of healthy Asian subjects: from birth to adulthood. *Cytometry* **26**, 8-15 (1996). **https://doi.org/10.1002/(sici)1097-0320(19960315)26:1**<8::Aid-cyto2>3.0.Co;2-e

172 Uppal, S. S., Verma, S. & Dhot, P. S. Normal values of CD4 and CD8 lymphocyte subsets in healthy indian adults and the effects of sex, age, ethnicity, and smoking. *Cytometry B Clin Cytom* **52**, 32-36 (2003). **https://doi.org/10.1002/cyto.b.10011**

173 Afshan, G., Afzal, N. & Qureshi, S. CD4+CD25(hi) regulatory T cells in healthy males and females mediate gender difference in the prevalence of autoimmune diseases. *Clin Lab* **58**, 567-571 (2012).

174 Souyris, M. *et al.* TLR7 escapes X chromosome inactivation in immune cells. *Sci Immunol* **3** (2018). **https://doi.org/10.1126/sciimmunol.aap8855**

175 Berghöfer, B. *et al.* TLR7 ligands induce higher IFN-alpha production in females. *J Immunol* **177**, 2088-2096 (2006). **https://doi.org/10.4049/jimmunol.177.4.2088**

176 Griesbeck, M. *et al.* Sex Differences in Plasmacytoid Dendritic Cell Levels of IRF5 Drive Higher IFN-α Production in Women. *J Immunol* **195**, 5327-5336 (2015). **https://doi.org/10.4049/jimmunol.1501684**

177 Beisel, C. *et al.* Sex differences in the percentage of IRF5 positive B cells are associated with higher production of TNF-α in women in response to TLR9 in humans. *Biol Sex Differ* **14**, 11 (2023). **https://doi.org/10.1186/s13293-023-00495-x**

178 Torcia, M. G. *et al.* Sex differences in the response to viral infections: TLR8 and TLR9 ligand stimulation induce higher IL10 production in males. *PLoS One* **7**, e39853 (2012). **https://doi.org/10.1371/journal.pone.0039853**

179 Moxley, G. *et al.* Sexual dimorphism in innate immunity. *Arthritis Rheum* **46**, 250-258 (2002). **https://doi.org/10.1002/1529-0131(200201)46:1**<250::Aid-art10064>3.0.Co;2-t

180 Aomatsu, M., Kato, T., Kasahara, E. & Kitagawa, S. Gender difference in tumor necrosis factor-α production in human neutrophils stimulated by lipopolysaccharide and interferon-γ. *Biochem Biophys Res Commun* **441**, 220-225 (2013). **https://doi.org/10.1016/j.bbrc.2013.10.042**

181 Sankaran-Walters, S. *et al.* Sex differences matter in the gut: effect on mucosal immune activation and inflammation. *Biol Sex Differ* **4**, 10 (2013). **https://doi.org/10.1186/2042-6410-4-10**

182 Hewagama, A., Patel, D., Yarlagadda, S., Strickland, F. M. & Richardson, B. C. Stronger inflammatory/cytotoxic T-cell response in women identified by microarray analysis. *Genes Immun* **10**, 509-516 (2009). **https://doi.org/10.1038/gene.2009.12**

183 Girón-González, J. A. *et al.* Consistent production of a higher TH1:TH2 cytokine ratio by stimulated T cells in men compared with women. *Eur J Endocrinol* **143**, 31-36 (2000). **https://doi.org/10.1530/eje.0.1430031**

184 Zhang, M. A. *et al.* Peroxisome proliferator-activated receptor (PPAR)α and -γ regulate IFNγ and IL-17A production by human T cells in a sex-specific way. *Proc Natl Acad Sci U S A* **109**, 9505-9510 (2012). **https://doi.org/10.1073/pnas.1118458109**

185 Furman, D. *et al.* Systems analysis of sex differences reveals an immunosuppressive role for testosterone in the response to influenza vaccination. *Proc Natl Acad Sci U S A* **111**, 869-874 (2014). **https://doi.org/10.1073/pnas.1321060111**

186 Whitacre, C. C., Reingold, S. C. & O'Looney, P. A. A gender gap in autoimmunity. *Science* **283**, 1277-1278 (1999). **https://doi.org/10.1126/science.283.5406.1277**

187 Gold, S. M., Willing, A., Leypoldt, F., Paul, F. & Friese, M. A. Sex differences in autoimmune disorders of the central nervous system. *Semin Immunopathol* **41**, 177-188 (2019). **https://doi.org/10.1007/s00281-018-0723-8**

188 Rhie, A. *et al.* The complete sequence of a human Y chromosome. *Nature* (2023). **https://doi.org/10.1038/s41586-023-06457-y**

189 Fish, E. N. The X-files in immunity: sex-based differences predispose immune responses. *Nat Rev Immunol* **8**, 737-744 (2008). **https://doi.org/10.1038/nri2394**

190 Abdel-Hafiz, H. A. *et al.* Y chromosome loss in cancer drives growth by evasion of adaptive immunity. *Nature* (2023). **https://doi.org/10.1038/s41586-023-06234-x**

191 Li, J. *et al.* Histone demethylase KDM5D upregulation drives sex differences in colon cancer. *Nature* (2023). **https://doi.org/10.1038/s41586-023-06254-7**

192 Loda, A., Collombet, S. & Heard, E. Gene regulation in time and space during X-chromosome inactivation. *Nat Rev Mol Cell Biol* **23**, 231-249 (2022). **https://doi.org/10.1038/s41580-021-00438-7**

193 Tukiainen, T. *et al.* Landscape of X chromosome inactivation across human tissues. *Nature* **550**, 244-248 (2017). **https://doi.org/10.1038/nature24265**

194 Balaton, B. P. & Brown, C. J. Contribution of genetic and epigenetic changes to escape from X-chromosome inactivation. *Epigenetics Chromatin* **14**, 30 (2021). **https://doi.org/10.1186/s13072-021-00404-9**

195 Mousavi, M. J., Mahmoudi, M. & Ghotloo, S. Escape from X chromosome inactivation and female bias of autoimmune diseases. *Mol Med* **26**, 127 (2020). **https://doi.org/10.1186/s10020-020-00256-1**

196 Cheng, M. I. *et al.* The X-linked epigenetic regulator UTX controls NK cell-intrinsic sex differences. *Nat Immunol* **24**, 780-791 (2023). **https://doi.org/10.1038/s41590-023-01463-8**

197 Gubbels Bupp, M. R. & Jorgensen, T. N. Androgen-Induced Immunosuppression. *Front Immunol* **9**, 794 (2018). **https://doi.org/10.3389/fimmu.2018.00794**

198 Moulton, V. R. Sex Hormones in Acquired Immunity and Autoimmune Disease. *Front Immunol* **9**, 2279 (2018). **https://doi.org/10.3389/fimmu.2018.02279**

199 Mohammad, I. *et al.* Estrogen receptor α contributes to T cell-mediated autoimmune inflammation by promoting T cell activation and proliferation. *Sci Signal* **11** (2018). **https://doi.org/10.1126/scisignal.aap9415**

200 Vasanthakumar, A. *et al.* Sex-specific adipose tissue imprinting of regulatory T cells. *Nature* **579**, 581-585 (2020). **https://doi.org/10.1038/s41586-020-2040-3**

201 Anderson, M. S. & Su, M. A. AIRE expands: new roles in immune tolerance and beyond. *Nat Rev Immunol* **16**, 247-258 (2016). **https://doi.org/10.1038/nri.2016.9**

202 Dragin, N. *et al.* Estrogen-mediated downregulation of AIRE influences sexual dimorphism in autoimmune diseases. *J Clin Invest* **126**, 1525-1537 (2016). **https://doi.org/10.1172/jci81894**

203 Zhu, M. L. *et al.* Sex bias in CNS autoimmune disease mediated by androgen control of autoimmune regulator. *Nat Commun* **7**, 11350 (2016). **https://doi.org/10.1038/ncomms11350**

204 Ramien, C. *et al.* Sex effects on inflammatory and neurodegenerative processes in multiple sclerosis. *Neurosci Biobehav Rev* **67**, 137-146 (2016). **https://doi.org/10.1016/j.neubiorev.2015.12.015**

205 Voskuhl, R. R. The effect of sex on multiple sclerosis risk and disease progression. *Mult Scler* **26**, 554-560 (2020). **https://doi.org/10.1177/1352458519892491**

206 Alvarez-Sanchez, N. & Dunn, S. E. Immune Cell Contributors to the Female Sex Bias in Multiple Sclerosis and Experimental Autoimmune Encephalomyelitis. *Curr Top Behav Neurosci* **62**, 333-373 (2023). **https://doi.org/10.1007/7854_2022_324**

207 Koch-Henriksen, N. & Sorensen, P. S. The changing demographic pattern of multiple sclerosis epidemiology. *Lancet Neurol* **9**, 520-532 (2010). **https://doi.org/10.1016/S1474-4422(10)70064-8**

208 Orton, S. M. *et al.* Sex ratio of multiple sclerosis in Canada: a longitudinal study. *Lancet Neurol* **5**, 932-936 (2006). **https://doi.org/10.1016/S1474-4422(06)70581-6**

209 Rotstein, D. L. *et al.* Temporal trends in multiple sclerosis prevalence and incidence in a large population. *Neurology* **90**, e1435-e1441 (2018). **https://doi.org/10.1212/wnl.0000000000005331**

210 Dunn, S. E., Lee, H., Pavri, F. R. & Zhang, M. A. Sex-Based Differences in Multiple Sclerosis (Part I): Biology of Disease Incidence. *Curr Top Behav Neurosci* **26**, 29-56 (2015). **https://doi.org/10.1007/7854_2015_371**

211 Kalincik, T. *et al.* Sex as a determinant of relapse incidence and progressive course of multiple sclerosis. *Brain* **136**, 3609-3617 (2013). **https://doi.org/10.1093/brain/awt281**

212 Moldovan, I. R., Cotleur, A. C., Zamor, N., Butler, R. S. & Pelfrey, C. M. Multiple sclerosis patients show sexual dimorphism in cytokine responses to myelin antigens. *J Neuroimmunol* **193**, 161-169 (2008). **https://doi.org/10.1016/j.jneuroim.2007.10.010**

213 Held, U., Heigenhauser, L., Shang, C., Kappos, L. & Polman, C. Predictors of relapse rate in MS clinical trials. *Neurology* **65**, 1769-1773 (2005). **https://doi.org/10.1212/01.wnl.0000187122.71735.1f**

214 Pozzilli, C. *et al.* 'Gender gap' in multiple sclerosis: magnetic resonance imaging evidence. *Eur J Neurol* **10**, 95-97 (2003). **https://doi.org/10.1046/j.1468-1331.2003.00519.x**

215 Frischer, J. M. *et al.* Clinical and pathological insights into the dynamic nature of the white matter multiple sclerosis plaque. *Ann Neurol* **78**, 710-721 (2015). **https://doi.org/10.1002/ana.24497**

216 Runmarker, B., Andersson, C., Odén, A. & Andersen, O. Prediction of outcome in multiple sclerosis based on multivariate models. *J Neurol* **241**, 597-604 (1994). **https://doi.org/10.1007/bf00920623**

217 Tomassini, V. & Pozzilli, C. Sex hormones, brain damage and clinical course of Multiple Sclerosis. *J Neurol Sci* **286**, 35-39 (2009). **https://doi.org/10.1016/j.jns.2009.04.014**

218 Shirani, A., Zhao, Y., Kingwell, E., Rieckmann, P. & Tremlett, H. Temporal trends of disability progression in multiple sclerosis: findings from British Columbia, Canada (1975-2009). *Mult Scler* **18**, 442-450 (2012). **https://doi.org/10.1177/1352458511422097**

219 Ribbons, K. A. *et al.* Male Sex Is Independently Associated with Faster Disability Accumulation in Relapse-Onset MS but Not in Primary Progressive MS. *PLoS One* **10**, e0122686 (2015). **https://doi.org/10.1371/journal.pone.0122686**

220 Beatty, W. W. & Aupperle, R. L. Sex differences in cognitive impairment in multiple sclerosis. *Clin Neuropsychol* **16**, 472-480 (2002). **https://doi.org/10.1076/clin.16.4.472.13904**

221 Schoonheim, M. M. *et al.* Subcortical atrophy and cognition: sex effects in multiple sclerosis. *Neurology* **79**, 1754-1761 (2012). **https://doi.org/10.1212/WNL.0b013e3182703f46**

222 Koch, M., Kingwell, E., Rieckmann, P. & Tremlett, H. The natural history of secondary progressive multiple sclerosis. *J Neurol Neurosurg Psychiatry* **81**, 1039-1043 (2010). **https://doi.org/10.1136/jnnp.2010.208173**

223 Papenfuss, T. L. *et al.* Sex differences in experimental autoimmune encephalomyelitis in multiple murine strains. *J Neuroimmunol* **150**, 59-69 (2004). **https://doi.org/10.1016/j.jneuroim.2004.01.018**

224 Bebo, B. F., Jr., Vandenbark, A. A. & Offner, H. Male SJL mice do not relapse after induction of EAE with PLP 139-151. *J Neurosci Res* **45**, 680-689 (1996). **https://doi.org/10.1002/(sici)1097-4547(19960915)45:6**<680::Aid-jnr4>3.0.Co;2-4

225 Pöllinger, B. *et al.* Spontaneous relapsing-remitting EAE in the SJL/J mouse: MOG-reactive transgenic T cells recruit endogenous MOG-specific B cells. *J Exp Med* **206**, 1303-1316 (2009). **https://doi.org/10.1084/jem.20090299**

226 Dhaeze, T. *et al.* Sex-dependent factors encoded in the immune compartment dictate relapsing or progressive phenotype in demyelinating disease. *JCI Insight* **4** (2019). **https://doi.org/10.1172/jci.insight.124885**

227 Cahill, L. S. *et al.* Aged hind-limb clasping experimental autoimmune encephalomyelitis models aspects of the neurodegenerative process seen in multiple sclerosis. *Proc Natl Acad Sci U S A* **116**, 22710-22720 (2019). **https://doi.org/10.1073/pnas.1915141116**

228 Wiedrick, J. *et al.* Sex differences in EAE reveal common and distinct cellular and molecular components. *Cell Immunol* **359**, 104242 (2021). **https://doi.org/10.1016/j.cellimm.2020.104242**

229 Massilamany, C., Thulasingam, S., Steffen, D. & Reddy, J. Gender differences in CNS autoimmunity induced by mimicry epitope for PLP 139-151 in SJL mice. *J Neuroimmunol* **230**, 95-104 (2011). **https://doi.org/10.1016/j.jneuroim.2010.09.011**

230 Voskuhl, R. R., Pitchekian-Halabi, H., MacKenzie-Graham, A., McFarland, H. F. & Raine, C. S. Gender differences in autoimmune demyelination in the mouse: implications for multiple sclerosis. *Ann Neurol* **39**, 724-733 (1996). **https://doi.org/10.1002/ana.410390608**

231 Voskuhl, R. R. *et al.* Estriol combined with glatiramer acetate for women with relapsing-remitting multiple sclerosis: a randomised, placebo-controlled, phase 2 trial. *Lancet Neurol* **15**, 35-46 (2016). **https://doi.org/10.1016/s1474-4422(15)00322-1**

232 Kurth, F. *et al.* Neuroprotective effects of testosterone treatment in men with multiple sclerosis. *Neuroimage Clin* **4**, 454-460 (2014). **https://doi.org/10.1016/j.nicl.2014.03.001**

233 Bove, R. *et al.* Exploration of changes in disability after menopause in a longitudinal multiple sclerosis cohort. *Mult Scler* **22**, 935-943 (2016). **https://doi.org/10.1177/1352458515606211**

234 Benagiano, G., Benagiano, M., Bianchi, P., D'Elios, M. M. & Brosens, I. Contraception in autoimmune diseases. *Best Pract Res Clin Obstet Gynaecol* **60**, 111-123 (2019). **https://doi.org/10.1016/j.bpobgyn.2019.05.003**

235 Palaszynski, K. M., Loo, K. K., Ashouri, J. F., Liu, H. B. & Voskuhl, R. R. Androgens are protective in experimental autoimmune encephalomyelitis: implications for multiple sclerosis. *J Neuroimmunol* **146**, 144-152 (2004). **https://doi.org/10.1016/j.jneuroim.2003.11.004**

236 Voskuhl, R. R. & Palaszynski, K. Sex hormones in experimental autoimmune encephalomyelitis: implications for multiple sclerosis. *Neuroscientist* **7**, 258-270 (2001). **https://doi.org/10.1177/107385840100700310**

237 Morales, L. B. *et al.* Treatment with an estrogen receptor alpha ligand is neuroprotective in experimental autoimmune encephalomyelitis. *J Neurosci* **26**, 6823-6833 (2006). **https://doi.org/10.1523/jneurosci.0453-06.2006**

238 Kim, R. Y. *et al.* Oestrogen receptor β ligand acts on CD11c+ cells to mediate protection in experimental autoimmune encephalomyelitis. *Brain* **141**, 132-147 (2018). **https://doi.org/10.1093/brain/awx315**

239 Sawalha, A. H., Harley, J. B. & Scofield, R. H. Autoimmunity and Klinefelter's syndrome: when men have two X chromosomes. *J Autoimmun* **33**, 31-34 (2009). **https://doi.org/10.1016/j.jaut.2009.03.006**

240 Seminog, O. O., Seminog, A. B., Yeates, D. & Goldacre, M. J. Associations between Klinefelter's syndrome and autoimmune diseases: English national record linkage studies. *Autoimmunity* **48**, 125-128 (2015). **https://doi.org/10.3109/08916934.2014.968918**

241 Arnold, A. P. Mouse models for evaluating sex chromosome effects that cause sex differences in non-gonadal tissues. *J Neuroendocrinol* **21**, 377-386 (2009). **https://doi.org/10.1111/j.1365-2826.2009.01831.x**

242 Lovell-Badge, R. & Robertson, E. XY female mice resulting from a heritable mutation in the primary testis-determining gene, Tdy. *Development* **109**, 635-646 (1990). **https://doi.org/10.1242/dev.109.3.635**

243 Arnold, A. P. Sex chromosomes and brain gender. *Nat Rev Neurosci* **5**, 701-708 (2004). **https://doi.org/10.1038/nrn1494**

244 Smith-Bouvier, D. L. *et al.* A role for sex chromosome complement in the female bias in autoimmune disease. *J Exp Med* **205**, 1099-1108 (2008). **https://doi.org/10.1084/jem.20070850**

245 Itoh, Y. *et al.* The X-linked histone demethylase Kdm6a in CD4+ T lymphocytes modulates autoimmunity. *J Clin Invest* **129**, 3852-3863 (2019). **https://doi.org/10.1172/jci126250**

246 Foster, S. C., Daniels, C., Bourdette, D. N. & Bebo, B. F., Jr. Dysregulation of the hypothalamic-pituitary-gonadal axis in experimental autoimmune encephalomyelitis and multiple sclerosis. *J Neuroimmunol* **140**, 78-87 (2003). **https://doi.org/10.1016/s0165-5728(03)00177-2**

247 Maret, A. *et al.* Estradiol enhances primary antigen-specific CD4 T cell responses and Th1 development in vivo. Essential role of estrogen receptor alpha expression in hematopoietic cells. *Eur J Immunol* **33**, 512-521 (2003). **https://doi.org/10.1002/immu.200310027**

248 Fox, H. S., Bond, B. L. & Parslow, T. G. Estrogen regulates the IFN-gamma promoter. *J Immunol* **146**, 4362-4367 (1991).

249 Kim, S. & Voskuhl, R. R. Decreased IL-12 production underlies the decreased ability of male lymph node cells to induce experimental autoimmune encephalomyelitis. *J Immunol* **162**, 5561-5568 (1999).

250 Castellazzi, M. *et al.* Multiplex Matrix Metalloproteinases Analysis in the Cerebrospinal Fluid Reveals Potential Specific Patterns in Multiple Sclerosis Patients. *Front Neurol* **9**, 1080 (2018). **https://doi.org/10.3389/fneur.2018.01080**

251 Brahmachari, S. & Pahan, K. Gender-specific expression of beta1 integrin of VLA-4 in myelin basic protein-primed T cells: implications for gender bias in multiple sclerosis. *J Immunol* **184**, 6103-6113 (2010). **https://doi.org/10.4049/jimmunol.0804356**

252 Kuhlmann, T. *et al.* Gender differences in the histopathology of MS? *J Neurol Sci* **286**, 86-91 (2009). **https://doi.org/10.1016/j.jns.2009.07.014**

253 Dasgupta, S., Jana, M., Liu, X. & Pahan, K. Myelin basic protein-primed T cells of female but not male mice induce nitric-oxide synthase and proinflammatory cytokines in microglia: implications for gender bias in multiple sclerosis. *J Biol Chem* **280**, 32609-32617 (2005). **https://doi.org/10.1074/jbc.M500299200**

254 Thion, M. S. *et al.* Microbiome Influences Prenatal and Adult Microglia in a Sex-Specific Manner. *Cell* **172**, 500-516.e516 (2018). **https://doi.org/10.1016/j.cell.2017.11.042**

255 Guillot-Sestier, M. V. *et al.* Microglial metabolism is a pivotal factor in sexual dimorphism in Alzheimer's disease. *Commun Biol* **4**, 711 (2021). **https://doi.org/10.1038/s42003-021-02259-y**

256 Hanamsagar, R. *et al.* Generation of a microglial developmental index in mice and in humans reveals a sex difference in maturation and immune reactivity. *Glia* **66**, 460 (2018). **https://doi.org/10.1002/glia.23277**

257 Schneider-Hohendorf, T. *et al.* Sex bias in MHC I-associated shaping of the adaptive immune system. *Proc Natl Acad Sci U S A* **115**, 2168-2173 (2018). **https://doi.org/10.1073/pnas.1716146115**

258 Alley, J. *et al.* More severe neurologic deficits in SJL/J male than female mice following Theiler's virus-induced CNS demyelination. *Exp Neurol* **180**, 14-24 (2003). **https://doi.org/10.1016/s0014-4886(02)00054-7**

259 Fuller, A. C. *et al.* Gender bias in Theiler's virus-induced demyelinating disease correlates with the level of antiviral immune responses. *J Immunol* **175**, 3955-3963 (2005). **https://doi.org/10.4049/jimmunol.175.6.3955**

260 Tejera-Alhambra, M. *et al.* Perforin expression by CD4+ regulatory T cells increases at multiple sclerosis relapse: sex differences. *Int J Mol Sci* **13**, 6698-6710 (2012). **https://doi.org/10.3390/ijms13066698**

261 Bettelli, E. *et al.* IL-10 is critical in the regulation of autoimmune encephalomyelitis as demonstrated by studies of IL-10- and IL-4-deficient and transgenic mice. *J Immunol* **161**, 3299-3306 (1998).

262 Bebo, B. F., Jr., Schuster, J. C., Vandenbark, A. A. & Offner, H. Androgens alter the cytokine profile and reduce encephalitogenicity of myelin-reactive T cells. *J Immunol* **162**, 35-40 (1999).

263 Liva, S. M. & Voskuhl, R. R. Testosterone acts directly on CD4+ T lymphocytes to increase IL-10 production. *J Immunol* **167**, 2060-2067 (2001). **https://doi.org/10.4049/jimmunol.167.4.2060**

264 Tillack, K. *et al.* Gender differences in circulating levels of neutrophil extracellular traps in serum of multiple sclerosis patients. *J Neuroimmunol* **261**, 108-119 (2013). **https://doi.org/10.1016/j.jneuroim.2013.05.004**

265 Wilcoxen, S. C., Kirkman, E., Dowdell, K. C. & Stohlman, S. A. Gender-dependent IL-12 secretion by APC is regulated by IL-10. *J Immunol* **164**, 6237-6243 (2000). **https://doi.org/10.4049/jimmunol.164.12.6237**

266 Miteva, L., Trenova, A., Slavov, G. & Stanilova, S. IL12B gene polymorphisms have sex-specific effects in relapsing-remitting multiple sclerosis. *Acta Neurol Belg* **119**, 83-93 (2019). **https://doi.org/10.1007/s13760-018-01066-3**

267 Siracusa, M. C., Overstreet, M. G., Housseau, F., Scott, A. L. & Klein, S. L. 17beta-estradiol alters the activity of conventional and IFN-producing killer dendritic cells. *J Immunol* **180**, 1423-1431 (2008). **https://doi.org/10.4049/jimmunol.180.3.1423**

268 de Andrés, C. *et al.* Activation of Blood CD3(+)CD56(+)CD8(+) T Cells during Pregnancy and Multiple Sclerosis. *Front Immunol* **8**, 196 (2017). **https://doi.org/10.3389/fimmu.2017.00196**

269 Karrenbauer, V. D., Bedri, S. K., Hillert, J. & Manouchehrinia, A. Cerebrospinal fluid oligoclonal immunoglobulin gamma bands and long-term disability progression in multiple sclerosis: a retrospective cohort study. *Sci Rep* **11**, 14987 (2021). **https://doi.org/10.1038/s41598-021-94423-x**

270 Luders, E., Gaser, C., Narr, K. L. & Toga, A. W. Why sex matters: brain size independent differences in gray matter distributions between men and women. *J Neurosci* **29**, 14265-14270 (2009). **https://doi.org/10.1523/jneurosci.2261-09.2009**

271 Wooten, G. F., Currie, L. J., Bovbjerg, V. E., Lee, J. K. & Patrie, J. Are men at greater risk for Parkinson's disease than women? *J Neurol Neurosurg Psychiatry* **75**, 637-639 (2004). **https://doi.org/10.1136/jnnp.2003.020982**

272 Uchoa, M. F., Moser, V. A. & Pike, C. J. Interactions between inflammation, sex steroids, and Alzheimer's disease risk factors. *Front Neuroendocrinol* **43**, 60-82 (2016). **https://doi.org/10.1016/j.yfrne.2016.09.001**

273 Du, S. *et al.* XY sex chromosome complement, compared with XX, in the CNS confers greater neurodegeneration during experimental autoimmune encephalomyelitis. *Proc Natl Acad Sci U S A* **111**, 2806-2811 (2014). **https://doi.org/10.1073/pnas.1307091111**

274 Meyer, C. E. *et al.* Neuroprotection in Cerebral Cortex Induced by the Pregnancy Hormone Estriol. *Lab Invest* **103**, 100189 (2023). **https://doi.org/10.1016/j.labinv.2023.100189**

275 Itoh, N. *et al.* Estrogen receptor beta in astrocytes modulates cognitive function in mid-age female mice. *Nat Commun* **14**, 6044 (2023). **https://doi.org/10.1038/s41467-023-41723-7**

276 Alvarez-Sanchez, N. & Dunn, S. E. Potential biological contributers to the sex difference in multiple sclerosis progression. *Front Immunol* **14**, 1175874 (2023). **https://doi.org/10.3389/fimmu.2023.1175874**

277 Schenkel, A. R., Mamdouh, Z., Chen, X., Liebman, R. M. & Muller, W. A. CD99 plays a major role in the migration of monocytes through endothelial junctions. *Nat Immunol* **3**, 143-150 (2002). **https://doi.org/10.1038/ni749**

278 Lou, O., Alcaide, P., Luscinskas, F. W. & Muller, W. A. CD99 is a key mediator of the transendothelial migration of neutrophils. *J Immunol* **178**, 1136-1143 (2007). **https://doi.org/10.4049/jimmunol.178.2.1136**

279 Winger, R. C. *et al.* Cutting Edge: CD99 Is a Novel Therapeutic Target for Control of T Cell-Mediated Central Nervous System Autoimmune Disease. *J Immunol* **196**, 1443-1448 (2016). **https://doi.org/10.4049/jimmunol.1501634**

280 Dworzak, M. N. *et al.* Flow cytometric assessment of human MIC2 expression in bone marrow, thymus, and peripheral blood. *Blood* **83**, 415-425 (1994).

281 Yu, F. *et al.* Cell Adhesion Molecule CD99 in Cancer Immunotherapy. *Curr Mol Med* **23**, 1028-1036 (2023). **https://doi.org/10.2174/1566524023666221007143513**

282 Riggi, N., Suvà, M. L. & Stamenkovic, I. Ewing's Sarcoma. *N Engl J Med* **384**, 154-164 (2021). **https://doi.org/10.1056/NEJMra2028910**

283 Baldauf, M. C. *et al.* Robust diagnosis of Ewing sarcoma by immunohistochemical detection of super-enhancer-driven EWSR1-ETS targets. *Oncotarget* **9**, 1587-1601 (2018). **https://doi.org/10.18632/oncotarget.20098**

284 Scotlandi, K. *et al.* Targeting CD99 in association with doxorubicin: an effective combined treatment for Ewing's sarcoma. *Eur J Cancer* **42**, 91-96 (2006). **https://doi.org/10.1016/j.ejca.2005.09.015**

285 Ali, A., Vaikari, V. P. & Alachkar, H. CD99 in malignant hematopoiesis. *Exp Hematol* **106**, 40-46 (2022). **https://doi.org/10.1016/j.exphem.2021.12.363**

286 Vestweber, D. How leukocytes cross the vascular endothelium. *Nat Rev Immunol* **15**, 692-704 (2015). **https://doi.org/10.1038/nri3908**

287 Pasello, M., Manara, M. C. & Scotlandi, K. CD99 at the crossroads of physiology and pathology. *J Cell Commun Signal* **12**, 55-68 (2018). **https://doi.org/10.1007/s12079-017-0445-z**

288 Mapunda, J. A., Tibar, H., Regragui, W. & Engelhardt, B. How Does the Immune System Enter the Brain? *Front Immunol* **13**, 805657 (2022). **https://doi.org/10.3389/fimmu.2022.805657**

289 Bixel, G. *et al.* Mouse CD99 participates in T-cell recruitment into inflamed skin. *Blood* **104**, 3205-3213 (2004). **https://doi.org/10.1182/blood-2004-03-1184**

290 Dufour, E. M., Deroche, A., Bae, Y. & Muller, W. A. CD99 is essential for leukocyte diapedesis in vivo. *Cell Commun Adhes* **15**, 351-363 (2008). **https://doi.org/10.1080/15419060802442191**

291 Watson, R. L. *et al.* Endothelial CD99 signals through soluble adenylyl cyclase and PKA to regulate leukocyte transendothelial migration. *J Exp Med* **212**, 1021-1041 (2015). **https://doi.org/10.1084/jem.20150354**

292 Wimmer, I. *et al.* PECAM-1 Stabilizes Blood-Brain Barrier Integrity and Favors Paracellular T-Cell Diapedesis Across the Blood-Brain Barrier During Neuroinflammation. *Front Immunol* **10**, 711 (2019). **https://doi.org/10.3389/fimmu.2019.00711**

293 Nishihara, H. *et al.* Human CD4(+) T cell subsets differ in their abilities to cross endothelial and epithelial brain barriers in vitro. *Fluids Barriers CNS* **17**, 3 (2020). **https://doi.org/10.1186/s12987-019-0165-2**

294 Zhou, F. *et al.* GDF6-CD99 Signaling Regulates Src and Ewing Sarcoma Growth. *Cell Rep* **33**, 108332 (2020). **https://doi.org/10.1016/j.celrep.2020.108332**

295 Waclavicek, M. *et al.* CD99 engagement on human peripheral blood T cells results in TCR/CD3-dependent cellular activation and allows for Th1-restricted cytokine production. *J Immunol* **161**, 4671-4678 (1998).

296 Oh, K. I. *et al.* CD99 activates T cells via a costimulatory function that promotes raft association of TCR complex and tyrosine phosphorylation of TCR zeta. *Exp Mol Med* **39**, 176-184 (2007). **https://doi.org/10.1038/emm.2007.20**

297 Brémond, A. *et al.* Regulation of HLA class I surface expression requires CD99 and p230/golgin-245 interaction. *Blood* **113**, 347-357 (2009). **https://doi.org/10.1182/blood-2008-02-137745**

298 Laopajon, W. *et al.* Triggering of CD99 on monocytes by a specific monoclonal antibody regulates T cell activation. *Cell Immunol* **335**, 51-58 (2019). **https://doi.org/10.1016/j.cellimm.2018.10.012**

299 Takheaw, N., Earwong, P., Laopajon, W., Pata, S. & Kasinrerk, W. Interaction of CD99 and its ligand upregulates IL-6 and TNF-α upon T cell activation. *PLoS One* **14**, e0217393 (2019). **https://doi.org/10.1371/journal.pone.0217393**

300 Takheaw, N., Pata, S., Laopajon, W., Roytrakul, S. & Kasinrerk, W. The presence of membrane bound CD99 ligands on leukocyte surface. *BMC Res Notes* **13**, 496 (2020). **https://doi.org/10.1186/s13104-020-05347-0**

301 Goswami, D. *et al.* Endothelial CD99 supports arrest of mouse neutrophils in venules and binds to neutrophil PILRs. *Blood* **129**, 1811-1822 (2017). **https://doi.org/10.1182/blood-2016-08-733394**

302 Li, Y. T. *et al.* Blood flow guides sequential support of neutrophil arrest and diapedesis by PILR-β1 and PILR-α. *Elife* **8** (2019). **https://doi.org/10.7554/eLife.47642**

303 Balaton, B. P., Cotton, A. M. & Brown, C. J. Derivation of consensus inactivation status for X-linked genes from genome-wide studies. *Biol Sex Differ* **6**, 35 (2015). **https://doi.org/10.1186/s13293-015-0053-7**

304 Goodfellow, P. N. *et al.* MIC2: a human pseudoautosomal gene. *Philos Trans R Soc Lond B Biol Sci* **322**, 145-154 (1988). **https://doi.org/10.1098/rstb.1988.0122**

305 Carrel, L. & Willard, H. F. X-inactivation profile reveals extensive variability in X-linked gene expression in females. *Nature* **434**, 400-404 (2005). **https://doi.org/10.1038/nature03479**

306 Mattisson, J. *et al.* Leukocytes with chromosome Y loss have reduced abundance of the cell surface immunoprotein CD99. *Sci Rep* **11**, 15160 (2021). **https://doi.org/10.1038/s41598-021-94588-5**

307 Trolle, C. *et al.* Widespread DNA hypomethylation and differential gene expression in Turner syndrome. *Sci Rep* **6**, 34220 (2016). **https://doi.org/10.1038/srep34220**

308 Wang, H. *et al.* Bioinformatic Analysis Identifies Potential Key Genes in the Pathogenesis of Turner Syndrome. *Front Endocrinol (Lausanne)* **11**, 104 (2020). **https://doi.org/10.3389/fendo.2020.00104**

309 Consortium, I. M. S. G. Locus for severity implicates CNS resilience in progression of multiple sclerosis. *Nature* (2023). **https://doi.org/10.1038/s41586-023-06250-x**

310 Beecham, A. H. *et al.* Analysis of immune-related loci identifies 48 new susceptibility variants for multiple sclerosis. *Nat Genet* **45**, 1353-1360 (2013). **https://doi.org/10.1038/ng.2770**

311 Concordet, J. P. & Haeussler, M. CRISPOR: intuitive guide selection for CRISPR/Cas9 genome editing experiments and screens. *Nucleic Acids Res* **46**, W242-w245 (2018). **https://doi.org/10.1093/nar/gky354**

312 Remy, S. *et al.* Generation of gene-edited rats by delivery of CRISPR/Cas9 protein and donor DNA into intact zygotes using electroporation. *Sci Rep* **7**, 16554 (2017). **https://doi.org/10.1038/s41598-017-16328-y**

313 Liu, Q. *et al.* A proximity-tagging system to identify membrane protein-protein interactions. *Nat Methods* **15**, 715-722 (2018). **https://doi.org/10.1038/s41592-018-0100-5**

314 Battle, A., Brown, C. D., Engelhardt, B. E. & Montgomery, S. B. Genetic effects on gene expression across human tissues. *Nature* **550**, 204-213 (2017). **https://doi.org/10.1038/nature24277**

315 Hagen, S. H., Hennesen, J. & Altfeld, M. Assessment of escape from X chromosome inactivation and gene expression in single human immune cells. *STAR Protoc* **2**, 100641 (2021). **https://doi.org/10.1016/j.xpro.2021.100641**

316 Winger, R. C., Koblinski, J. E., Kanda, T., Ransohoff, R. M. & Muller, W. A. Rapid remodeling of tight junctions during paracellular diapedesis in a human model of the blood-brain barrier. *J Immunol* **193**, 2427-2437 (2014). **https://doi.org/10.4049/jimmunol.1400700**

317 Pata, S. *et al.* Association of CD99 short and long forms with MHC class I, MHC class II and tetraspanin CD81 and recruitment into immunological synapses. *BMC Res Notes* **4**, 293 (2011). **https://doi.org/10.1186/1756-0500-4-293**

318 Kasinrerk, W., Tokrasinwit, N., Moonsom, S. & Stockinger, H. CD99 monoclonal antibody induce homotypic adhesion of Jurkat cells through protein tyrosine kinase and protein kinase C-dependent pathway. *Immunol Lett* **71**, 33-41 (2000). **https://doi.org/10.1016/s0165-2478(99)00165-0**

319 Yu, B. *et al.* B cell-specific XIST complex enforces X-inactivation and restrains atypical B cells. *Cell* **184**, 1790-1803.e1717 (2021). **https://doi.org/10.1016/j.cell.2021.02.015**

320 Sado, T. Does XIST safeguard against sex-biased human diseases? *Mol Cell* **81**, 1598-1600 (2021). **https://doi.org/10.1016/j.molcel.2021.03.036**

321 Tan, M. H., Li, J., Xu, H. E., Melcher, K. & Yong, E. L. Androgen receptor: structure, role in prostate cancer and drug discovery. *Acta Pharmacol Sin* **36**, 3-23 (2015). **https://doi.org/10.1038/aps.2014.18**

322 Hoffmann, J. P., Liu, J. A., Seddu, K. & Klein, S. L. Sex hormone signaling and regulation of immune function. *Immunity* **56**, 2472-2491 (2023). **https://doi.org/10.1016/j.immuni.2023.10.008**

323 Suh, Y. H. *et al.* Cloning, genomic organization, alternative transcripts and expression analysis of CD99L2, a novel paralog of human CD99, and identification of evolutionary conserved motifs. *Gene* **307**, 63-76 (2003). **https://doi.org/10.1016/s0378-1119(03)00401-3**

324 Park, S. H. *et al.* Rapid divergency of rodent CD99 orthologs: implications for the evolution of the pseudoautosomal region. *Gene* **353**, 177-188 (2005). **https://doi.org/10.1016/j.gene.2005.04.023**

325 Gal-Oz, S. T. *et al.* ImmGen report: sexual dimorphism in the immune system transcriptome. *Nat Commun* **10**, 4295 (2019). **https://doi.org/10.1038/s41467-019-12348-6**

326 Lu, T. & Mar, J. C. Investigating transcriptome-wide sex dimorphism by multi-level analysis of single-cell RNA sequencing data in ten mouse cell types. *Biol Sex Differ* **11**, 61 (2020). **https://doi.org/10.1186/s13293-020-00335-2**

327 Nam, G. *et al.* Interaction of CD99 with its paralog CD99L2 positively regulates CD99L2 trafficking to cell surfaces. *J Immunol* **191**, 5730-5742 (2013). **https://doi.org/10.4049/jimmunol.1203062**

328 Bixel, M. G. *et al.* A CD99-related antigen on endothelial cells mediates neutrophil but not lymphocyte extravasation in vivo. *Blood* **109**, 5327-5336 (2007). **https://doi.org/10.1182/blood-2006-08-043109**

329 Schenkel, A. R., Dufour, E. M., Chew, T. W., Sorg, E. & Muller, W. A. The murine CD99-related molecule CD99-like 2 (CD99L2) is an adhesion molecule involved in the inflammatory response. *Cell Commun Adhes* **14**, 227-237 (2007). **https://doi.org/10.1080/15419060701755966**

330 Seelige, R. *et al.* Cutting edge: Endothelial-specific gene ablation of CD99L2 impairs leukocyte extravasation in vivo. *J Immunol* **190**, 892-896 (2013). **https://doi.org/10.4049/jimmunol.1202721**

331 Samus, M., Seelige, R., Schäfer, K., Sorokin, L. & Vestweber, D. CD99L2 deficiency inhibits leukocyte entry into the central nervous system and ameliorates neuroinflammation. *J Leukoc Biol* **104**, 787-797 (2018). **https://doi.org/10.1002/jlb.1a0617-228r**

332 Hrastelj, J. *et al.* CSF-resident CD4(+) T-cells display a distinct gene expression profile with relevance to immune surveillance and multiple sclerosis. *Brain Commun* **3**, fcab155 (2021). **https://doi.org/10.1093/braincomms/fcab155**

333 Pappalardo, J. L. *et al.* Transcriptomic and clonal characterization of T cells in the human central nervous system. *Sci Immunol* **5** (2020). **https://doi.org/10.1126/sciimmunol.abb8786**

334 Efremova, M., Vento-Tormo, M., Teichmann, S. A. & Vento-Tormo, R. CellPhoneDB: inferring cell-cell communication from combined expression of multi-subunit ligand-receptor complexes. *Nat Protoc* **15**, 1484-1506 (2020). **https://doi.org/10.1038/s41596-020-0292-x**

335 Yue, S., Xu, P., Cao, Z. & Zhuang, M. PUP-IT2 as an alternative strategy for PUP-IT proximity labeling. *Front Mol Biosci* **9**, 1007720 (2022). **https://doi.org/10.3389/fmolb.2022.1007720**

336 Sevim, H. *et al.* Clofarabine induces ERK/MSK/CREB activation through inhibiting CD99 on Ewing sarcoma cells. *PLoS One* **16**, e0253170 (2021). **https://doi.org/10.1371/journal.pone.0253170**

337 Çelik, H. *et al.* Clofarabine inhibits Ewing sarcoma growth through a novel molecular mechanism involving direct binding to CD99. *Oncogene* **37**, 2181-2196 (2018). **https://doi.org/10.1038/s41388-017-0080-4**

338 Balaraman, K. *et al.* Design, synthesis and biological evaluation of Nucleosidic CD99 inhibitors that selectively reduce Ewing sarcoma viability. *Eur J Med Chem* **251**, 115244 (2023). **https://doi.org/10.1016/j.ejmech.2023.115244**

339 Wingett, D., Forcier, K. & Nielson, C. P. A role for CD99 in T cell activation. *Cell Immunol* **193**, 17-23 (1999). **https://doi.org/10.1006/cimm.1999.1470**

340 Zumwalde, N. A., Domae, E., Mescher, M. F. & Shimizu, Y. ICAM-1-dependent homotypic aggregates regulate CD8 T cell effector function and differentiation during T cell activation. *J Immunol* **191**, 3681-3693 (2013). **https://doi.org/10.4049/jimmunol.1201954**

341 Manara, M. C. *et al.* Engagement of CD99 activates distinct programs in Ewing sarcoma and macrophages. *Cancer Immunol Res* (2023). **https://doi.org/10.1158/2326-6066.Cir-23-0440**

V. Publication list

Partial results of this work have been submitted for publication to the Journal Biology of Sex Differences on the 7th of November 2023:

Winschel I, Willing A, Engler JB, Walkenhorst M, Meurs N, Binkle-Ladisch L, Woo MS, Pfeffer LK, Sonner JK, Borgmeyer U, Hagen SH, Grünhagel B, Claussen JM, Altfeld M, Friese MA. Sex- and species-specific contribution of CD99 to T cell costimulation during multiple sclerosis. Under review.

Witt G, Keminer O, Leu J, Tandon R, Meiser I, Willing A, **Winschel I**, Abt JC, Brändl B, Sébastien I, Friese MA, Müller FJ, Neubauer JC, Claussen C, Zimmermann H, Gribbon P, Pless O. An automated and high-throughput-screening compatible pluripotent stem cell-based test platform for developmental and reproductive toxicity assessment of small molecule compounds. Cell Biol Toxicol. 2021 Apr;37(2):229-243.

Walkenhorst M, Sonner JK, Kursawe N, Engler JB, Bauer S, **Winschel I**, Raich L, Salinas G, Lantz O, Friese MA, Willing A. TCR-activated MAIT cells promote recovery from CNS inflammation. 2023. In revision.

Woo MS, Bal LC, **Winschel I**, Manca E, Walkenhorst M, Kachegia B, Sonner JK, Di Liberto G, Mayer C, Binkle-Ladisch L, Rothammer N, Unger L, Raich L, Vieira V, Meurs N, Wagner I, Cocco C, Stephens SB, Glatzel M, Merkler D, Friese MA. Neuroinflammation-induced NR4A2-VGF pathway activation fuels neurodegeneration through increased neuronal glycolysis. November 2023. Under review.

VI. Acknowledgements

First of all, I thank Prof. Dr. Manuel Alexander Friese for the opportunity to work on this intriguing project at the INIMS as well as for great supervision and constant support. I am grateful for the opportunity to expand my scientific and soft skills on international workshops and conferences.

I thank Prof. Dr. Tim-Wolf Gilberger for co-supervising my work and the evaluation of my thesis as well as for encouragement during my project.

I want to thank Prof. Dr. Tim-Wolf Gilberger, Prof. Dr. Thomas Oertner and Prof. Dr. Marcus Altfeld for being members of my examination commission as well as Dr. Thomas Jacobs and Dr. Guido Hermey for being members of my ZMNH thesis committee with all of them supporting my project with their scientific experience.

Many thanks to Dr. Anne Willing for excellent supervision, knowledge, proof-reading of this thesis and motivational support whenever needed – not only science wise. I enjoyed working together and am grateful for all I have learned from that.

I would like to thank Dr. Dr. Jan Broder Engler for bioinformatic contribution as well as Dr. Mark Walkenhorst, Dr. Lars Binkle-Ladisch, Dr. Marcel Seungsu Woo, Dr. Jana Sonner and Dr. Kristina Pfeffer for their scientific expertise and experimental help to this work. Special thanks to Nina Meurs for invaluable support with experimental procedures.

I thank Dr. Uwe Borgmeyer and Dr. Irm Hermans-Borgmeyer for the generation of *Cd99*-deficient mice. Many thanks to Prof. Dr. Marcus Altfeld, Dr. Sven Hendrik Hagen, Benjamin Grünhagel and Janna Claussen for XCI experiments as well as for generously providing PBMC samples from trans men.

Moreover, I heartily thank Dr. Mark Walkenhorst and Dr. Iris Winkler as well as all other members of the INIMS for their help, scientific and non-scientific discussions and the good and cooperative atmosphere in the lab.

Last but foremost I am incredibly grateful to my family and friends, who paved the way and encouraged with unconditional support all along that journey.

VII. Affidavit

Hiermit erkläre ich an Eides statt, dass ich die vorliegende Dissertationsschrift selbst verfasst und keine anderen als die angegebenen Quellen und Hilfsmittel benutzt habe.

I hereby declare upon oath that I have written the present dissertation independently and have not used further resources and aids than those stated in the dissertation.

_____

Ort, den | City, date Unterschrift | Signature